Design and Construction of Pattern Reconfigurable Antenna with Fine Direction Resolution

A thesis submitted as partial fulfilment of the requirement of Doctor of Philosophy (Ph.D.)

by

Nur Farahwahida binti Ab Aziz

Electronic and Computer Engineering Department,

Brunel University, London.

January 2019

Abstract

Recent developments in modern communication system have led to high demand in antenna as a transmitter and receiver in every electronic device. Antenna with high performance, low cost and multi-function is mostly desirable to fit into the system. Reconfigurable antenna has attained a lot of attention from antenna researchers with regards to its unique performance. Frequency, pattern and polarisation reconfigurable antenna has resolved many antenna problems in these recent years.

The radiation pattern reconfigurable antenna has led to many novel designs of reconfigurable antennas using different techniques and have different phase covered. The objective of this thesis is to overcome the limitation of beam angle polarisation. A considerable amount of literature has been published on the radiation pattern reconfigurable antenna. However, most of the papers have a difficulty of covering all angles in a plane.

Thus, the aim of this research is to design and develop a radiation pattern reconfigurable antenna with fine direction resolution ensuring full coverage extension on the plane. There are numerous researches conducted on pattern reconfigurable antenna showing the ability of the smart antenna to change its radiation pattern, but not many has cover the full plane.

An antenna that has a radiation pattern with full coverage on azimuthal plane is beneficial for an application that would requires signal transmitted or received in all directions. In this thesis, the radiation pattern is configured by the insertion of metal rods around the patch antenna. The radiation pattern does change accordingly but with the cost of large size of the antenna build-up.

The complexity of the reconfigurable antenna design has also brought to more in-depth studies on the miniaturisation techniques. Modern communication technology demands a low cost and compact design to be fitted in the wireless devices. Most of the reconfigurable antennas available these days have a drawback of complicated design which is problematical to be applied into communication devices. The experiment is carried out to attain a design of low profile pattern reconfigurable antenna with least shortfall in the antenna performance.

Acknowledgements

With the name of Allah, The Most Gracious and The Most Merciful.

All praises is due to God alone.

Throughout this hard journey of finishing this thesis, I am forever in-debt and thankful to so many people that help and encouraged me during my hard time, giving me support when I am carrying my baby while doing the writing, push me to finish my research when I am about to give everything up.

First and foremost, I would like to thank my supervisor, Dr.Rajagopal Nilavalan for his endless support and encouragement throughout my PhD studies. He had helped me tremendously with my research progress as well as being my support when I need one. He also has been a great listener and provides good moral support during my time away from family.

To the lab technician, Mr. Michael Lateo and his friend, Mr. Schkzamian William, thank you very much. You had provided a great hospitality and huge help during my experiment in Tower B. The remarkable experience and awe-inspiring knowledge during the preparation of antenna prototype and hardware arrangement will be great memories to us all.

I also owe special thanks to my husband for his unconditional support and consideration through the whole journey and also for his limitless understanding in our long distance relationship. He has also been very patient with my everyday mood swing during my early trimester of pregnancy.

Not to forget, my parents, parent-in-law, siblings and friends who gave me tremendous moral support and encouragement throughout my PhD journey.

Table of Contents

List of Figures

List of Tables

List of Symbols

RF	Radio frequency
VNA	Vector network analyser
f_H	Higher frequency
f_L	Lower frequency
f_0	Operating frequency
dB	Decibels
η	Efficiency
D	Directivity
HFSS	High Frequency Structural Simulator
MEMS	Microelectromechanical switches
RHCP	Right-handed circularly polarized
LHCP	Left-handed circularly polarized
WiMAX	Worldwide Interoperability for Microwave Access
WLAN	Wireless local area network
DC	Direct current
FDTD	Finite Different Time Domain
MoM	Moment of Method
FEM	Finite Element Method
f_r	Resonant frequency
ϵ_r	Dielectric constant
h	Height of the substrate
α	Actual radius of patch antenna
α_{eff}	Effective radius of patch antenna
d	Distance between shorting pin and centre of patch
RAM	Radiation Absorbing Material
dBm	decibel-milliwatts
FTB	Front-to-back ratio
λ	Free-space wavelength

Chapter 1 Introduction

1.1 Antennas

An antenna is a transitional structure between free-space and a guiding device designed to radiate or receive electromagnetic waves, as shown in Figure 1.1. The IEEE Standard for Definitions of Terms for Antenna defines it as part of receiving and transmitting system which radiates or receives electromagnetic waves[1]. In the transmitting modes, an antenna is used to convert guided waves within the transmission line to radiated free-space waves, and vice versa[2]. The device was known as areal or an elevated wire until the term antenna was first introduced by Guglielmo Marconi. In 1895, Guglielmo Marconi had come out with a way to transmit and receive electromagnetic waves up to a distance of 1.5 km during his experiment using Hertz' equipment.

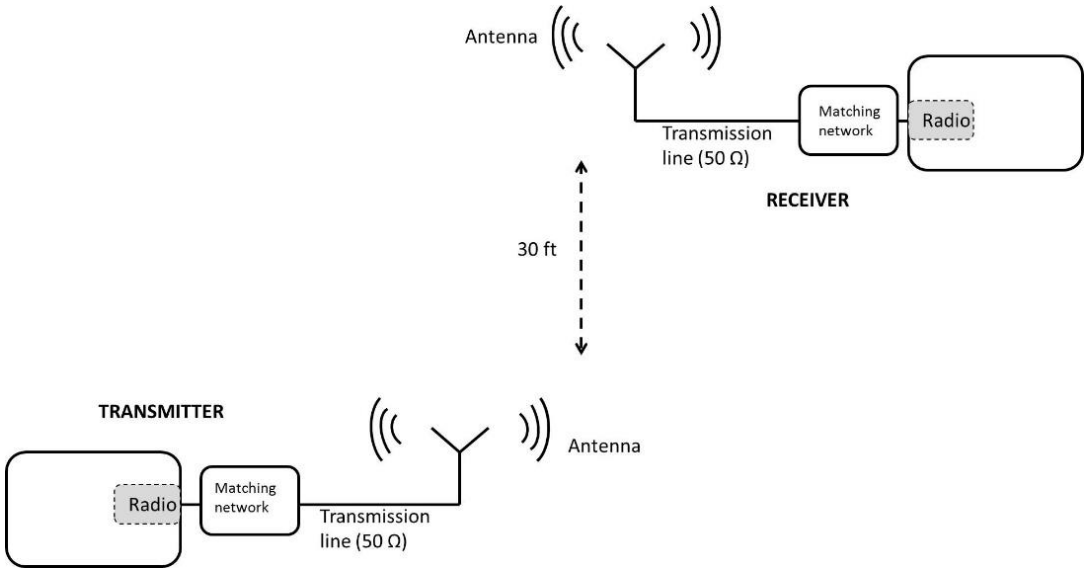

Figure 1.1 An example of wireless communication system.

1.2 General background

There are different types of antennas for different applications. Some example of antenna types are wire and microstrip antenna. Wire antennas are they are made of conducting wire and mainly applied in cars and television. The production cost of wire antennas are low compared to other antennas and they are usually operated at low frequencies[3]. The fabrication of this type of antenna is simple and straightforward. The length of the antenna can be modified to resonate at the desired wavelength. Some example of wire antennas are dipole, helical and loop antenna. Half-wavelength dipole antenna is widely used in radio transmitting and receiving application as it is very simple model. It consists of two identical conductive elements with total length of half wavelength, connected and fed at the centre to an RF feed line.

Figure 1.2 Example of dipole antenna prototype[4].

Another type of antenna is microstrip antenna. Microstrip antenna consists of mainly metallic structure on top of a grounded substrate. It is widely used because it is easy to fabricate and analyse on top of it low profile design. Some examples of microstrip antennas are rectangular and circular patch antenna, depending on the shape of metallic structure. Microstrip antenna has the advantage of low cross Polarisation radiation and very flexible in terms of its radiation pattern, operating frequency and impedance[5].

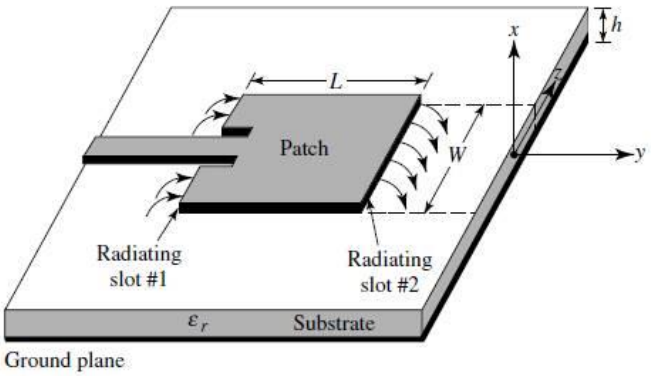

Figure 1.3 Microstrip antenna[5]

.

1.3 Main parameters of Antenna

There are some important parameters that need to be considered for the antenna design. This parameter will have a huge impact on the antenna performance. The parameters are listed as below.

1.3.1 S-parameter

S-parameters measured in a Vector Network Analyser (VNA) signifies the input and output connection between ports in an electrical system. It is obtained by measuring the voltage travelling waves between the ports to determine the impedance of an antenna. Antenna impedance is crucial as it affects the amount of power delivered or received in an antenna. Antenna impedance is required to be close to transmission line impedance to ensure a good design.

The first number in the subscript of S-parameters is the output port and the input port is represented by the second number. For instance, if there are two ports called Port 1 and Port 2 respectively, S12 represents the power transferred from Port 2 to Port 1. As a general rule, S_{NM} represents the power transferred from Port M to Port N in a multi-port network.

The most common parameter in regards to antenna is S11. S11 also known as reflection coefficient measures the amount of power reflected back when delivered from Port 1. It measures the amount of reflected power Port 1 trying to deliver to Port 1. S-parameters are a function of frequency and it also represents at which frequency does the antenna radiates best. When S11 (dB) is equal to zero, it means all the power is

reflected back and nothing is radiated. When S11 is equal to -10 dB, only small amount of power is reflected and the rest is radiated+. At this point of frequency, the antenna radiates well.

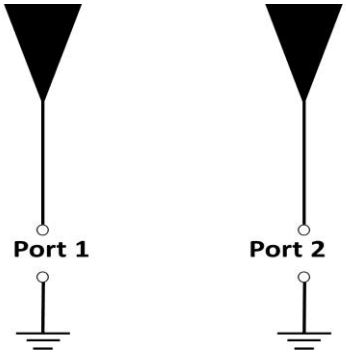

Figure 1.4 Two port network.

1.3.2 Impedance bandwidth

Impedance bandwidth is used to describe the bandwidth over where the antenna has acceptable losses due to mismatch. It can also be defined as the frequency range when the reflected power is less than -10 dB using S_{11} plot, as shown in Figure 1.5. In this range, the antenna radiates best as only small power is reflected back. The bandwidth can be calculated using the equation

$$\text{Bandwidth} = \frac{f_H - f_L}{f_0} \times 100\%$$

where f_H : Higher frequency
f_L : Lower frequency
f_0 : Operating frequency

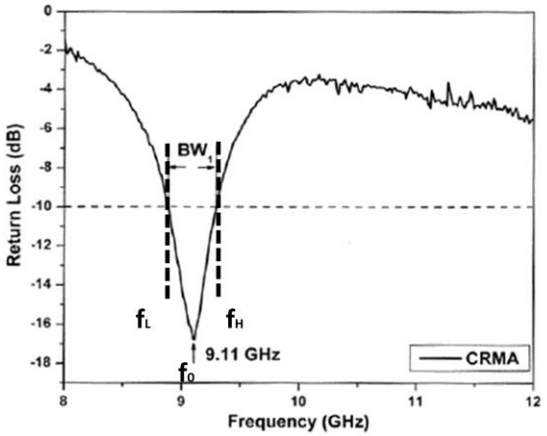

Figure 1.5 Impedance bandwidth measurement[6].

1.3.3 Directivity

Directivity of an antenna, as defined by [1], is the ratio of the radiation intensity in a given direction from the antenna to the radiation intensity averaged over all directions. In other words, it measures the intensity of the radiation pattern direction. A patch antenna will have a high directivity as it is a directional antenna, while an antenna with omnidirectional radiation pattern will have a directivity of 1 or 0 dB. The higher the directivity means a more focused antenna, which is beneficial in some applications but often comes with a price of large dimensions[6]. Figure below demonstrates directivity in a clearer way.

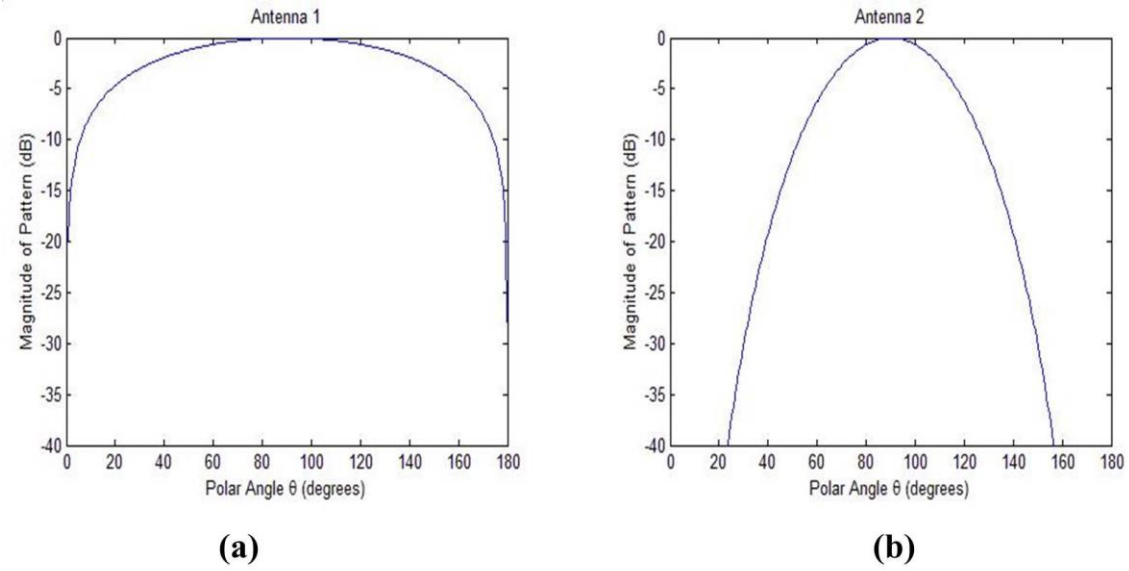

Figure 1.6 Radiation patterns for an antenna with (a) low directivity and (b) high directivity[7].

1.3.4 Radiation pattern

Radiation pattern of an antenna can be defined as a mathematical function or a graphical representation of the radiation properties of the antennas as a function of space coordinates[1]. In other words, radiation pattern can be defined as the variation of the power radiated by an antenna as a function of the direction away from the antenna. Typically, radiation pattern is measured in far-field region and represented in two- or three- dimensional space. When plotting the radiation pattern, the units or magnitude of the pattern are mostly measured in antenna gain[7]. An antenna which transmits or receives signal equally on a single plane has an omnidirectional radiation pattern as shown in Figure 1.7. The radiation pattern analysis is more significant for directional antenna as it express the directive properties of the antenna. In general, an

omnidirectional antenna has a comparatively low gain compared to directional antennas as the power radiates in all directions. Monopole antenna is an example of antenna with omnidirectional radiation pattern, and horn antenna is a good example of directional antenna.

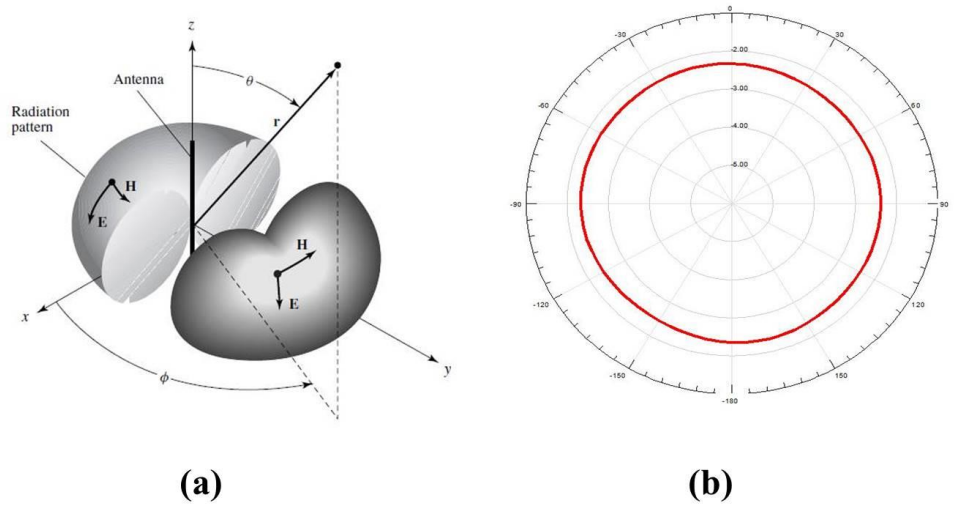

Figure 1.7 Example of omnidirectional radiation pattern plotted in (a) 3-dimension[8] and (b) 2-dimension[9].

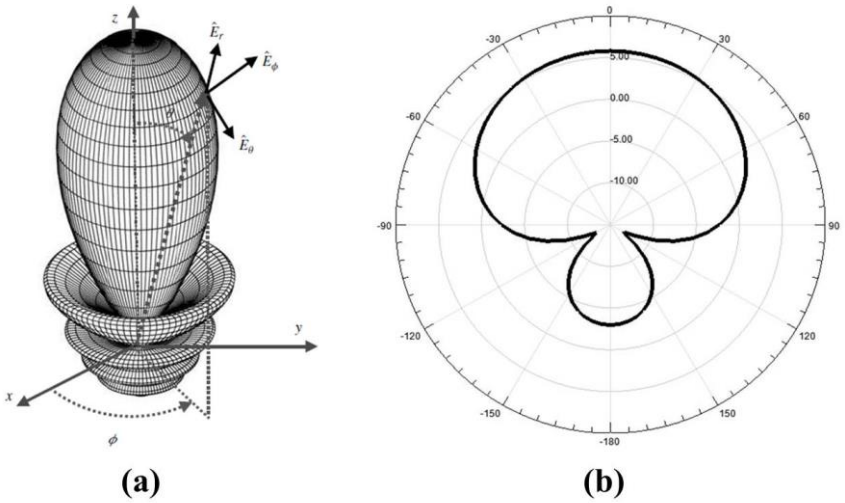

Figure 1.8 Example of directional radiation pattern plotted in (a) 3-dimension[5] and (b) 2-dimension.

1.3.5 Gain

Gain of an antenna is the ratio of radiation intensity of an antenna in a given direction to the radiation intensity that would be obtained by an isotropic antenna fed by the same power and it is measured in dBi. A high gain antenna is beneficial in a directional antenna, but then it is not appropriate for an antenna that receives and transmit signal from different directions. Gain of an antenna is closely related to the efficiency and directional capabilities of the antenna[8]. Therefore, gain of an antenna can be expressed as

$$\text{Gain} = \eta \, . \, D$$

where η is the efficiency and D is the directivity.

1.4 Main objectives

The demand in modern communication technology has been expanding rapidly, thus a smart antenna with the ability to change its parameter according to the system need is crucial and beneficial. Advanced wireless system necessitates an antenna with the ability to transmit and receive signal in all horizontal direction equally, and at the same time can be a directional antenna when preferred.

Primarily, the first objective of this thesis is to design an antenna with full coverage extension. An antenna with omnidirectional radiation pattern is beneficial for an application that would requires signal transmitted or received in all directions, i.e. mobile base station. Therefore, a conventional patch antenna is modified to give an omnidirectional radiation pattern with insertion of shorting pin.

After that, the radiation pattern is configured using the insertion of metal rods around the patch antenna. An antenna with a deviation in radiation pattern in all manner of angles in single plane is very beneficial for modern communication system. The addition of metal rods resulted in the antenna becoming a directional antenna according to which metal rod activated. The radiation pattern does change accordingly but with the cost of large size of the antenna build-up.

The radiation pattern reconfigurable antenna in the earlier part of this research has an extensive dimension. A compact design is more tempting for an application in modern communication technology. Patch antenna has been acknowledged to have low profile design and easy to fabricate, thus it is opted for this experiment. Thus, a

miniaturisation of the pattern reconfigurable antenna is an attempt in the later part of this research.

1.5 Main Contribution

All in all, the main contributions from this research are listed as below.

1. A compact size patch antenna with omnidirectional radiation pattern is developed by the manipulation of shorting pin location and using air as a substrate.
2. A reconfigurable antenna with radiation pattern agility incorporating fine direction resolution throughout azimuth plane is proposed. The pattern agility is acquired by the insertion of metal rods around the patch antenna.
3. A miniaturise reconfigurable antenna is presented by employing inductive loading with specific value into the parasitic structure.

First and foremost, a patch antenna with omnidirectional radiation pattern is designed. The full coverage of its radiation pattern is crucial before designing the reconfigurable antenna. A conventional patch antenna has a directional radiation pattern. A conventional patch antenna is modified to give an omnidirectional radiation pattern. Patch antenna is applied due to its lightweight, low profile, less cost, and its ease of fabrication. Furthermore, it is easier to integrate patch antenna with other radio frequency devices as compared to other antennas. In a conventional patch antenna, the low frequency of operation will result in large size of patch antenna. The introduction of shorted pin into the patch antenna design resulted in reduction of antenna size. There are other techniques available to reduce the antenna size yet resulted in high cost and degraded the performance of the antenna.

There are many studies conducted on radiation pattern reconfigurable antenna. However, not many have a go on radiation pattern reconfigurable antenna comprising full angle coverage in a single plane. In this research, the variation of radiation patterns comprises of whole angle on an azimuth plane of the antenna. This improvement improves the performance of telecommunication system that requires transmitting and receiving signals from all directions. In a mobile base station, for example, the signal transmissions are expected from all direction thus a good reconfigurable radiation pattern antenna covering the whole plane is desired.

The complexity of the reconfigurable antenna design has also brought to more in-depth studies on the miniaturization techniques. Modern communication technology demanded a low cost and compact design to be fitted in the wireless devices. Most of the reconfigurable antennas available these days have a drawback of complicated design which is problematical to be applied into communication devices. The experiment is carried out to attain a design of low profile pattern reconfigurable antenna with least shortfall in the antenna performance.

During the completion of this research, the author has successfully published:

1. Nur Ab Aziz, Alaa H.Radhi and R. Nilavalan, "A reconfigurable radiation pattern annular slot antenna," Loughborough Antenna and Propagation Conference, Loughborough, 2016 (IEEE Conference).

2. Nur Farahwahida Ab Aziz ; R. Nilavalan, "Pattern reconfigurable using half-wave dipole antenna," International Workshop on Electromagnetics: Applications and Student Innovation Competition, London, 2017 (IEEE Conference).

1.6 Scope of Thesis

The arrangement of this thesis is conducted as follow. The first part of the thesis is on the general knowledge of an antenna. Different type of antenna and all the important parameters for an antenna is described briefly. The following chapter described various types of reconfigurable antennas available in the present days. Different techniques in attempting the frequency, radiation pattern and Polarisation reconfigurable antennas are described concisely in this chapter. Different methods to do an analysis on antenna are also included in this chapter.

Chapter 3 discussed the construction of a patch antenna with an omnidirectional radiation pattern. The miniaturisation of the antenna has also been discussed here. The construction of radiation pattern reconfigurable antenna is described comprehensively in chapter 4. The principle of operation to achieve variation in radiation pattern is justified in the former part of the chapter followed by the simulation and experiment results from the measurement. The miniaturisation of the reconfigurable antenna is conducted in chapter 5 of this thesis. The principle behind the operation is explained briefly and the proposed antenna is simulated using HFSS. Then, the proposed antenna is fabricated and put under test. The comparison results from simulation and experiment are presented comprehensively in this chapter.

Chapter 2 Reconfigurable antennas

2.1 Introduction

Reconfigurable antenna is fast becoming a key instrument in communication technology nowadays. Modern wireless communication devices require an antenna with a capability to work in more than one operational mode in a single structure. Thus, reconfigurable antennas are designed to resolve the problem as well as offer new capabilities to adapt in future wireless applications. In this chapter, the history of reconfigurable antenna is discussed in detail. Different types of reconfigurable antenna, such as frequency reconfigurable, pattern reconfigurable, and polarisation reconfigurable are presented in Section 2.2. In Section 2.3, multiple techniques in attaining reconfigurable characteristic are discussed and studied closely. The example for each technique is also presented in this section. The analysis of antenna performance can be conducted through various ways. The analysis method for antenna performance is discussed briefly in Section 2.4, which contributes to the introduction of Ansys HFSS. Ansys HFSS is applied vastly in the development of the antenna design in this study. The advantages of using the software are all presented in Section 2.5.

2.2 Type of reconfigurable antenna

There are three types of reconfigurable antenna; frequency, polarisation and pattern reconfigurable antenna which will be discussed thoroughly in this chapter. In addition, due to rapid development in communication technology, an antenna that can achieve a combination of two or more reconfiguration characteristics in one structure is developed.

2.2.1 Frequency reconfigurable antenna

Frequency reconfigurable antenna has the ability to change its operating frequency without changing the radiation pattern and polarisation characteristic of the antenna. Currently, there are a large number of frequency reconfigurable antenna designs which comes in a wide arrangement of frequency band (broadband) or functioning among multiple frequency bands (multiband). In other words, frequency reconfigurable antenna is put into operation to replace multiple antennas switched into multiple transceivers to cover different frequency ranges, resulted in huge reduction of product size and complexity. The main advantage of reconfigurable antenna is that it provides efficient frequency usage in a limited spectrum with better noise rejection in the unused bands and dynamic spectral allocation. Furthermore, it is useful for reducing the adverse effects such as co-site interference and jamming.

The frequency reconfiguration can be achieved through numerous methods with regards to the extended literature review. The basic method to attain frequency reconfiguration in an antenna is by having variations of current distribution over the antenna geometry. For an instance, frequency reconfigurable antenna can be achieved by controlling the effective length of the radiator[10][11] or meandering with the radiator shape[12][13]. Operating frequency of an antenna is determined mainly from the effective length of the radiator. With the integration of switching system such as RF-MEMS, PIN diodes or varactor diodes, the operating frequency of the antenna can be controlled. The antenna designed in [14] has six PIN diodes to achieve 36 frequency bands (2.35 GHz-3.43 GHz) while maintaining unidirectional radiation patterns. The diodes are positioned such that it controls the electrical length of the radiator. The antenna design uses a simple dc bias and single RF feed line which make it favourable for a small devices application.

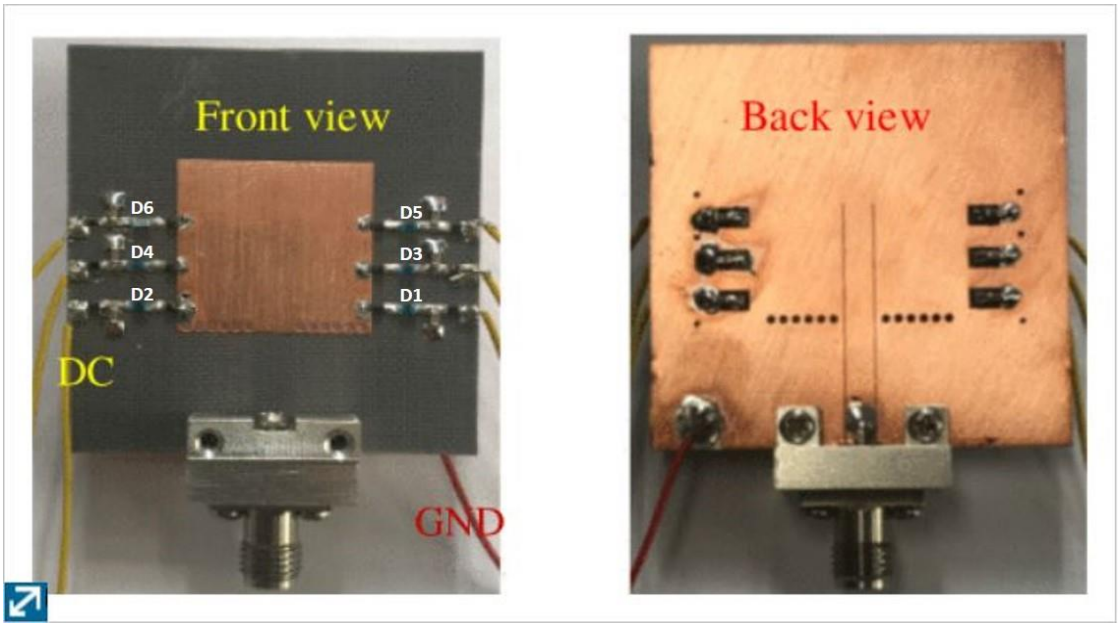

Figure 2.1 Compact frequency reconfigurable antenna with 6 diodes for 36 states of frequency operating bands[15].

Multiband operation in printed antennas can be achieved by introducing slot in the radiating patch. With the insertion of slot into the antenna design, the current patch in the radiator is shifted, hence change the antenna performance. There are relatively a lot of studies on the introduction of slot and the impact on the antenna performance[16][17][18]. In [19], the Vivaldi antenna is designed to have a three-quarter free-space wavelength to cover all the operating frequencies. The manipulation of RF switches will determine the operating frequency band of the antenna. The antenna design provides high isolation by manipulating the length of open-circuit stub of the microstrip feed line.

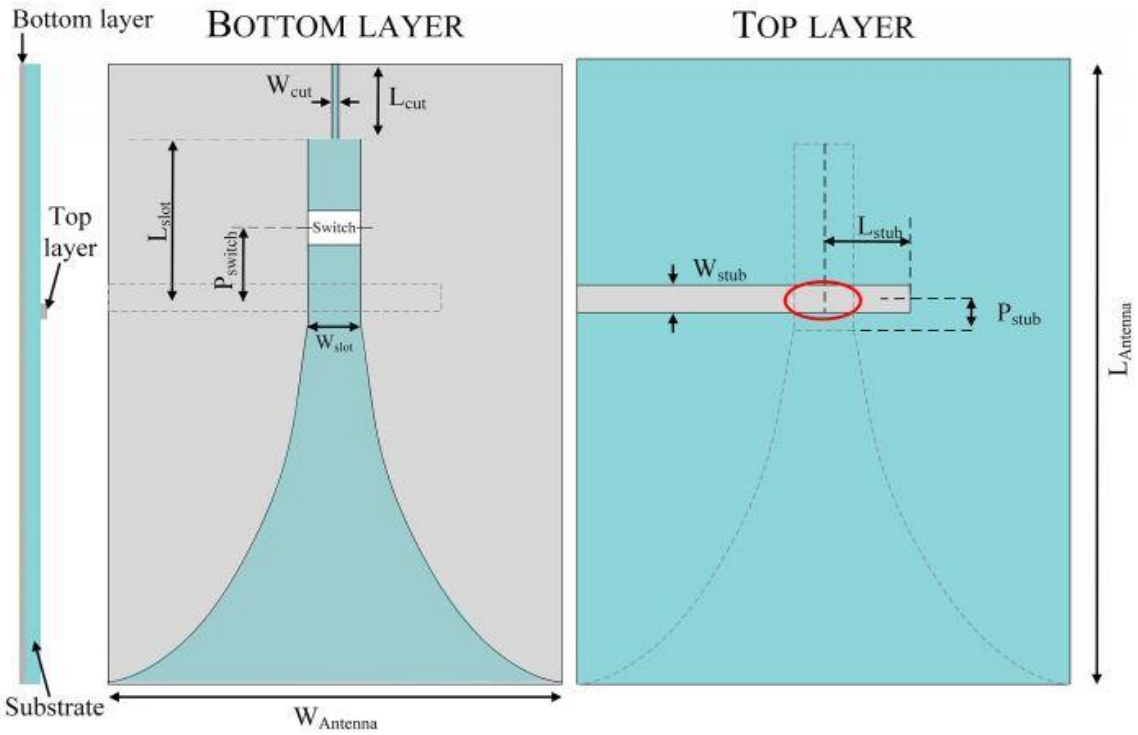

Figure 2.2 The construction of the two-band frequency reconfigurable Vivaldi antenna [10].

Another method for frequency reconfigurable antenna is by applying multilayer substrates design with aperture-coupled feeding technique[20][21][22]. The aperture coupled feeding technique is applied into the antenna design to reduce the spurious radiations generated between the radiating patch and the feed line. The radiating patches are etched on different substrate layers and designed with their respective operating frequency. Switching mechanism, for instance PIN diode is integrated to activate the selected aperture slots to achieve frequency reconfigurability. In another design, varactor diode is introduced to allow for a continuous dual frequency-tunable characteristic[23]. Also, with the increased number of sub layers, the antenna array provides better isolation and the integration of the switches is less complicated compared to single substrate design. The stacked reconfigurable antenna fed by aperture-coupled feeding technique also has improved gain and bandwidth performance.

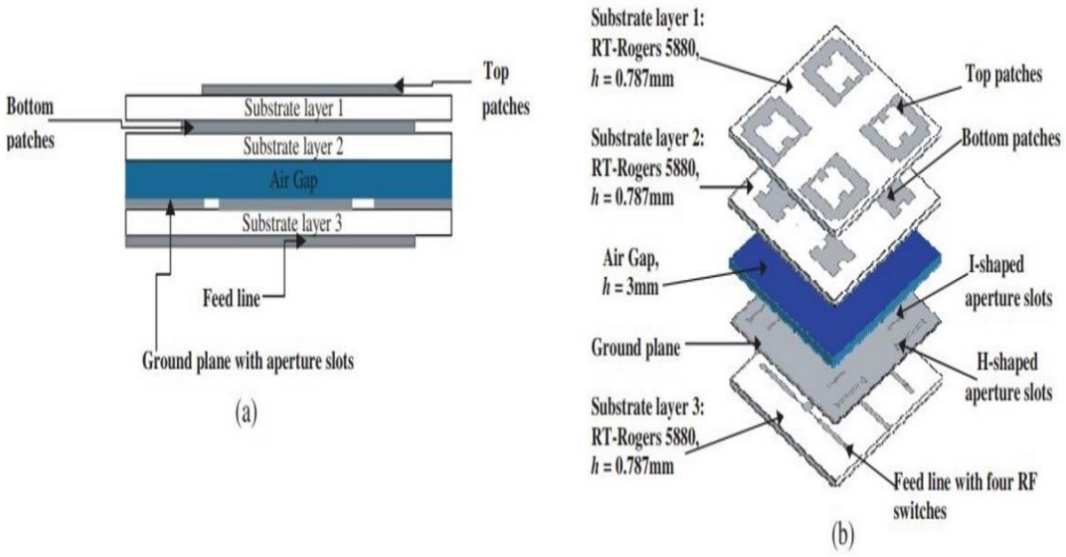

Figure 2.3 Geometry of frequency reconfigurable stacked patch antenna fed by aperture-coupled feeding technique (a) side view and (b) 3D view [13].

2.2.2 Radiation pattern reconfigurable antenna

Another category of reconfigurable antenna is radiation pattern reconfigurable antenna, where the antenna has the capability of changing the shape of radiation pattern and steer the direction of radiation to maximise the antenna gain while maintaining the frequency and polarisation of the antenna. Pattern reconfigurable antenna can provide diversity in the radiation pattern which leads to an increase of the number of users in wireless communication system without increasing the number of array elements[24]. Furthermore, the overall performance of modern wireless communication system is greatly improved as the antennas can be used to avoid inter-user interference, improve security as well as saving energy by directing the signal to the right direction[25].

There is a growing body of literature that recognizes the importance of radiation pattern reconfigurable antenna, such as in [26] and [27]. Generally, the radiation pattern can be changed in two different ways subjected to system requirements: 1) shifting the main beam while maintain the beam shape or 2) shifting the main beam while changing the beam shape. The microstrip Yagi-Uda antenna design in [28] is a good example of the first case. The peak beam direction of the planar Yagi-Uda antenna switched in opposite direction (±180˚) while maintaining the beam shape and matching bandwidths at a fixed operating frequency. The maximum gain of the antenna is not significant; however more focus is given to the front-to-back ratio. For the latter case, a simple

configuration of pattern reconfiguration antenna with three switches that control the radiation pattern from omnidirectional to directional pattern is presented in [29] [30].

A number of techniques have been developed to obtain radiation pattern reconfiguration characteristic. One of them is by inserting parasitic structures, such as reflector and director into the antenna design. A monopole antenna in [30][31][32] and Yagi antenna[33] attained multiple radiation pattern by the manipulation of switches which connect the antenna to either director or reflector to improve the gain. In [30], a quarter-wavelength monopole antenna mounted on an octagonal copper board and connected through switches to eight concentric parasitic elements. The parasitic element behaves as director and reflector with the manipulation of switches to give three different configurations. Another means of improving the gain in the right direction and reducing interference gain in the other direction is shown in [34]. The gain and front-to-back ratio of the antenna design is improved significantly from 4.5 to 8.2 dB when reconfigurable artificial structures (RASs) are loaded on Vivaldi shape slot antenna. The antenna has a windmill-shaped reconfigurable feeding network with four switches embedded which gives four end-fire patterns on azimuth plane.

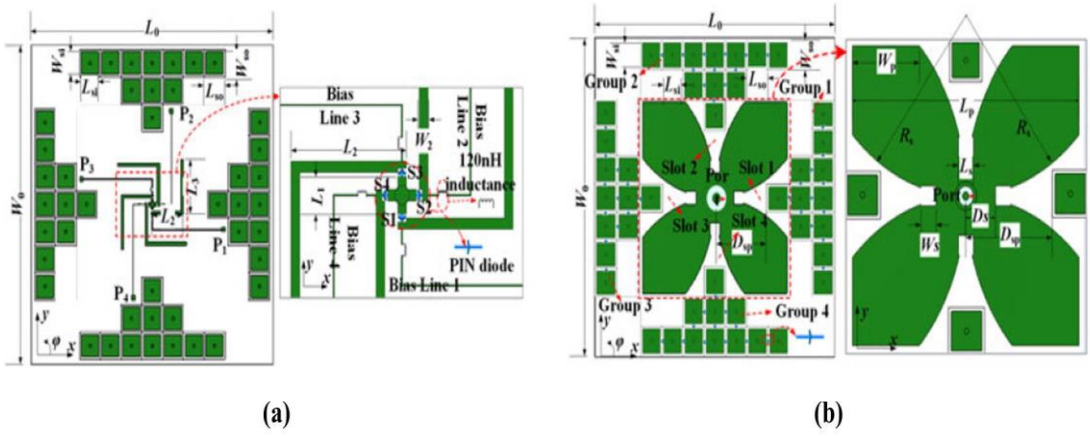

Figure 2.4 The construction of Vivaldi antenna with improved gain (a)top layer and (b)bottom layer [25].

Radiation pattern agility characteristics can also be obtained through the adaptation of element shifting; i.e. reflector and director, or through implementation of different phase of signal in array of antennas. There are quite a numbers of academic journals wrote on the subject of using phased array for pattern reconfigurable antennas, which are fed by equal amplitude and proper phase signals [35][36][37]. Feeding network of the antenna could be a cascade of power dividers and phase shifters. The orientation of the radiated beam depends on the phase shifter values. As proposed in

[38], the output of the feed network made by three Wilkinson power dividers controls the two modes of operation for the antenna. When one mode is selected, the outputs from feed network are of equal magnitude and phase, thus conical pattern of a monopole antenna is produced. When another mode is selected, the outputs from feed network are equal but a 90° phase difference is introduced which leads to broadside beam radiation pattern.

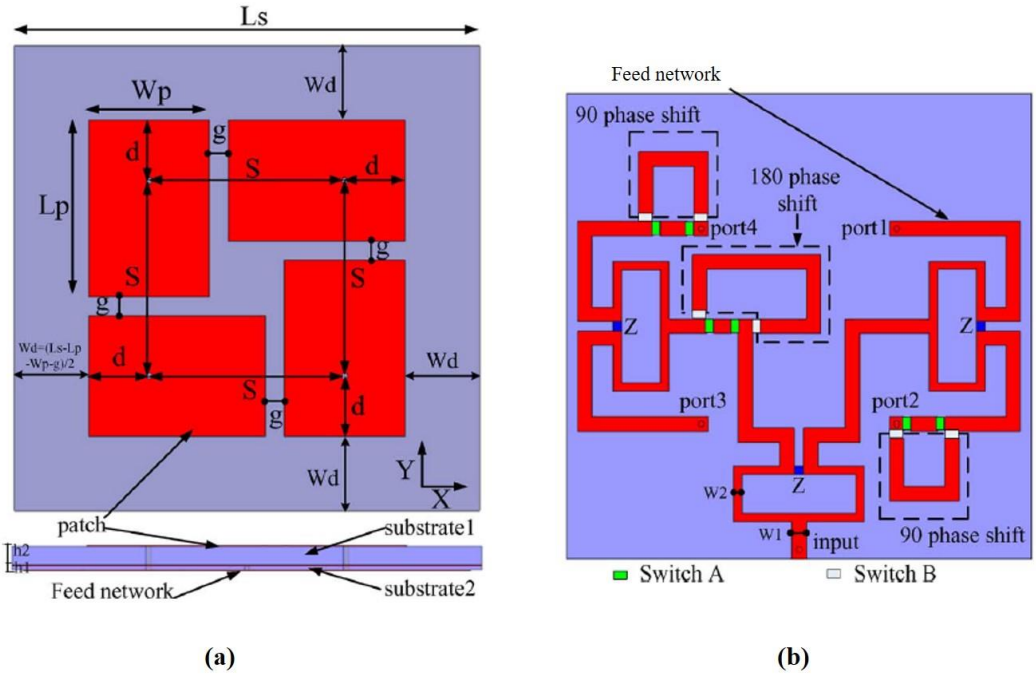

Figure 2.5 Geometry of pattern reconfigurable antenna (a) four radiating patches and (b) feed network made by three Wilkinson power dividers[38]**.**

2.2.3 Polarisation reconfigurable antenna

Polarisation reconfigurable antenna is another type of reconfigurable antenna where the antenna has the capability to change its polarisation while maintaining its frequency and pattern characteristics. Polarisation refers to the electric field vector as a function of time. The polarisation will also determine the orientation of the antenna. Therefore, it is most important that the polarisation of transmitter and receiver to have the same polarisation to avoid loss of signal. There are three forms of polarisation: linear, circular and elliptic. Polarisation reconfigurable antenna has the advantage of expending the capability of communication systems and reduce fading loss causes by multipath effects[38]. Furthermore, antenna designs with polarisation diversity can be used to filter in-band interference[39] and increase channel capacity[40].

Extensive research has been conducted on antenna with polarisation agility techniques. A good example of polarisation reconfigurable antenna is by using annular ring slot as its circular polarisation can be easily reconfigured by loading different kinds of perturbation slots[41] or coupling strips (feeding lines) across the ring slot[42][43]. Due to extensive number of research, there are many antenna designs that have been successfully reconfigured to switch between a left-handed circularly polarized (LHCP) and right-handed circularly polarized (RHCP) using slot antennas. Monopole antenna [44] and patch antenna[45][46] have also offered a simple and low cost design for polarisation reconfigurable antenna. By adding two wide strips with specific distance from the top of the ground plane, the monopole antenna[44] can switch from linear polarisation to RHCP or LHCP using two PIN diodes. The wide strips are connected using two PIN diodes for different configurations. When none of the PIN diode is activated, the horizontal induced surface current on the ground plane and the strips will cancel each other and leave behind only the vertical surface current on monopole arm and ground plane. The antenna will have a linear polarisation. When one of the PIN diode is activated, the surface current on the ground plane and the strips are rearranged, resulted in horizontal component for either LHCP or RHCP. This antenna offers a less complex design by reducing number of diodes employed in the radiating element.

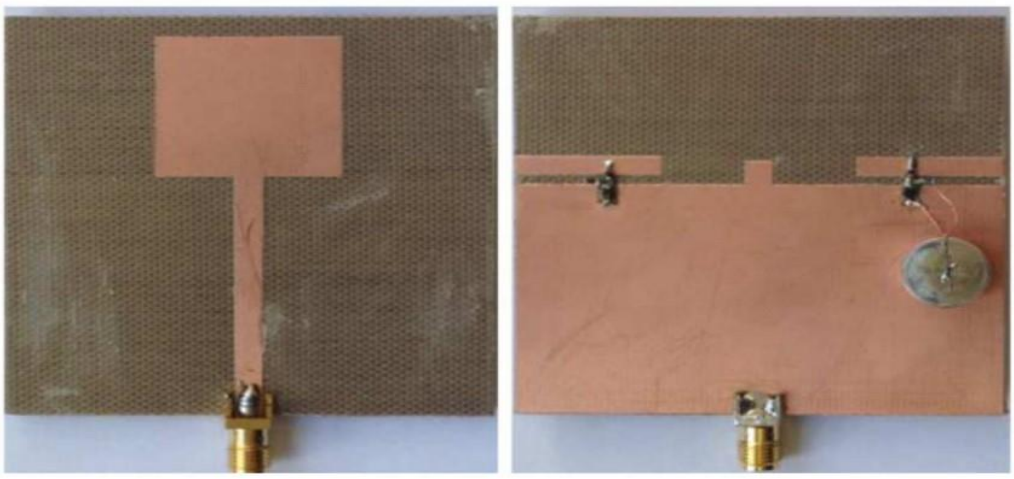

Figure 2.6 Polarisation reconfigurable antenna using monopole antenna (a)front view and (b)back view[44].

2.2.4 Combination of any reconfiguration characteristics

Along with the rapid development in communication technology, more antenna design has been developed which incorporated two or three reconfigurable characteristics to fulfil the demand. In a recent research paper by [47], the frequency and radiation pattern of the circular array antenna can be altered without adapting a switching mechanism into the design. The antenna features a power divider and eight horn antenna elements with respective band stop filters uniformly distributed around the circular ground plane. A directional radiation pattern can be generated at a particular frequency by controlling the band notch filters and the frequency is controlled by voltage applied to the varactor inside the filters. When none of the filters are activated, an omnidirectional radiation pattern on azimuth plane is produced. The antenna design successfully operating between 0.8 to 3 GHz with six different modes including omnidirectional radiation pattern. However, in this paper, the element is disconnected to represent when the filter is not activated.

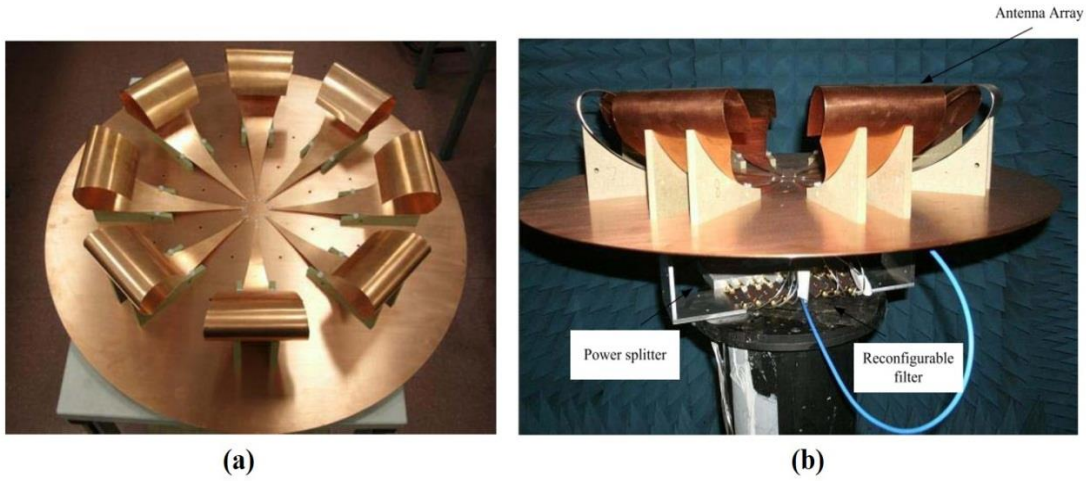

Figure 2.7 The arrangement of frequency and radiation pattern reconfigurable antenna (a)circular array antenna and (b)the whole antenna system[35].

Following high demand for low profile reconfigurable antenna, another antenna design with frequency reconfigurability and radiation pattern characteristics has been proposed in [48][49][50]. The antenna in [48] operates in three frequency bands, depending on the length of the slot with the manipulation of two switches. The introduction of four slits in the ground plane of the slot antenna held many functions in the antenna design. Not only it serves as biasing circuit, it is also exploited to attain reconfigurability in radiation pattern of the antenna. Each slit is installed with three

switches to control the length as well as terminating it in each different configuration. In this design, the radiation pattern emitted is independent of the frequency band. By switching the upper and bottom part of the slits, the beam angle can be shifted into +15˚, 0˚ and -15˚. Even though the antenna has a high efficiency in all frequency bands, the shifted angle introduced by the slits is not major and restricted on one direction only despite of the four slits fitted on the design.

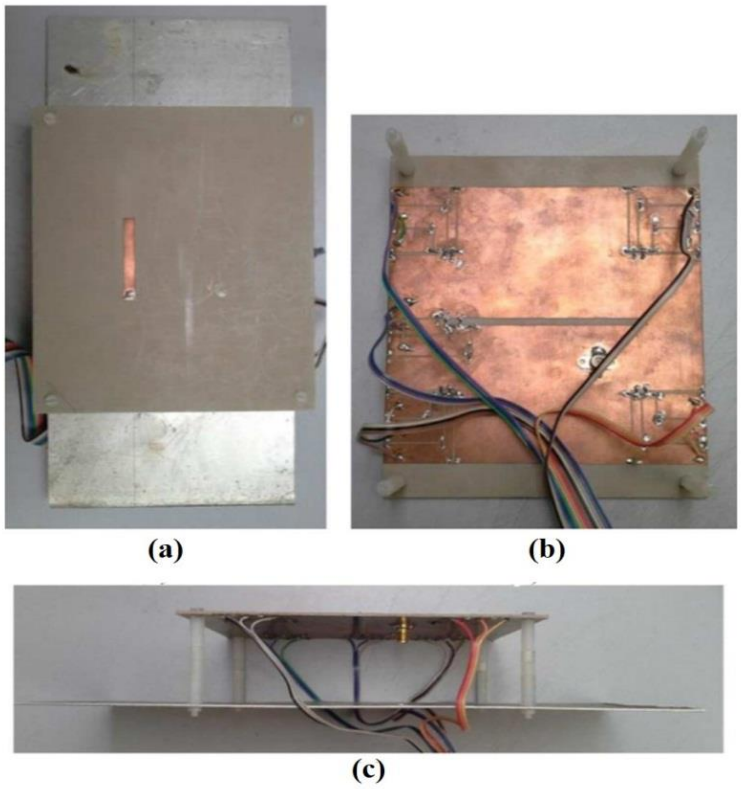

Figure 2.8 The construction of slot antenna with freqeuncy and pattern reconfigurable characteristics (a)front view, (b)back view and (c)side view[48].

2.3 Different techniques for reconfigurability

In general, the techniques to attain reconfigurable antenna designs can be grouped into electrical, optical, physical and also through material change. By applying switching mechanism using electrical and optical controls, different arrangement of reconfigurable antennas can be achieved. The physical and material change is rarely used, but still efficient in antenna design.

2.3.1 Electrical

There are extended literature research has been conducted on reconfigurable antennas by the adaptation of electronic switches such as PIN diodes, varactor and radio frequency microelectromechanical (RF-MEMS) switches. The frequency, pattern and polarisation agility characteristic of an antenna can be achieved by basically controlling the current distribution in the antenna with manipulation of the switches.

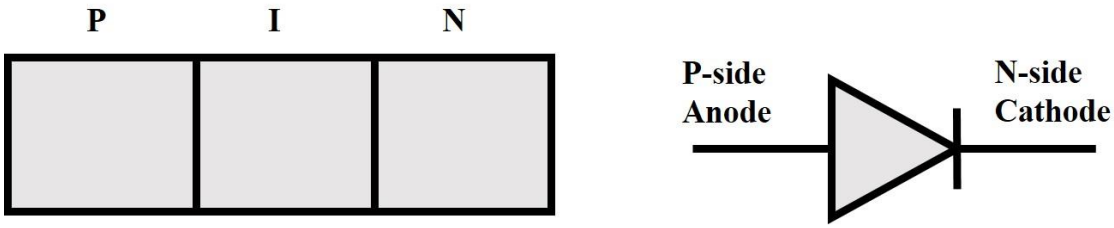

Figure 2.9 The construction of PIN diode.

Over the past decade, most research in reconfigurable antenna has emphasized the use of PIN diodes to attain diversity in radiation pattern[51][52] and frequency[53][54]. PIN diodes has been widely used in numbers of design due to its fast response, low resistance at high frequency and less susceptible to electrostatic discharge damage[55][56]. PIN diode has a heavily doped p-type and n-type regions, which are separated by a wide, lightly-doped intrinsic region as shown in the figure above. Forward biasing a PIN diode creates a very low resistance at high frequencies which constitute when the switch is ON, while reverse biasing results in an open circuit or OFF mode. Figure 2.10 shows an equivalent circuit of PIN diode during ON and OFF state. The advantage of PIN diode is that it can handle high current using much smaller levels of control power[57].

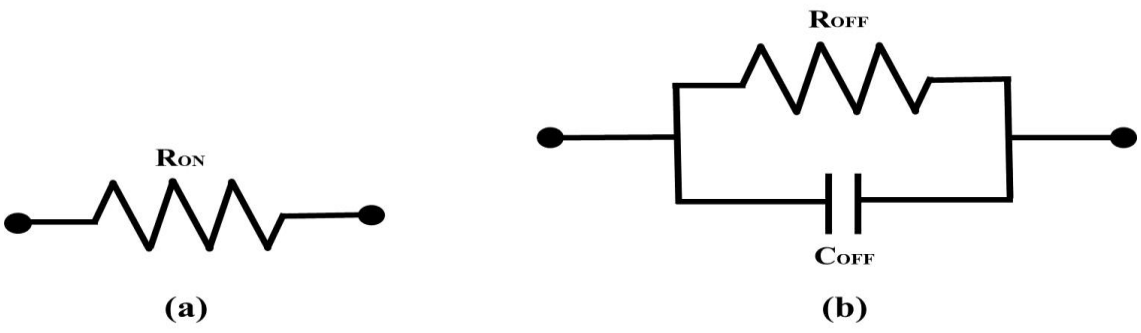

Figure 2.10 Equivalent circuit of PIN diode switch (a) ON state and (b) OFF state.

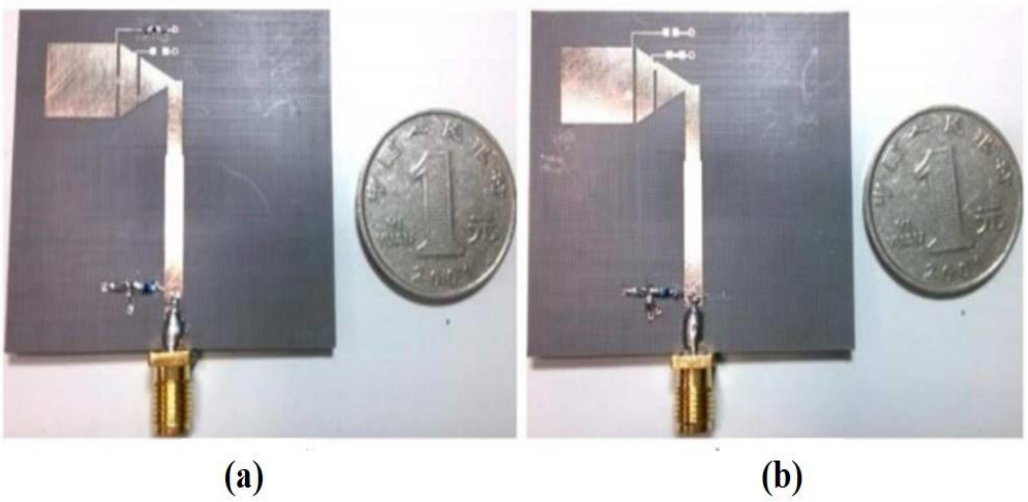

Figure 2.11 Bow-tie antena with multiband frequency using PIN diodes at (a)2.4 GHz and (b) 3.5 GHz [53].

Another popular RF switches is MEMS, which use mechanical movement to achieve a short circuit or an open circuit in RF transmission line. The forces required for the mechanical movement can be obtained using the electrostatic, magneto static, piezoelectric or thermal designs[58] according to their actuation mechanism. RF-MEMS component has been applied as switches to reconfigure the radiation pattern[59][60], polarisation[61] and engage in multi-frequency application[62][63][64]. A functional multiband frequency with pattern and polarisation diversity system using MEMS switches is demonstrated in [65] to study the feasibility and impact of real MEMS switches during operation. Some tricky part of MEMS switches is due to the contact stiction [66] and the problematical protective package of the switch[67]. However, the switch has the advantage of low power consumption and low insertion loss with high isolation, but then again, it has a limited power handling capability and high-priced. Also, MEMS switches require high voltage for dc biasing and has slow speed switching compared to PIN diodes.

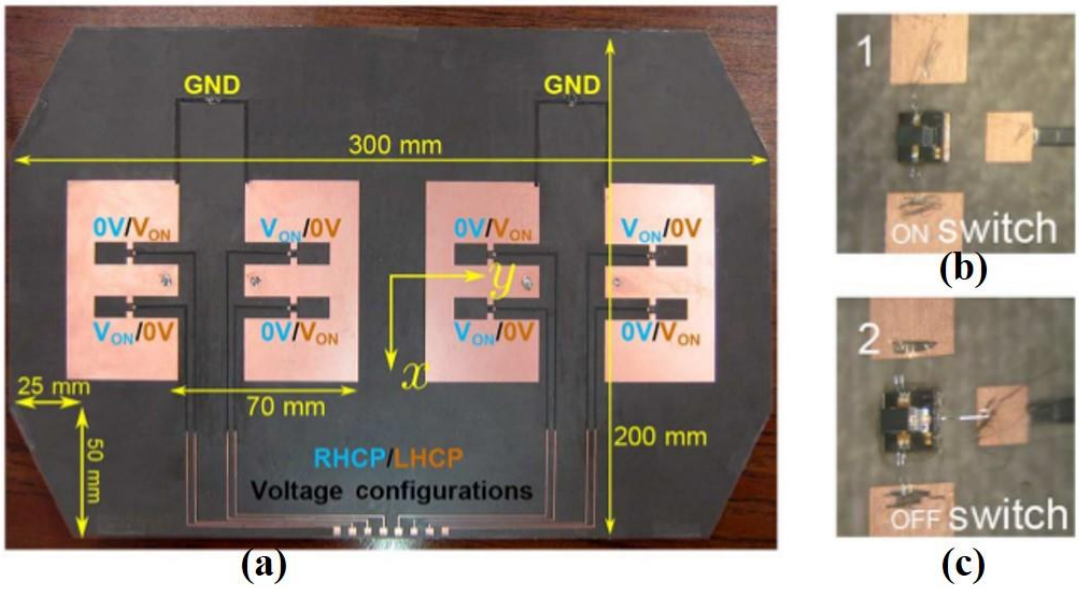

Figure 2.12 Polarisation reconfigurable E-shaped patch antenna using MEMS switches (a)top view, (b)MEMS switch ON state and (c)MEMS switch OFF state[59].

In overall, these two types of switching is bi-static switch, which does not allow for a continuous switching. Varactor has been effectively adopted in [68][33] to achieve a continuous frequency and null pattern scanning. Varactor consists of a small junction capacitance with varied voltage. The capacitance change when different bias voltage is applied to the diode. The capacitance of a varactor decreases when the voltage gets larger. A tuning varactor can be represented by the electrical equivalent circuit shown in Figure 2.13. However, varactor suffers from poor linearity[3].

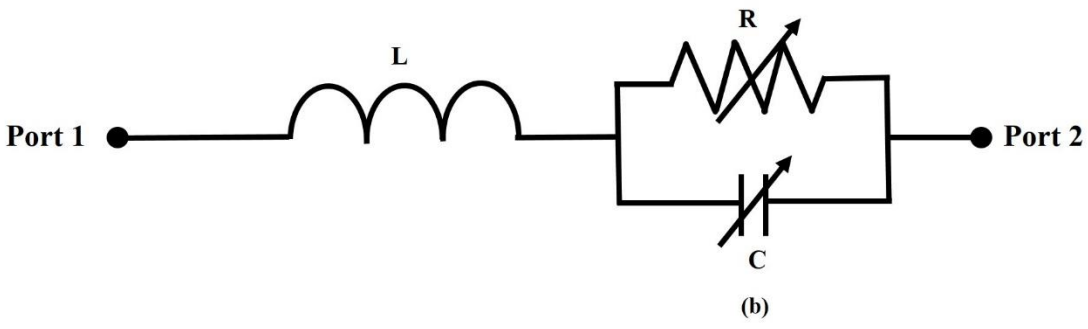

Figure 2.13 Electrical circuit of varactor diode.

2.3.2 Optical

Optical control has been employed as a switching mechanism for reconfigurable antenna design. The fundamental construction of optical control switch has been based on the manipulation of the electrons capability to move from valence band to conduction band when appropriately lit by certain wavelength of light. In other words, the optical switch will be activated when light of pertinent wavelength from a laser diode is given. The major advantage of using optically driven switches is that it eradicates the need of metallic biasing line which leads to interference in radiation pattern.

The solution was then assayed for the frequency reconfiguration using optically control switch method as shown in [69]. By using three optical switches, the coplanar fed microstrip antenna is working on three different frequency bands: WiMAX (3.5 GHz), WLAN (5.5 GHz) and X-band satellite communication (8.4 GHz). In [70], two different approaches of optical control are implemented as a switch in a planar antenna design with microstrip radiators to attain pattern reconfiguration. The p-i-n photodetector in the first approach allows a good insertion loss but has a poor isolation, while the second approach using optical illumination of a phototransistor exhibits a low loss, less cost and less affected by the noise in the laser source even though it has a quite complex design compared to the first approach. Thus, it is more favourable for the antenna design. The thermal and electrical isolation from the control circuitry make the photonic switching technique a very attractive solution relative to conventional dc control of lumped elements.

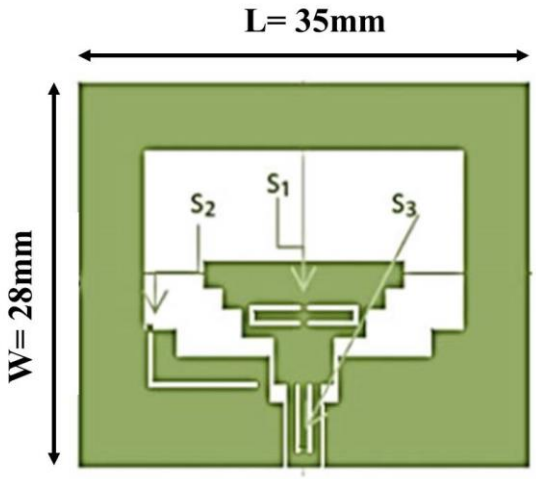

Figure 2.14 Frequency reconfigurable ultra-wideband antenna design using optical switch[69].

2.3.3 Physical

Reconfigurable antenna using physical changes is an alternative to switching mechanism to achieve antenna reconfiguration. Commonly, the technique involves rotors, actuators, or other tools to move some part in the antenna structure to change the electrical properties of the antenna. Using this alternative configuration, even though the speed is definitely slower than any switching component, but it is enough for most application. The importance of this technique is that it does not rely on any switching mechanisms, biasing lines, or optical fibre/laser diode integration. On the other hand, this technique depends on the limitation of the device to be physically reconfigured[58].

The antenna in [71] has discussed the operation of the frequency reconfigurable antenna using physical controlled method. The operating frequency of the antenna is shifted by adjusting the degree of spiral tightness. A step motor is installed to control the rolling mechanism in a shielded box below the ground plane. When the metal sheet is rolled, it stretches the radius between outermost and innermost cylinder. The rolled planar antenna introduces a parasitic capacitance due to strong mutual coupling between the adjacent layers and inductance due to the spiral cross section. Changing the configurations of the antenna changes the parasitic capacitances and inductance so that the resonance frequency varied. The antenna has a frequency range of 2.9 to 15 GHz.

The radiation pattern of the antenna maintains an omnidirectional pattern in all frequency bands. The antenna has high efficiency throughout the spectrum and not affected by the dielectric loading of the mechanical parts. A physical control reconfigurable antenna has a robust antenna performance as no RF devices applied in the design. However, higher power handling is possible with high voltage requirements for the turning motor. The slow tuning speed and small reconfiguration capabilities are another setback in the antenna design.

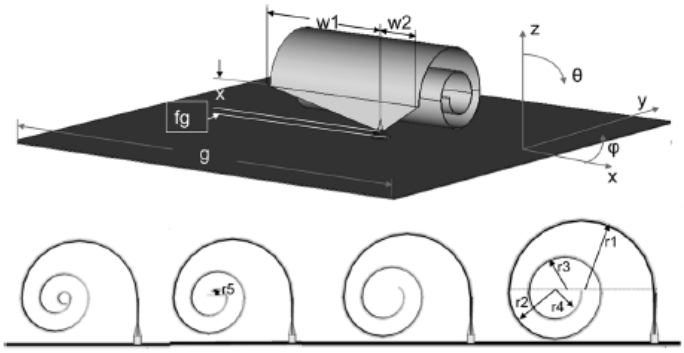

Figure 2.15 Physical control frequency reconfigurable antenna[71].

2.3.4 Material changes

Another method to attain reconfigurable antenna is by adapting specific material properties into the antenna design such as grapheme plasmonics[72][73][74] and liquid crystals[75]. These materials have the ability to change the chemical potential by applying different voltage values. As can be seen in the figure below, when DC bias voltage is applied, the perpendicular orientation of liquid crystal transition into parallel orientation. The BL038 liquid crystal dielectric properties change when in perpendicular and parallel orientation. Thus, varying the DC voltage resulted in varying permittivity of the liquid crystals which can be manipulated in frequency tuning antenna. This design has it drawback since it requires a complicated feeding network for each patch.

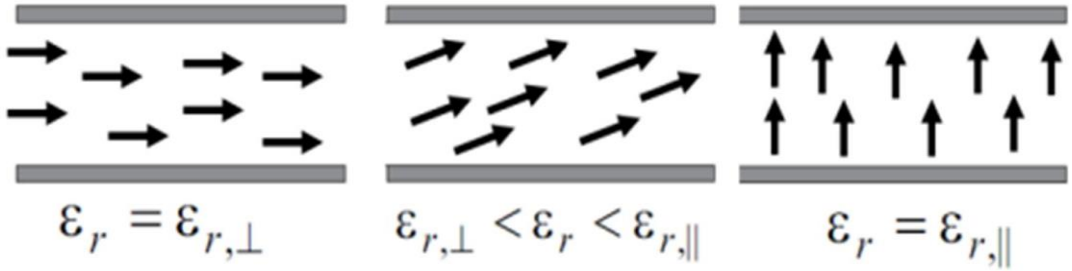

Figure 2.16 Illustration of liquid crystal as bias volatge applied[75].

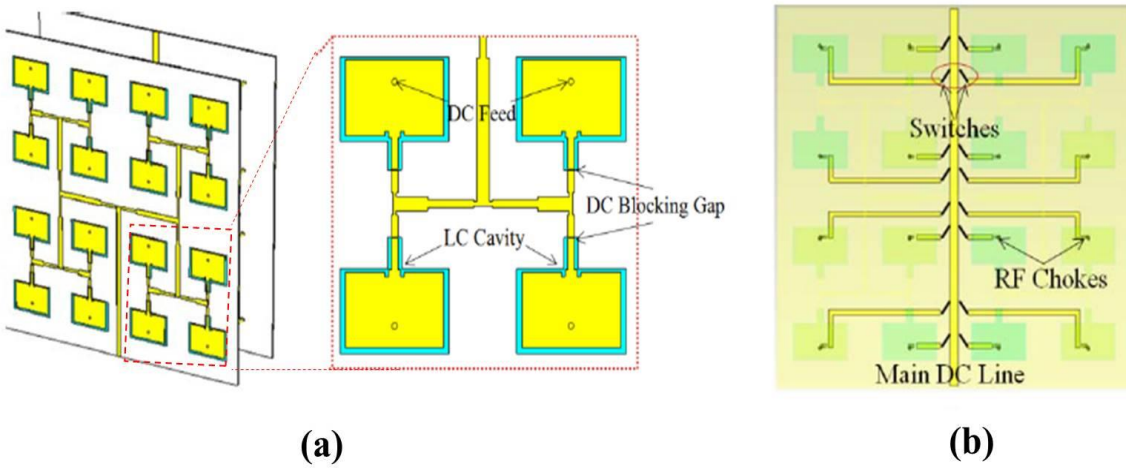

Figure 2.17 Frequency reconfigurable patch array using liquid crystal (a) top section and (b) feeding network in the bottom section[75].

Recently, pattern reconfigurable antenna by using metamaterial-inspired concept[76][77] has received much attention due to their feasible design. Metamaterials are materials engineered to have properties that are not naturally existed. Metamaterials derive their properties not from the properties of the base materials, but from their newly designed structures and appropriately designed metamaterials can affect waves of electromagnetic radiation. An example of antenna design with metamaterial manipulation is shown in beam tilting bow-tie antenna[78] where H-shaped unit-cell metamaterial structure with high refractive index is incorporated into the antenna design.

2.4 Analysis method

There are many method of analysis that has been developed by researchers up to this present day. These methods can be divided into two: 1) Time-domain analysis and 2) Frequency-domain analysis. Based on these two methods, many commercial software have been developed to help in analysis of radio frequency design. In this part of the chapter, the foundation principles for each technique are explained briefly.

2.4.1 Finite Different Time Domain (FDTD)

The Finite Different Time Domain (FDTD) is a widely used method to solve several electromagnetic problems. The literature on FDTD is extensive and has been used in various microwave analysis such as antenna designs, propagation, filter designs and many other microwave analysis. However, the shortcoming of FDTD comes as it is not suitable for electrically huge system but good for system involving pulses. This method did not gain considerable attention despite its usefulness to handle electromagnetic problems until the computing costs become affordable. The FDTD iteratively calculates the field values in the problem space that is discretised into unit cells. Each unit cell is assigned with three orthogonal electric and three orthogonal fields.

2.4.2 Moment of Method (MoM)

The Moment of Method (MoM) is a numerical method of solving electromagnetic problems or volume integral equation in the frequency domain. Numerical Electromagnetic Code (NEC) is the most well-known of the codes using

MoM to solve problems that can be defined as sets of one or more wires. The method is simple and adaptable to the problem. Furthermore, the MoM technique has been widely used to solve electromagnetic scattering and radiation problems based on reducing the operator equations to a system of linear equations written in matrix form. The result from the analysis is accurate as it uses exact equations and provides direct numerical solution for the equations. However, the disadvantage of this technique lies in the large amount of computation it required.

2.4.3 Finite Element Method (FEM)

The finite element method (FEM) is a mathematical technique used for finding approximate solutions of partial equations as well as of integral equations. The solution is based on reducing the differential equations, and then integrated numerically using Euler's method which is a standard technique such as the Runge-Kutta. FEM is a method used to solve frequency domain boundary valued electromagnetic problems using a variation form. There are generally two types of analysis that are used in FEM, which is 2-D and 3-D canonical elements of differing shape. Even though 2-D conserves simplicity and allow itself to be run from a normal computer, the results are less accurate compared to 3-D. The 3-D canonical element gives a more accurate result by working effectively on faster computer. The FEM is often used in frequency domain for computing the frequency distribution in complex, closed regions such as cavities and waveguides.

2.5 Introduction to HFSS

All the experiment and simulation to study the electromagnetic field of an antenna is conducted in ANSYS High Frequency Structural Simulator (HFSS). Ansys HFSS is graphic design software with industry standard for executing accurate and rapid designs in high frequency and high speed electronic devices. It takes some time to become proficient at HFSS including designing the antenna structure with precise dimension and element. HFSS plays a great role in analysing all the important parameters in antenna, such as antenna gain, bandwidth, radiation pattern, and reflection coefficient of an antenna. In this design, only cavity model and full-wave analysis can be conducted appropriately. High Frequency Simulation Software (HFSS) is used to conduct the full-wave analysis by solving Maxwell's Equation.

2.6 Summary

Reconfigurable antennas can be divided into three categories: frequency, radiation pattern and polarisation. With the rapid growth of telecommunication technology nowadays, there are antenna designs that combine more than one category of reconfigurable antenna to feed users demand. Various techniques have been discovered to attain the idea, i.e. electrically, optically, physically and using material change. Different methods indicated different end results. Some are simple, but causes more loss to the signal, while others have low-priced but very complicated design.

Chapter 3 Patch antenna with an omnidirectional radiation pattern.

3.1 Introduction

At present, there is a high demand for antennas that have the capability of transmitting and receiving signal in all directions, covering 360° on a single plane. The uniform coverage of omnidirectional antennas makes it widely applied for wireless devices like cellular telephone and wireless routers. Thus, it is crucial to design a compact size omnidirectional antenna to combat the hidden node problem due to improper use of directional antennas for a low frequency application. In the first part of this chapter, the construction of standard conventional patch antenna is presented. The dimension and performance of patch antenna are discussed concisely in Section 3.2. The primary objective of this part of the thesis is to design an antenna with omnidirectional radiation pattern at low frequency, precisely at 1 GHz. It is achieved by using air as a substrate, but with a cost of significant dimension of antenna design. The proposed antenna is designed in HFSS with a suspended ground plane to obtain omnidirectional radiation pattern and shorting pin is introduced to reduce the total size of the patch antenna. The proposed antenna design is explained in details in Section 3.3 and all the analysis is conducted thoroughly. The affecting parameters in the antenna construction are investigated and discussed in Section 3.4 of this chapter. The proposed antenna is fabricated and measurements on the antenna characteristics are conducted. The measurement result is compared with the simulation result. All the detailed results are presented in Section 3.5.

3.2 Patch antenna

Nowadays, modern communication system requires a cost-efficient, compact size, easy to install and a good performance antenna to complement with rapid development in mobile radio and wireless communication. Patch antenna has emerged as a practical solution to the problem. Patch antenna offers small size, light weight and low profile design, with less cost and less complicated to fabricate using modern printed-circuit technology[79]. Furthermore, the antenna design is versatile as the frequency, radiation pattern, polarisation and impedance of the antenna can be controlled by adding different loads between the patch and ground plane.

By using cavity model for an antenna operated in dominant mode, the patch and ground plane are treated as perfect electric conductors on top and bottom of the cavity with cylindrical perfect magnetic conductor set as a boundary for the cavity[80]. Rectangular microstrip antenna design tends to be more concerned with the width to length ratio in determining the operating mode whereas in circular patch design, the key parameter of the model lies in the radius of the radiating patch. A design procedure for the circular patch antenna is set off by specifying the resonant frequency (f_r), the dielectric constant (ϵ_r) and height of the substrate (h). In this dissertation, the frequency of operation for the circular patch antenna is set at a frequency of 1 GHz to demonstrate the size of patch antenna at low operating frequency. The circular patch antenna is printed on an FR4 substrate with the dielectric constant of 4.4 and height is set at 1.6 mm. It should be noted that throughout this thesis, the term standard patch antenna is used to describe a conventional quarter-wave circular patch antenna.

By referring to A.Balanis [5] in his book, the actual radius, α of the radiating patch of a circular patch antenna operating in dominant mode with very small substrate height (h<<λ_0) can be written as

$$\alpha = \frac{F}{\left\{1 + \frac{2h}{\pi\epsilon_r F}\left[\ln\left(\frac{\pi F}{2h}\right) + 1.7726\right]\right\}^{1/2}} \quad (3.1)\ [5]$$

where

$$F = \frac{8.791 \times 10^9}{f_r \sqrt{\epsilon_r}} \quad (3.2)$$

α : Actual radius of radiating patch
f_r : Resonant frequency
ϵ_r : Dielectric constant
h : Height of the substrate

Take note that all the calculations are in cm. Fringing effect causes the patch antenna electrically larger than its physical dimension. Equation (3.1) does not take into account the fringing effect. Thus, the effective radius of patch taken into account the fringing effect is given by

$$\alpha_{eff} = \alpha\left\{1 + \frac{2h}{\pi\epsilon_r \alpha}\left[\ln\left(\frac{\pi\alpha}{2h}\right) + 1.7726\right]\right\}^{1/2} \quad (3.3)[5]$$

α_{eff} : Radius of radiating patch with Fringing effect
α : Actual radius of radiating patch
f_r : Resonant frequency
ϵ_r : Dielectric constant
h : Height of the substrate

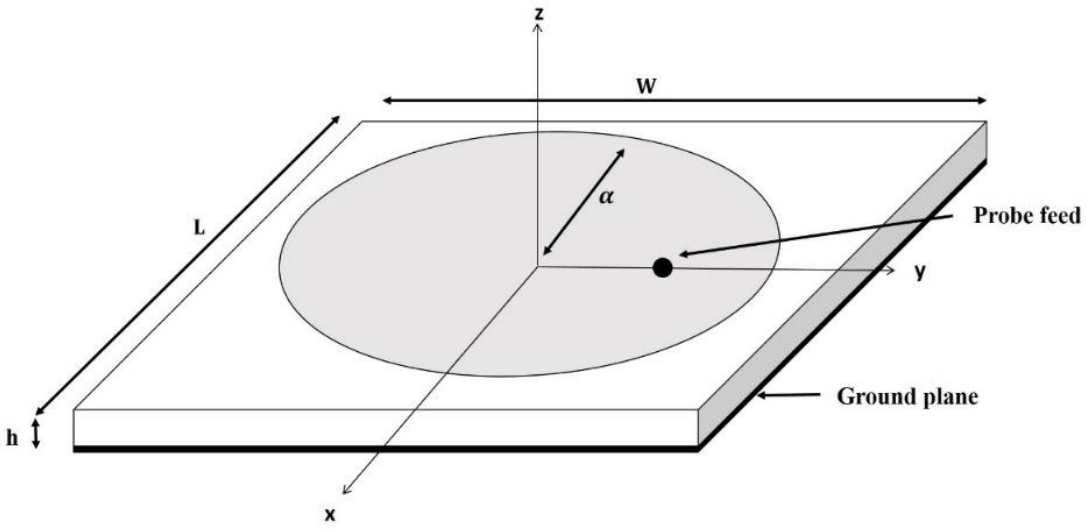

Figure 3.1 Conventional circular patch antenna.

The metal conductor is printed on one side of FR 4 substrate and the ground plane is printed on the other side of the substrate. A standard patch antenna has a configuration as shown in Figure 3.1. The specific dimension of the standard patch antenna is tabulated in Table 3.1 below. The ground plane length and width is given such that it should be greater than radiating patch by at least two or three times of substrate height, h for proper operation[81].

The calculation of antenna dimension as given in (3.1) has resulted in a standard patch antenna with frequency resonance at 1 GHz. The radiation pattern of the standard circular patch antenna is directional with low-level gain due to the surface wave losses in the dielectric substrate. In this study, an omnidirectional radiation pattern with appropriate gain level is anticipated. The omnidirectional radiation pattern is desirable as it permits the antenna to receive or transmit signals for any arbitrary angle over a full plane. The poor radiation performance can be improved by eliminating the surface wave losses in the dielectric substrate. For this purpose, air is used as substrate in the antenna design. The two resonators are separated by air with a specific distance resulted in omnidirectional radiation pattern with acceptable gain level. The distance between the ground plane and radiating patch is optimised using optimisation function in HFSS as well. Then again, the dimension of the antenna is modified and the optimal position for feeding point is located using parametric analysis so that the antenna has the best matching at 1 GHz. The detail dimensions and comparison for both circular patch with air substrate and standard patch antenna printed on FR 4 substrate are shown in Table 3.1.

Parameters	Patch antenna with FR 4 substrate (mm)	Patch antenna with air substrate (mm)
α_{eff}	41.5	88
L	90	180
W	90	180
h	1.6	3
ϵ_r	4.4	1

Table 3.1 The dimension of conventional patch antenna operating at 1 GHz.

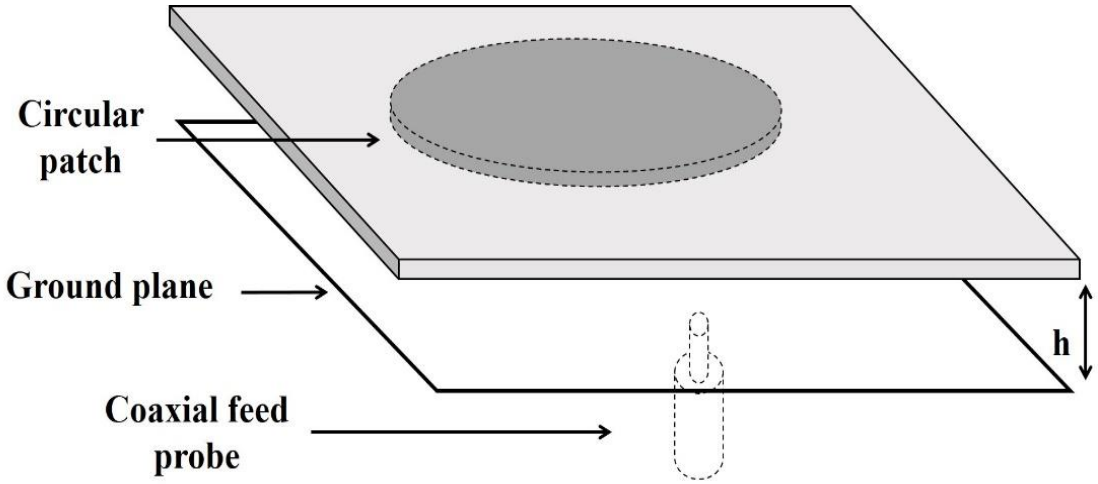

Figure 3.2 Conventional circular patch antenna with air substrate.

The configuration of patch antenna with air substrate is shown in Figure 3.2. The comparison for both antenna frequency responses is given in Figure 3.3. It is clear that both designs are operating at 1 GHz. The low gain level of the radiation pattern for conventional circular patch antenna is improved when using air as a substrate. Furthermore, the omnidirectional pattern from the antenna is crucial for many radio applications, such as point-to-multipoint transmission, radio frequency identification detection or sensing. The best position of feeding point is required to obtain a good impedance match. In both designs, the best location for coaxial feed is determined using adaptive solutions in HFSS software to find low input impedance or good matches between the transmission line and the port[82]. The analysis and simulation step has been done for all the feeding location points on azimuthal plane (X-Y plane).

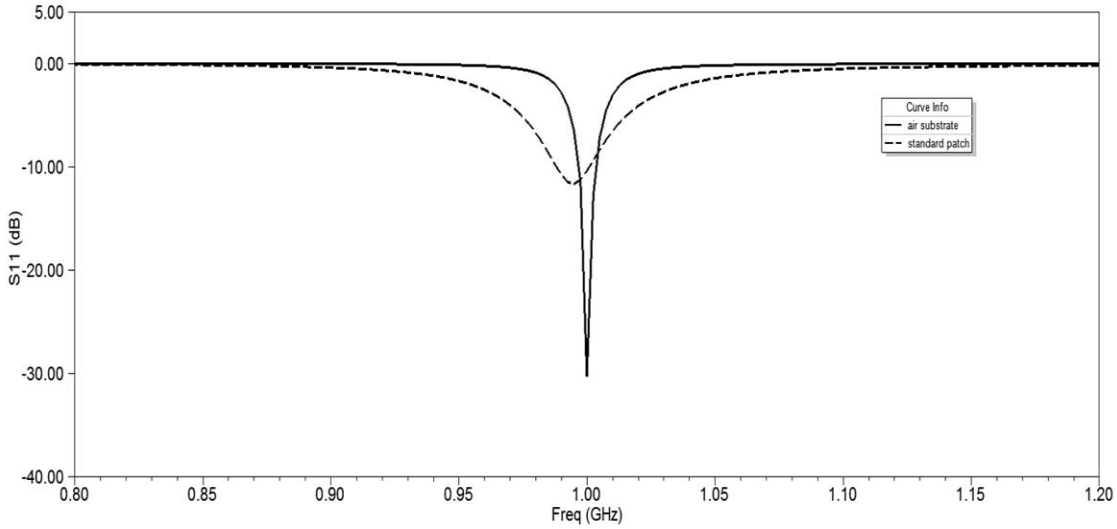

Figure 3.3 Comparison between frequency response of antenna with air substrate and dielectric substrate.

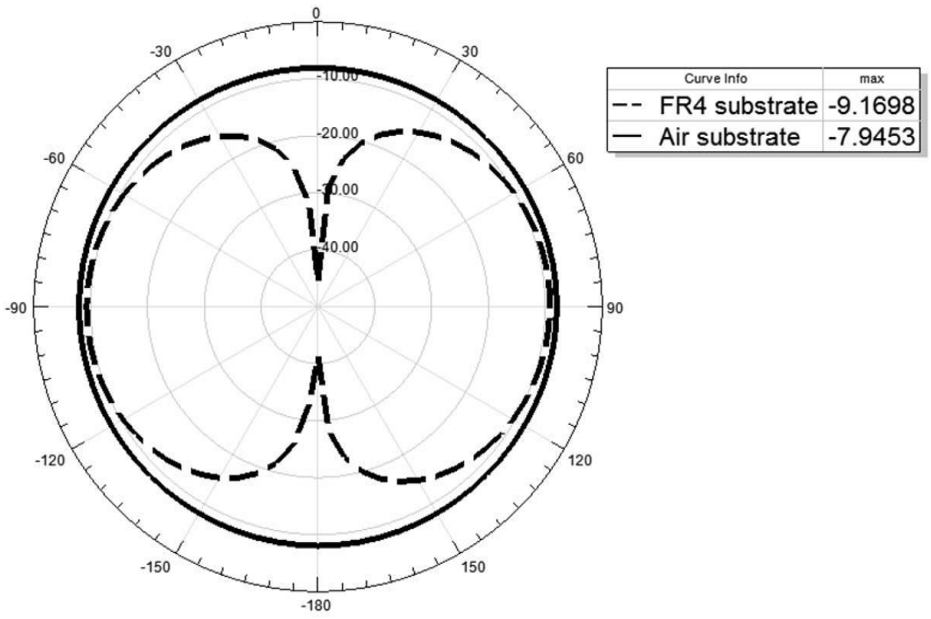

Figure 3.4 Comparison between radiation pattern of antenna with air substrate and dielectric substrate on azimuth plane.

3.3 Shorted circular patch antenna

A primary concern of standard circular patch antenna is the physically large dimension for an antenna operating at low frequency, for instance at 1 GHz frequency. The circular patch antenna design in Part 3.2 resulted in large physical dimension. With the insertion of shorting pin, the antenna dimension is reduced. The shorting pin causes the antenna to excite at lower frequency mode rather than the fundamental mode of the antenna. Using this approach, researchers have been able to reduce the overall length of resonating patch to less than half of free space wavelength[83][84][85].

The design procedure for the shorted circular patch antenna is similar in principle to the standard patch antenna. In the earlier design of microstrip patch antennas[86], the incorporation of shorting pin has been proven to result in electrically small printed antennas for mobile communications handset. The input impedance of the antenna depends on the position shorting pin and feed probe. The circular patch is designed to match for input impedance of 50 Ω at 1 GHz. In the proposed antenna design, fine adjustments were then made on the position of shorting pins with respect to the coaxial feed to achieve 50 Ω resonant. The radius of the radiating patch is also adjusted to give good impedance match and acceptable radiation characteristics. The spacing between the two resonators is increased to reduce the coupling of the probe feed. It should be noted that throughout this thesis, the term shorted patch is used to describe a patch antenna with shorting pins.

The formulation resonant length for shorted rectangular patch antenna is reported in [87], where the length and width of the rectangular are related to the modes index along the patch width. However, the formulation of resonant length for shorted circular patch antenna at any modes is not reported. The fringing field extensions length on a shorted patch is also not reported. Therefore, full-wave analysis on a shorted patch is the most accurate analysis for shorted patch antenna design. The electrical performance of the antenna can be studied using cavity model analysis. However, an analysis performed will be less accurate due to some approximation and assumption made in the calculation. Thus, a full wave analysis to obtain an accurate representation of electrical performance of the antenna is conducted.

3.3.1 Geometry of Circular Patch Antenna

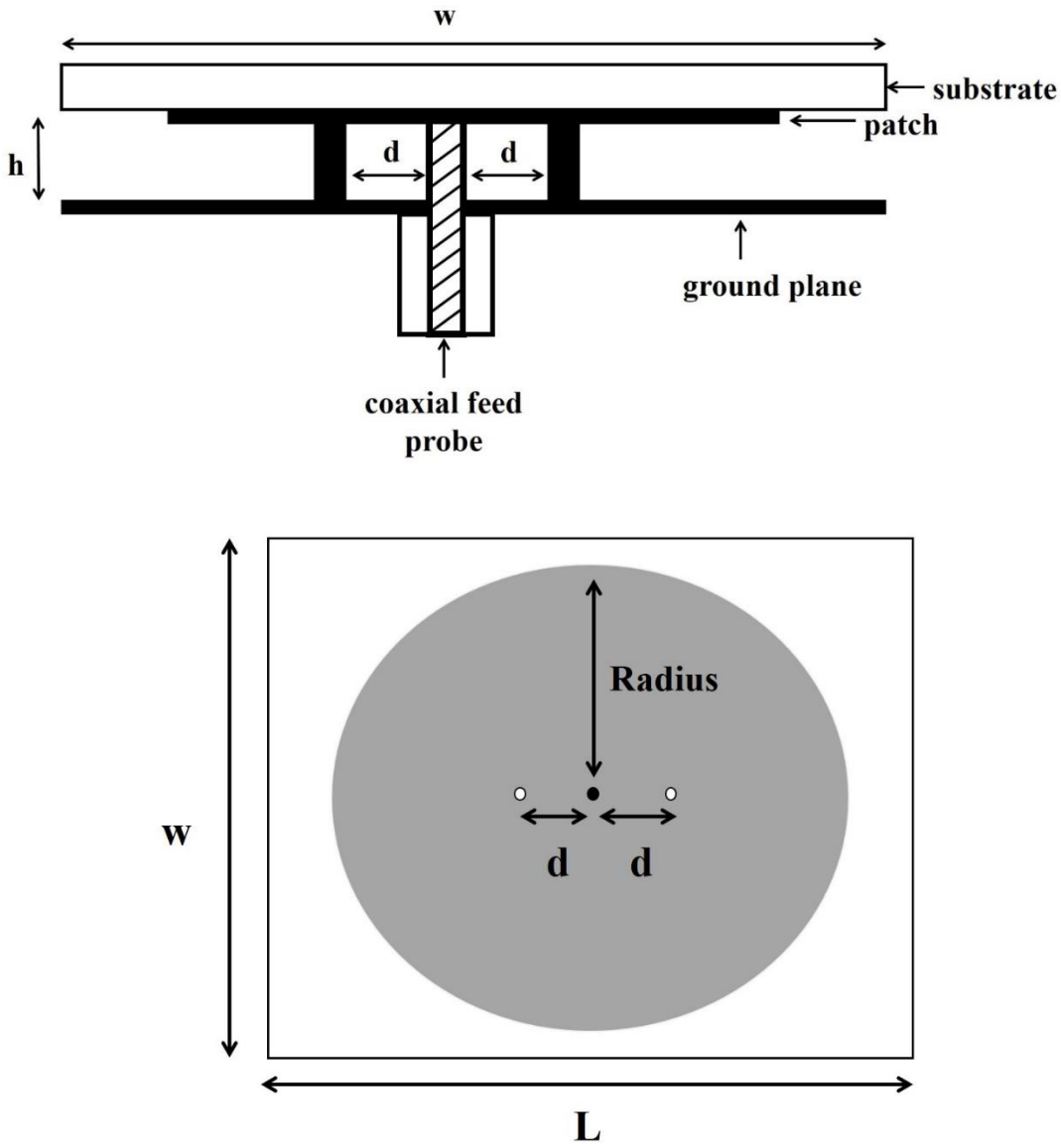

Figure 3.5 Dimensions of the proposed circular patch antenna.

The shorted circular patch antenna is constructed as shown in Figure 3.5 above. The patch antenna is designed to be located at origin coordinates x-y plane while the height of the substrate lies in z-direction in HFSS software. The radiating patch and ground plane are separated by air with a specific distance from each other. The surface wave loss is eliminated, thus permitting the antenna to have better gain as no power extracted from the radiation. By using air as a substrate, this resulted in omnidirectional radiation pattern characteristics for the proposed antenna. The distance between the two resonators is optimised to give the best gain level.

The radius of circular patch and the position of shorting pin have a perceptible effect on the radiation performance of the antenna and frequency response of the antenna respectively. Following the design procedure of standard patch antenna, an appropriate radius is selected then adjusted to give an acceptable radiation performance. A certain compromise is needed between finding a small size of printed antenna and a good performance of the antenna. The shorted patch antenna gives another degree of freedom in antenna design, as the size of radiating conductor is maintained at electrically small size with a reasonable radiation performance. The position of shorting pin is related straightforwardly to the frequency response of the proposed antenna. An additional shorting pin asymmetrical to that is added to provide a low cross polarisation in the antenna performance[88]. Furthermore, it is noted that by symmetrically loading a pair of shorting pins offer a more stable antenna performance during the design process.

Parameters	**Value (mm)**
Radius	38
L	80
W	80
h	3
d	4
Diameter of inner coax	0.869
Diameter of outer coax	2

Table 3.2 Specific fimension for the shorted circular patch antenna.

The feeding mechanism of the antenna is carried out using coaxial probe technique. A primary concern in conventional patch antenna design is the position of feeding point. The position of feed point is crucial during the design procedure in order to match 50 Ω input impedance of a coaxial probe[5]. In [89], the shorting pin is positioned close to the feeding point of a microstrip feed line patch antenna to match the input impedance of the antenna with its 50 Ω microstrip feeding line. The proposed antenna design is fed from the centre of ground plane throughout to the centre of radiating patch. The electrical performance of shorted patch antenna is dissimilar from conventional patch antenna. The coaxial feed probe is designed to feed the shorted patch antenna is represented by two conductors with a diameter of 0.869 mm and 2 mm respectively. The inner conductor (0.869 mm) is coupled to the radiating patch while

the outer conductor (2 mm) is attached to the ground plane. This two stages probe is excited properly to realise a practical wire diameter and obtain impedance matching of 50 Ω over the entire bandwidth.

The standard circular patch antenna gives a directional radiation pattern. By altering the position of ground plane, the omnidirectional radiation pattern is obtained at the expense of large dimension. However, with the insertion of shorting pin, the large size of patch antenna is reduced significantly. The comparison between the dimensions of three antenna designs is tabulated in Table 3.3 below. The operating frequency for all antennas is set at 1GHz. The radiation characteristics for each antenna at 1 GHz frequency is also shown below.

Parameters	**Conventional patch antenna (mm)**	**Patch antenna using air substrate (mm)**	**Shorted patch antenna (mm)**
Radius	41.5	83.7	38
L	90	181.5	80
W	90	181.5	80
The position of feeding point from the centre	25.5	22	0

Table 3.3 The specific dimensions for three patch antenna designs.

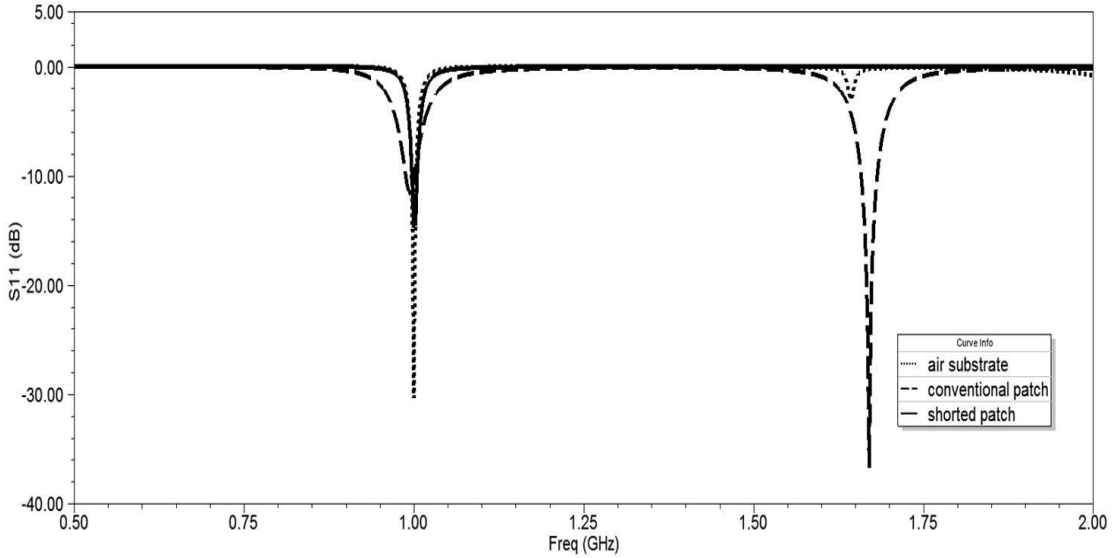

Figure 3.6 The comparison of return loss for three different patch antenna designs.

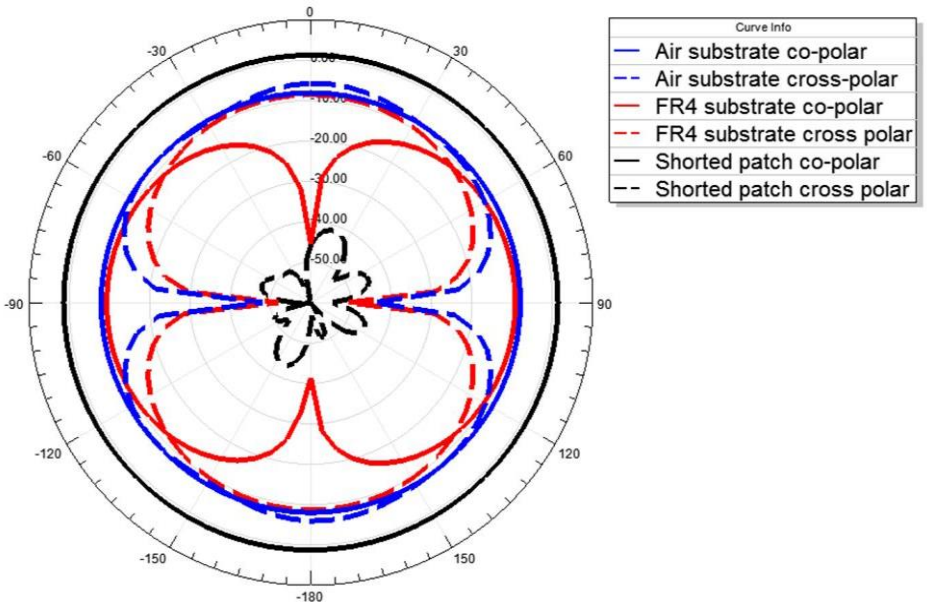

Figure 3.7 The comparison of radiation pattern in azimuth plane for three different patch antenna designs.

3.3.2 Operating frequency and radiation mechanism

The shorted patch antenna is excited at lower frequency mode contrast from a conventional patch antenna operated in dominant mode, thus resulted in an electrically small antenna. The return loss of the proposed antenna is shown in Figure 3.8 below. The input impedance at resonance of the antenna design is determined by the location of shorting pin. The shorting pins are positioned such that the frequency response is at 1 GHz.

The proposed circular patch antenna has radiation performance like a monopole antenna in regards to high gain level in all direction on azimuth plane. The omnidirectional radiation pattern is desirable in some application that requires uniform coverage such as, wireless access points and routers. Furthermore, as seen in Figure 3.9, the simulation result shows that the cross polarisation of the proposed antenna design is maintained at low level. The two identical pins with symmetric arrangement caused the surface current on the patch to be odd symmetric with respect to the H-plane and resulted in a low cross polarisation of the proposed antenna design compared to single pin loaded patch antenna[88].

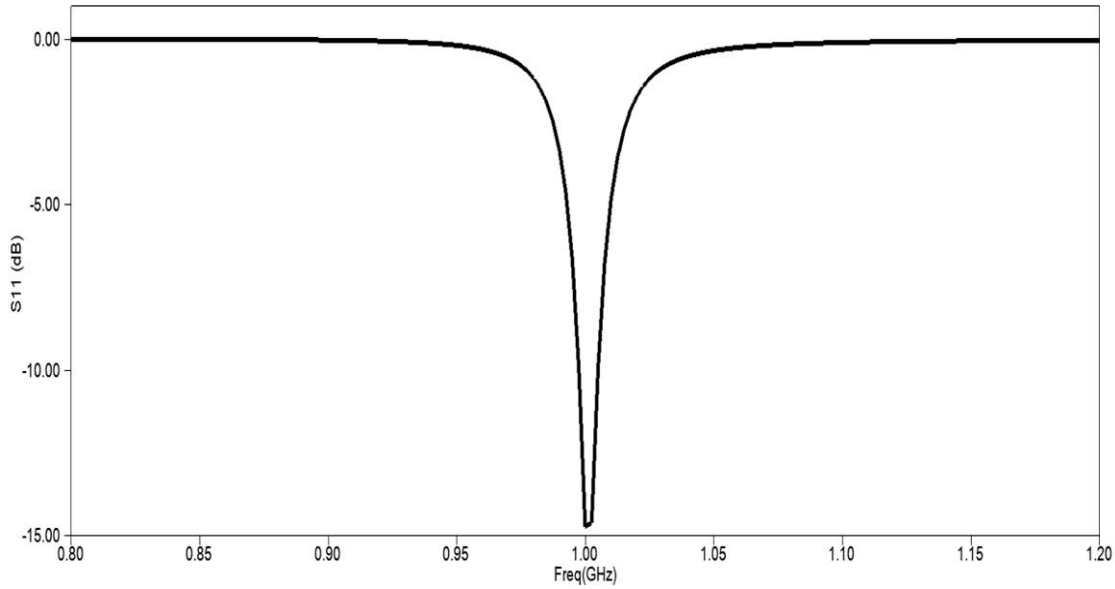

Figure 3.8 Return loss of shorted circular patch antenna.

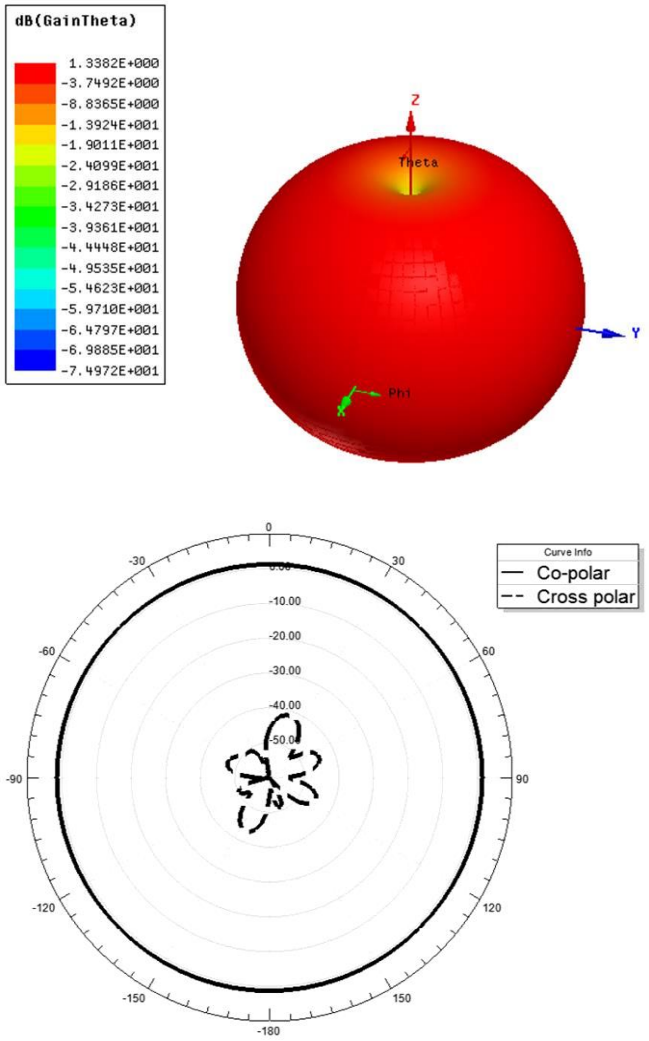

Figure 3.9 Co-polar and cross-polar radiation pattern in azimuth plane (XY-plane) for shorted patch antenna at 1GHz.

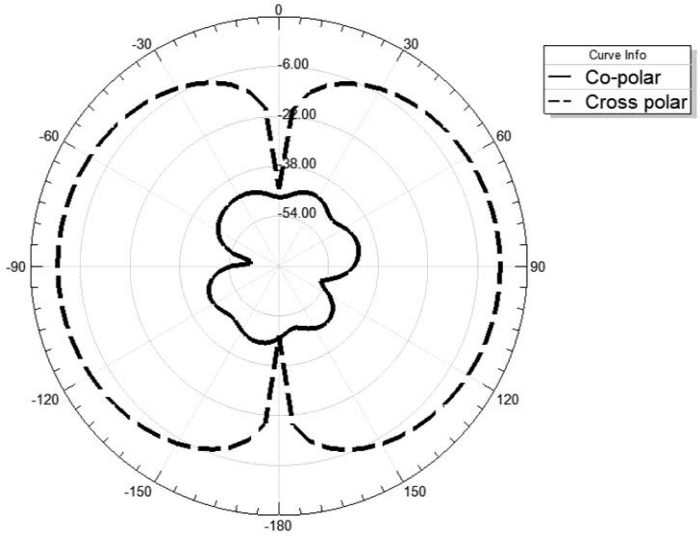

Figure 3.10 Co-polar and cross-polar radiation pattern in elevation plane (XZ-plane) for shorted patch antenna at 1GHz.

3.3.3 Current distribution of proposed antenna design

To understand the operation of a shorted patch antenna, the surface current distribution is plotted. The introduction of shorting pin into the antenna design resulted in the antenna operating at low frequency. The surface current distribution for the shorted patch antenna operated at 1 GHz frequency is shown in Figure 3.10. On this operating mode, the proposed antenna has a uniform current distribution about the aperture, which is equivalent to a DC current path[90]. When current flow through the shorting pins, it will give rise to the magnetic field circulating around the wire and excite electric fields between the radiating patch and ground plane. In the current distribution plot below, there is only one major current path concentrated around the shorting pins on the radiator.

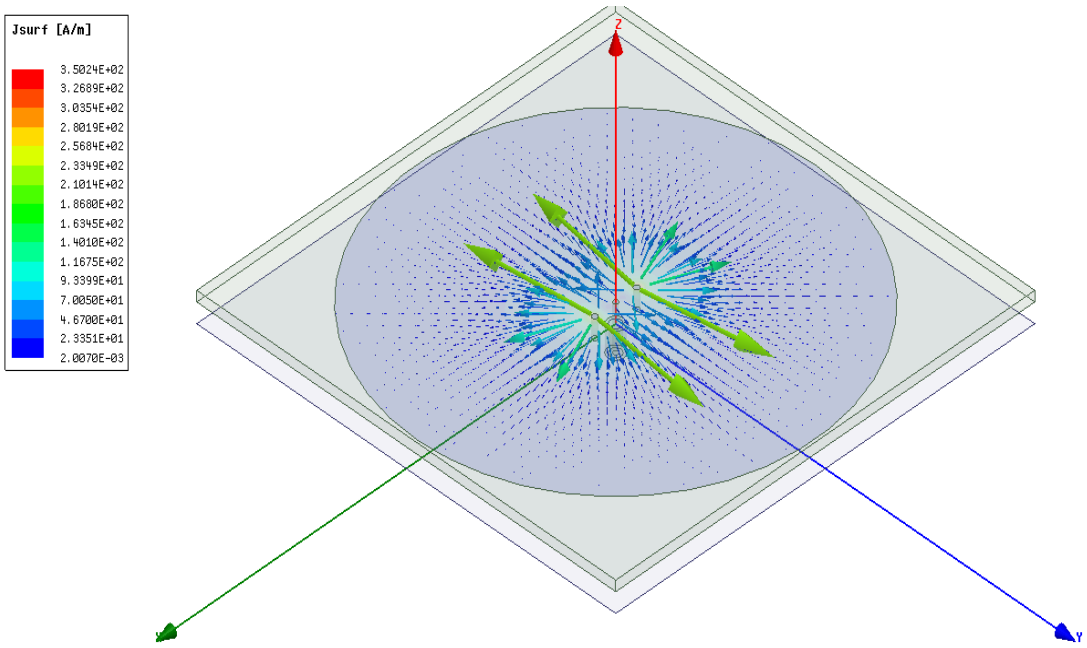

Figure 3.11 Current distribution for the shorted patch antenna.

3.4 Parametric analysis

Based on the construction of shorted patch antenna design, there are few parameters which cause a very noticeable effect on the antenna performance. The parametric studies on those parameters are conducted and the result is given in this section. The optimisation configuration for the proposed antenna design is simulated using HFSS software.

3.4.1 Effect of changing the radius

The frequency operating of an antenna is generally determined through the size of patch radiator. However, with the incorporation of shorting pins in shorted patch antenna, the radius of the circular patch is determined through full wave analysis conducted in HFSS. The size of the patch radiator in shorted patch antenna has been reduced significantly compared to standard patch antenna. The parametric analysis has been conducted on different radius of radiator patch. Even though the size of patch radiator is reduced, the effect of different radius on the patch is still considered as main parameter in the design. The operating frequency for each case has been maintained at 1GHz. The size of the patch radiator can be reduced even smaller while maintaining the input impedance matched at 1 GHz by varying the position of shorting pin but limited to practicality.

Table 3.4 shows the different radius and corresponding distance of shorting pins from the centre of the patch to obtain matching at 1 GHz frequency. Figure 3.12 shows the return loss for each case. As can be seen, all the designs are maintained at 1 GHz with good impedance matching. The shorting pins in each design are modified to give the best possible matching at 1GHz.

Case	Radius (mm)	Distance between shorting pins and centre patch (mm)
Case A	35	2
Case B	37	3.5
Case C	38	4
Case D	40	9

Table 3.4 Different radius of patch radiator with corresponding position of shorting pins.

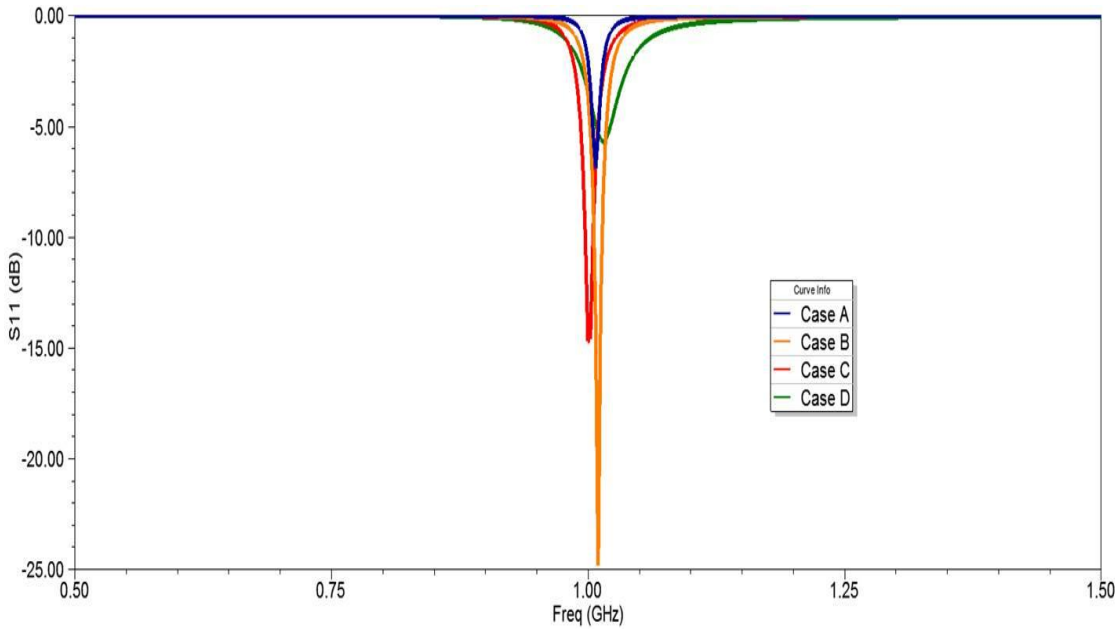

Figure 3.12 Frequency operating bands for different radius of patch antenna.

However, another aspect that needs consideration during the antenna design process is the antenna radiating performance. The radiation performance for each case is shown in Figure 3.13. As can be seen from Figure 3.13, the co-polar measurement taken for each cases show that the antenna are having an omnidirectional radiation pattern with around the same gain. However, the cross-polarisation measurement of Case C is lower compared to Case D with better matching. Thus, radius of 38 mm is selected for the proposed antenna design.

Since shorting pin can be used to shift frequency operating, thus the radius of the radiating patch can be minimised to get the best radiation performance. However, the dependency on the position of shorting pins need to be reduced as the practical realisation of the distance between shorting pin and feeding probe is very close. Furthermore, a smaller radius of patch antenna constitute to lower gain of co-polar measurement. Thus, proper size of the radiating patch is required to give the best radiation performance at the operating frequency desired.

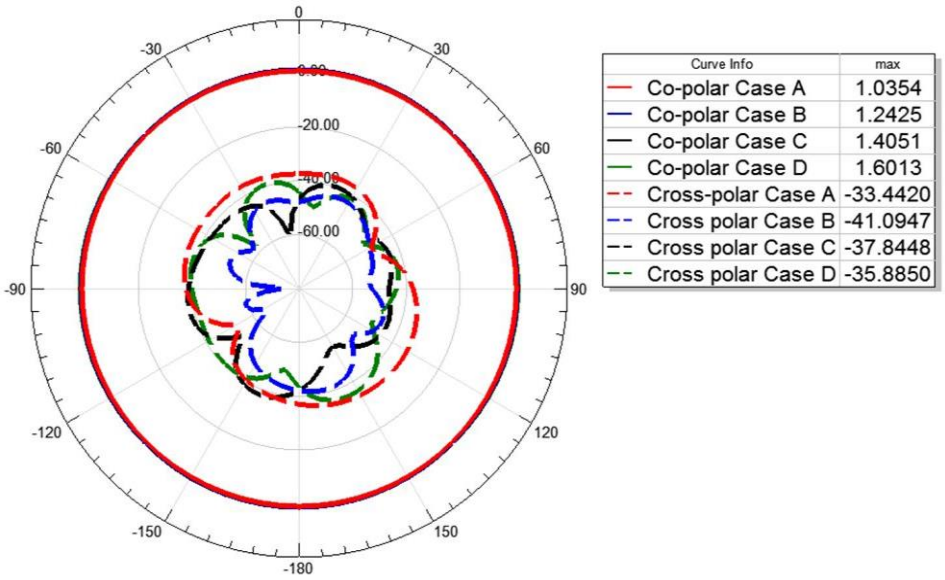

Figure 3.13 Co-polar and cross polar measurement on azimuth plane for each case simulated in HFSS.

3.4.2 Effect of changing the position of shorting pins

In the earlier design of microstrip patch antennas[86], the incorporation of shorting post has been proven to result in electrically small printed antennas for mobile communications handset. The patch size can be altered by varying the distance between the shorting pin from the feed while maintaining the exact operating frequency. In other words, when the dimension of the shorted patch antenna is fixed, the positioning of the shorting pins will affect the operating frequency of the antenna.

The impact of the shorting pin position can be seen on the frequency response of the shorted patch antenna after a parametric analysis on different positioning of shorting pins are conducted in HFSS. Following the design procedure of shorted patch antenna given earlier, the radius of circular patch radiator is set at 38 mm and the positioning of shorting pins is adjusted. The return loss or frequency response analysis of the antenna

is studied. Please note that d is the distance between the shorting pins and the centre of the patch. The practical size of feed point is also put into consideration.

The input impedance and return loss of the antenna are shown in the Figure 3.14 below. The match impedance obtained at 1 GHz frequency is dependent on the position of the shorting pins. Different shorting pin position impacted on the frequency response because of the variation in matching. Fine adjustment on the position of shorting pins was then made to obtain the desired input impedance behaviour at 1 GHz frequency.

With a continuous increase in the distance between the feed point and shorting pin, the operating frequency of the antenna is also shifted. This is beneficial in the design procedure of the shorted antenna compared to classic patch antenna, as the frequency operating of the antenna is independent of the patch size. As a result, small size patch antenna operating in low frequency is obtained.

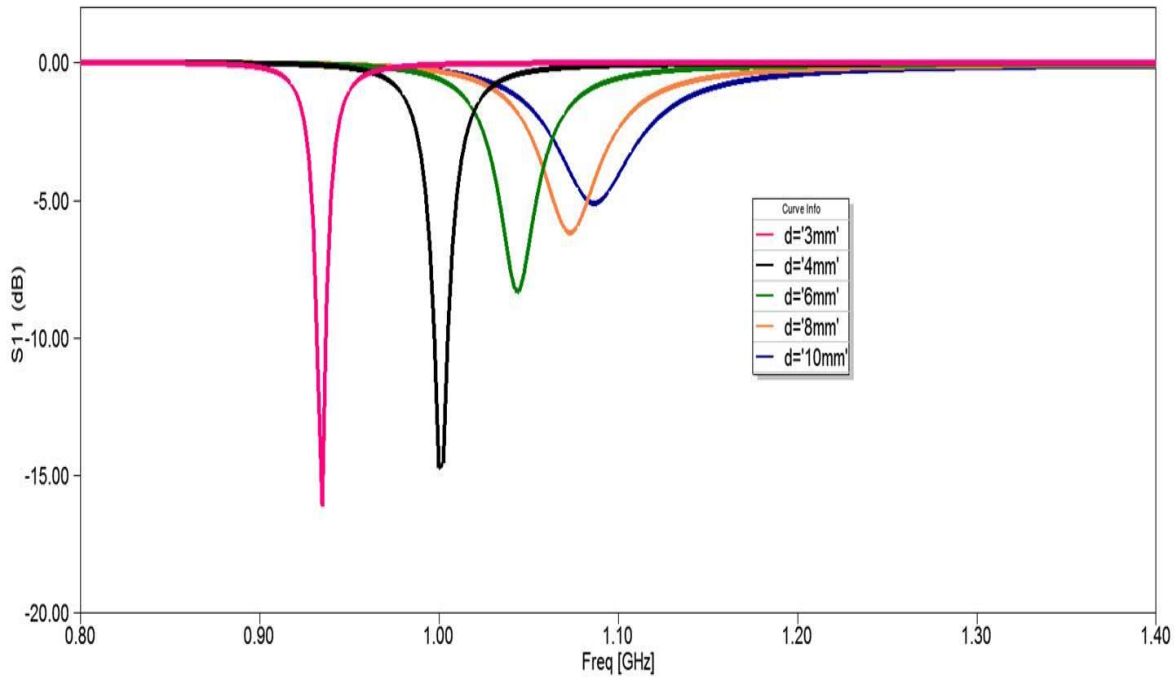

Figure 3.14 Frequency responses for different position of shorting pins. D is the distance from the centre of the patch.

3.5 Simulation and Measurements

3.5.1 Measurement setup

The circular patch antenna as mentioned above is fabricated and constructed. The radiating patch antenna is fabricated on FR4 board and attached to the ground plane using coaxial cable. The return loss and radiation performance of the shorted circular patch antenna is measured and compared with the simulation result from HFSS.

The measurement of the proposed antenna design is conducted using Power Network Analyser. The return loss value of the proposed antenna design is obtained by measuring the S11 using Network Analyser. The antenna measurement is optimally conducted in Anechoic Chamber. An anechoic chamber is a room that has a wall shielded with Radiation Absorbing Material (RAM) to ensure that all the radiation reflected from the measured antenna is totally absorbed. This is to ensure that no reflected radiation is disturbing the measurement conducted. However, due to lack of facility in Brunel University, the measurement is conducted in a spacious room big enough to avoid multipath effect from surrounding. The power of -5 dBm from the Power Network Analyser is conveyed to the transmitting antenna. Horn antenna is operated as transmitter while shorted patch antenna is regarded as receiver antenna.

3.5.2 Return loss and S11

The S11 analysis represents the amount of power reflected from the antenna, hence known as the reflection coefficient. As can be seen from the Figure 3.15 below, the shorted circular patch antenna is working at 1 GHz with a good impedance matching of more than -10 dB. The return loss of the shorted patch antenna as given by the Network Analyser is -13.8 dB. The comparison of return loss between the simulated and measured shorted patch antenna is shown in the Figure 3.16 below. From the measurement, it can be seen that the return loss is reduced compared to simulated data. It might be due to the noise and multipath effect during the experiment.

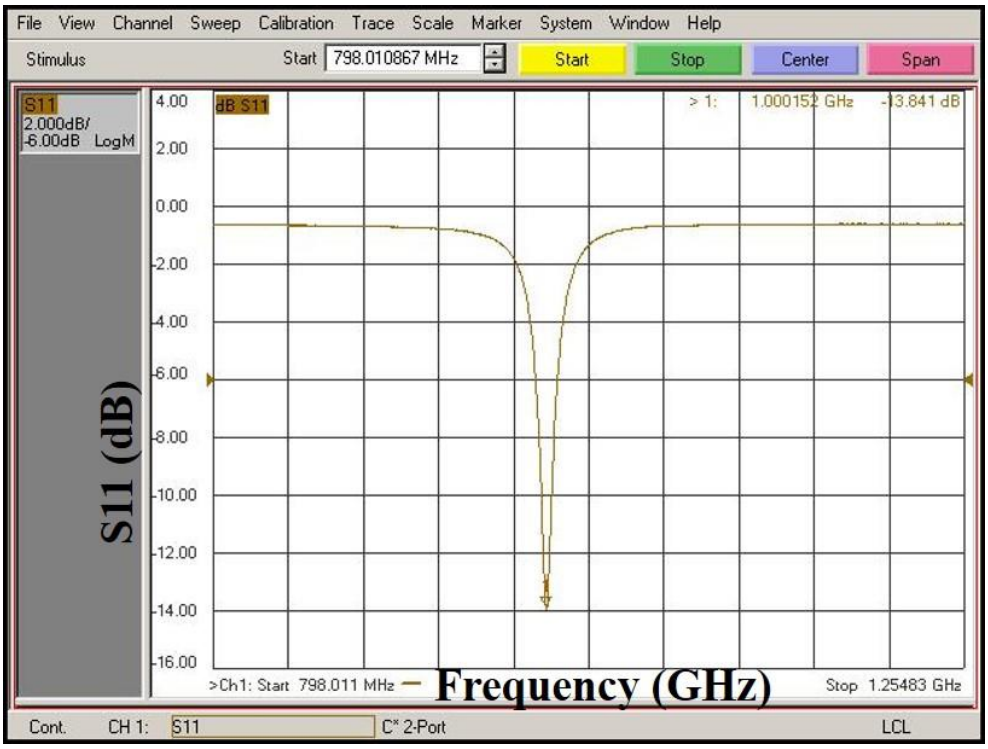

Figure 3.15 Measured return loss (S11) for the shorted patch antenna as given by Network Analyser.

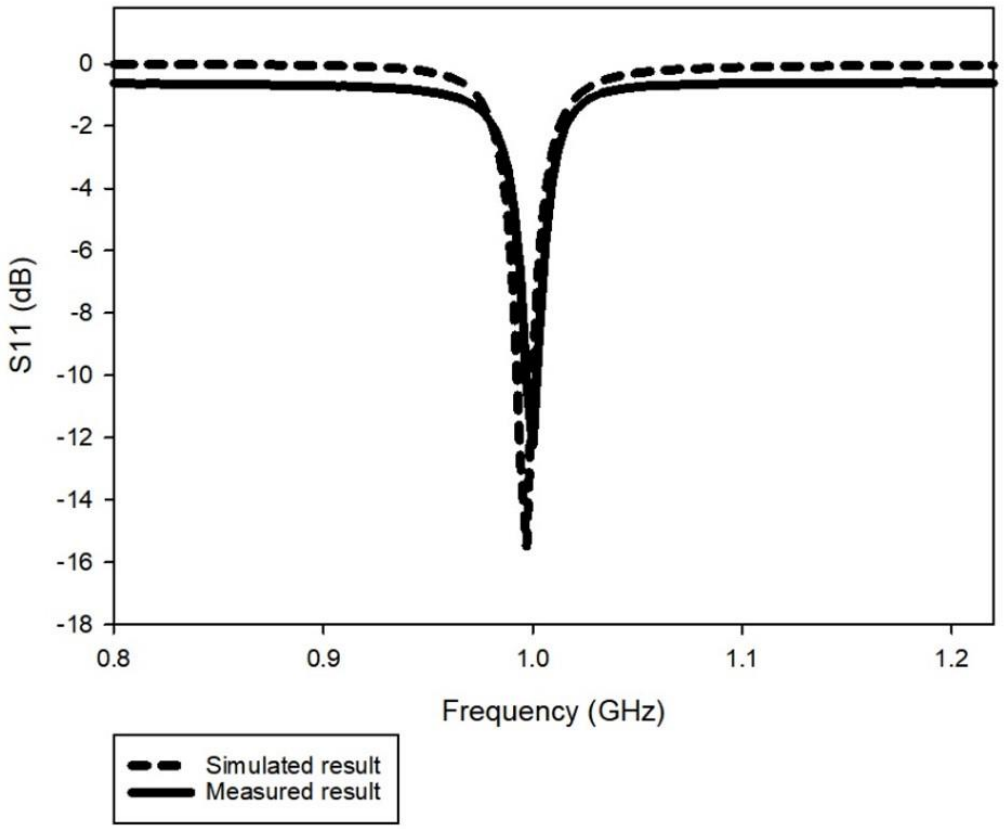

Figure 3.16 Simulated and measured return lost for the shorted circular patch antenna.

3.5.3 Measured gain and radiation efficiency

The radiation pattern measurement for the proposed antenna is obtained and presented in Figure 3.16 and Figure 3.17 below. Since the experiment is conducted manually, the gain of the shorted patch antenna is measured distinctly at each 10° angle position. After each measurement taken, the shorted patch antenna will be rotated 10° until all angles in the azimuthal plane are covered. The antenna under measurement is kept steady and maintained in equilibrium during the whole process.

As seen in the graph below, the radiation pattern of the proposed antenna has an omnidirectional shape on an azimuth plane (XY-plane). The gain level is approximately equal in all directions suggesting that the proposed antenna can transmits and receives equal power from all direction on the azimuth plane. The introduction of two identical pins makes the surface current on the patch symmetric with respect to the H-plane, thus keeping low cross polarisation as expected. However, there are some irregularities in the shape of radiation pattern that might be resulting from the multipath effect from the surrounding. The multipath effect still needs to be taken into consideration even though the experiment has been carried out in a large spacious room to minimise the impact. Another reason might be losses from cable, as both antennas are connected using coaxial cable approximately 5 meters from the Network Analyser.

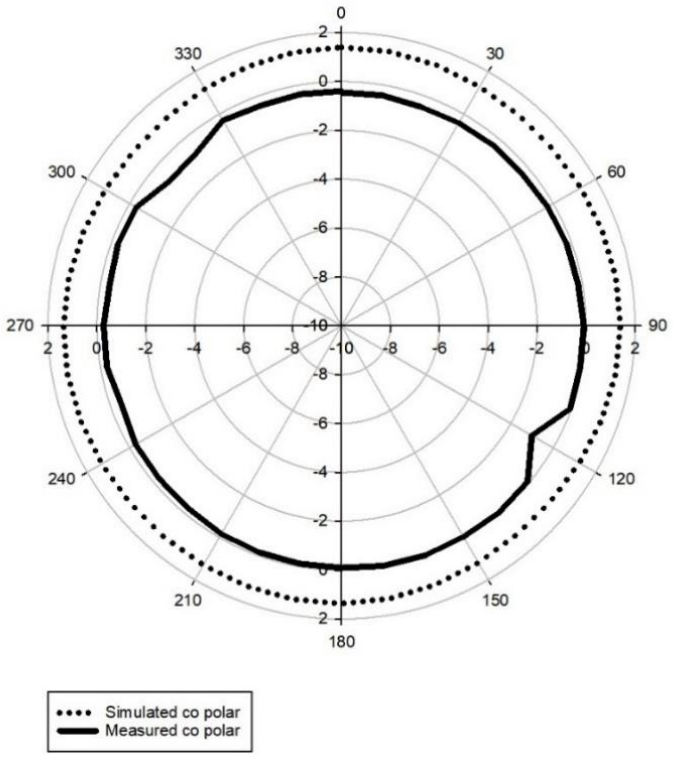

Figure 3.17 Simulated and measured co-polar radiation pattern on azimuth plane for the shorted circular patch antenna.

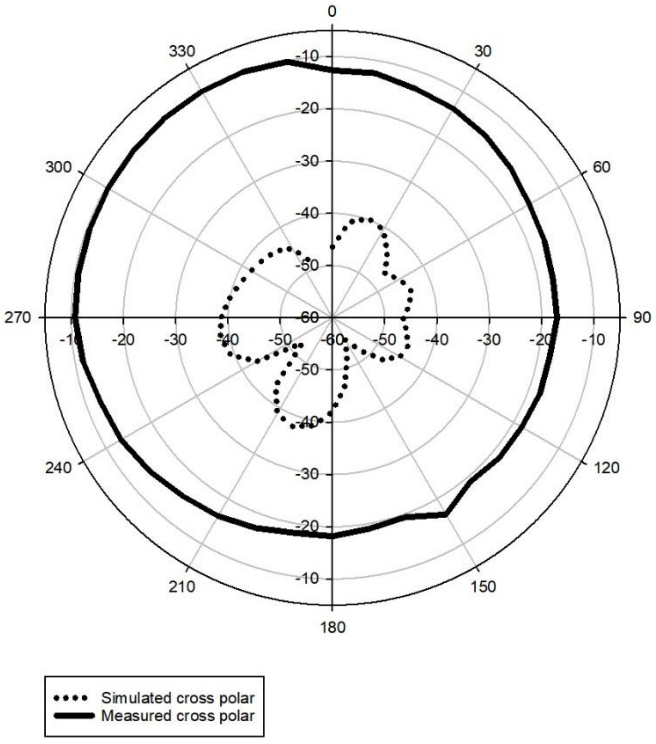

Figure 3.18 Simulated and measure cross-polar radiation pattern on elevation plane for the shorted circular patch antenna.

3.6 Summary

In this chapter, a shorted circular patch antenna is designed and all the key parameters are tested using HFSS for optimal design. The hardware prototype of the antenna is fabricated. The frequency response and radiation performance of the antenna is measured and compared with simulation result. The antenna is operating at 1 GHz frequency with an omnidirectional radiation pattern. An acceptable good gain level is resulted from using air as substrate. The shorted patch antenna has an omnidirectional radiation pattern which is beneficial for achieving the goals of this thesis.

Chapter 4 Radiation pattern reconfigurable antenna with fine direction resolution.

4.1 Introduction

Pattern reconfigurable antenna is crucial in modern communication system due to its adaptable quality to the system requirement. This smart antenna can unravel the hidden nodes due to lack of coverage problem by directing the signal toward the right directions. It has previously been observed that most pattern reconfigurable antenna design are capable of having multiple radiation pattern in a single design and does not support full beam coverage in one single plane. Alternatively, in this chapter, the shorted patch antenna from previous chapter is configured to have multiple radiation pattern characteristics with fine direction resolution on single plane. The mechanism of operation for the proposed antenna design of radiation pattern reconfigurable antenna is explained in Section 4.2 of this chapter. Radiation pattern reconfigurable characteristic of the circular patch antenna is achieved by adding a parasitic element in the design. The radiation pattern of the antenna can be modulated to a fine direction resolution of 10° when a single parasitic element is activated. The critical parameters of the proposed antenna are presented in Section 4.3. The return loss and radiation pattern of the proposed antenna are analysed and studied thoroughly. The parametric study on the proposed method is studied in Section 4.4. Then, the practical measurement of the antenna using proposed method is carried out. The result from the experiment is compared with the simulated data in Section 4.5.

4.2 Principle of Operation

The pattern reconfigurable manners of the proposed antenna design are constructed based on the operating principle of Yagi-Uda antenna, which was developed by H. Yagi and S. Uda at Tohoku Imperial University in Sendai, Japan[91][92]. The basic construction of Yagi –Uda antenna is comprised of a reflector, a driven element and a director. These will cause phase distribution to occur, which leads to Yagi-Uda antenna to function as an end-fire beam. It has conclusively been shown that the total phase of currents in the radiators is determined by the length and spacing between the radiators.

By adopting this concept, a metal element is introduced into the shorted circular patch antenna. An element which is physically longer than resonant length will become reflector. The impedance of reflector is inductive, and the induced currents lag in phase from the current induced by the driven element[93]. This causes phase distribution to occur. When the electric field from the metal rod met the electric field from the radiating patch, it will result in constructive wave collision in the opposite direction to the position of metal rod. Thus, it results in power reflected away from the parasitic element and the maximum power is in the opposite direction to the position of metal rod. Figure 4.1 and Figure 4.2 show the configuration of proposed antenna design and how the radiation pattern change respectively. The shorted circular patch antenna has a dimension as mentioned in Chapter 3 and the metal rod length is 150 mm, which is $\lambda/2$ and placed 58mm from the centre of radiating patch. Other components of the antenna are also verified to find the most desirable gain. Each metal cylinder has a radius of 0.5 mm to give maximum gain.

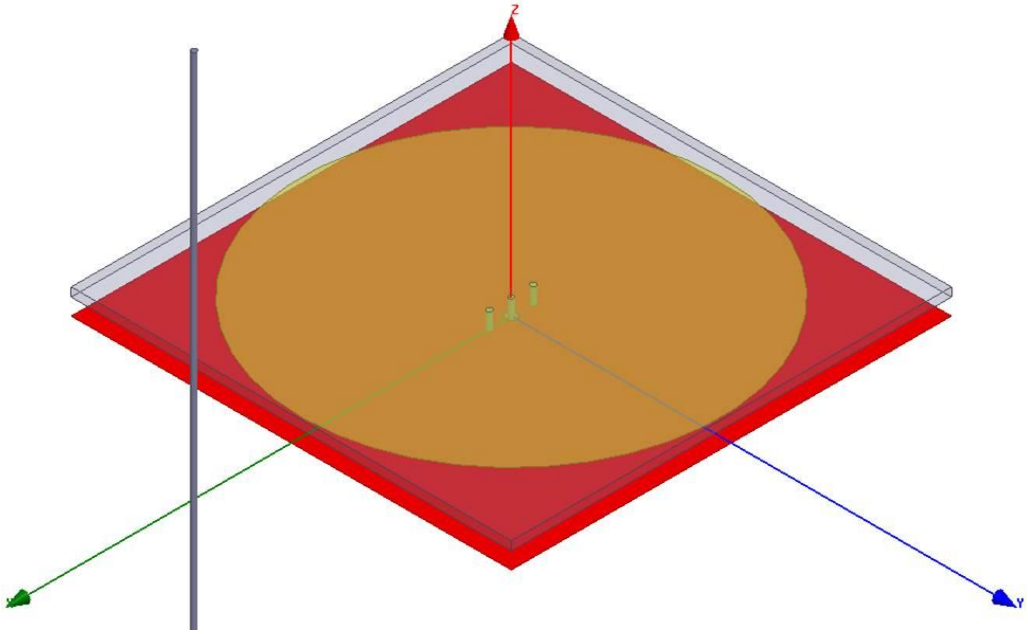

Figure 4.1 The construction of reconfigurable circular patch antenna using metal rod in HFSS.

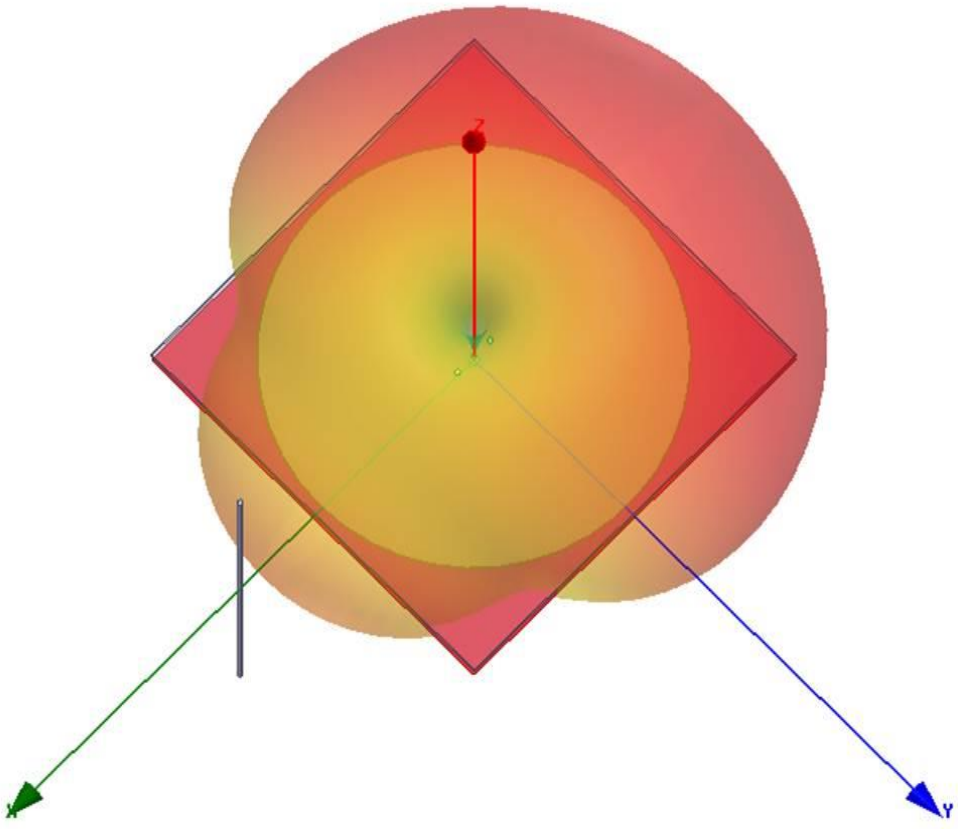

Figure 4.2 Radiation pattern change in 3D plot when metal rod is inserted.

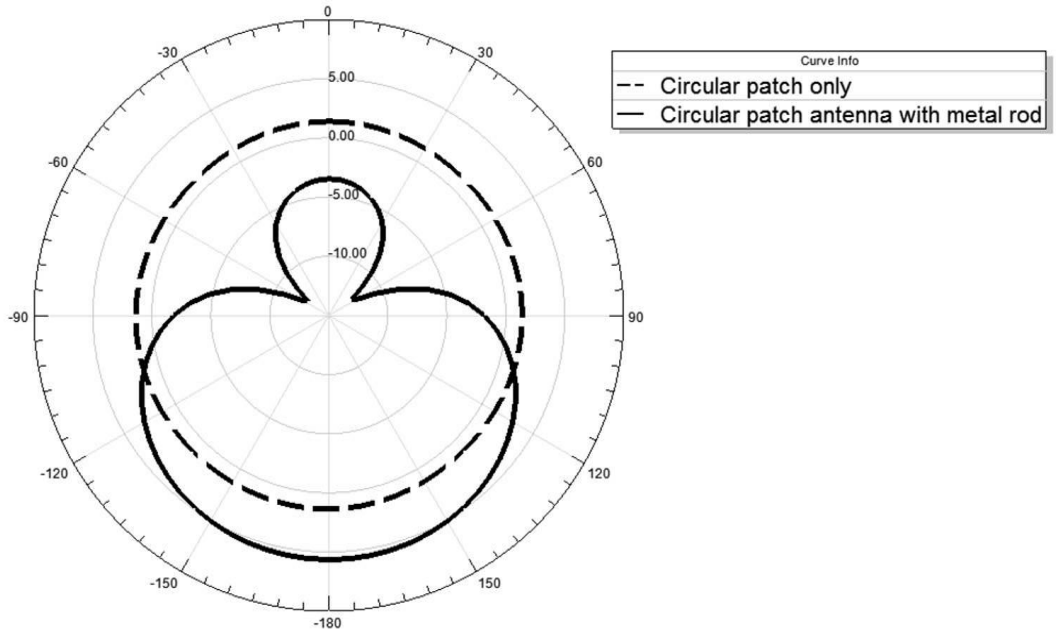

Figure 4.3 Radiation pattern on azimuth plane when metal rod is inserted.

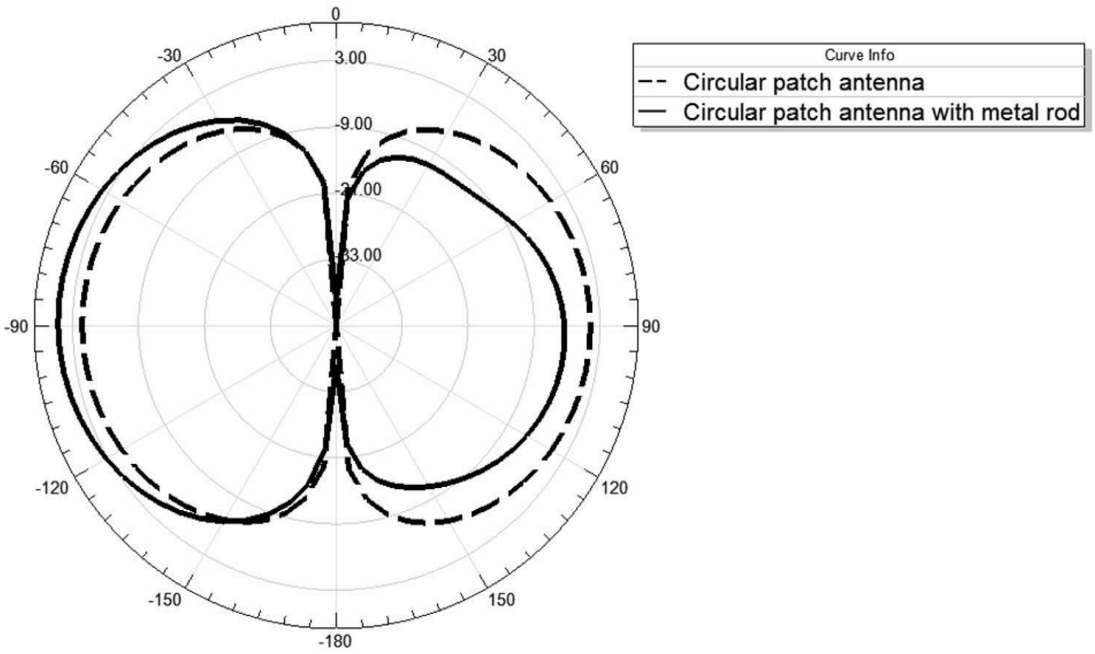

Figure 4.4 Radiation pattern on elevation plane when metal rod is inserted.

The reconfigurable characteristic of the antenna is controlled by having a different overall length of metal rod at one time. The length of metal rod is controlled using PIN diode as a switch. The PIN diode is located in the middle of the metal element. PIN diode serves to open or close a current path connecting the metal cylinder, which gives the total length of metal rod. PIN diodes are less susceptible to electrostatic discharge damage compared to other switches[57]. Forward biasing a PIN diode creates a very low resistance at high frequencies, while reverse biasing results in an open

circuit. The different position of the activated metal cylinder around the circular patch antenna will determine the shape of the radiation pattern accordingly. When the PIN diode is triggered, the metal rod will act as a reflector where the gain of the radiation pattern is highest in the opposite direction compared to other direction. In this study, the application of PIN diode as a switch is not studied as the primary focus is on proving the main concept. The activated metal rod will have a full length, while non-activated metal rod will be shorter than a full-length metal rod.

The full wave analysis of the reconfigurable antenna is conducted in HFSS. For the purpose of simulation, the metal cylinder is divided into two and separated by an empty cylinder to signify when the switch is off. When the switch is activated, the two metal cylinders are united which gives a total length of $\lambda/2$.

4.3 Performance analysis

4.3.1 Radiation pattern

As shown in the previous section, the radiation pattern of the proposed antenna changes with the insertion of a metal rod. When activated, the full-length metal rod operates as a reflector and the omnidirectional radiation pattern of the shorted patch antenna will change accordingly. The reconfigurable characteristics of the proposed antenna are attained by activating different metal rod at one time. The direction of maximum gain changes as different metal rod is activated. In this study, the main goal is to have a reconfigurable antenna covering all beam direction in azimuth plane. Following this objective, metal rods are placed around the shorted circular patch antenna to contend with the whole azimuth plane. The initial omnidirectional radiation pattern of shorted patch antenna allows more room in the radiation pattern reconfiguration.

The distance between the metal rods and the centre of radiating patch is maintained while the position of metal rod is varied. To see the changes in radiation pattern with the activation of different metal rod clearly, four metal rods are placed around the antenna. The metal rod is turn on individually and the changes in radiation pattern are observed. The radiation pattern of the reconfigurable antenna is shown in the figure below. When Metal 1 is activated, the radiation pattern has a maximum gain

opposing to the position of Metal 1and so on. Figure 4.5 shows the radiation pattern in 3D and 2D plane for each consecutive metal activated.

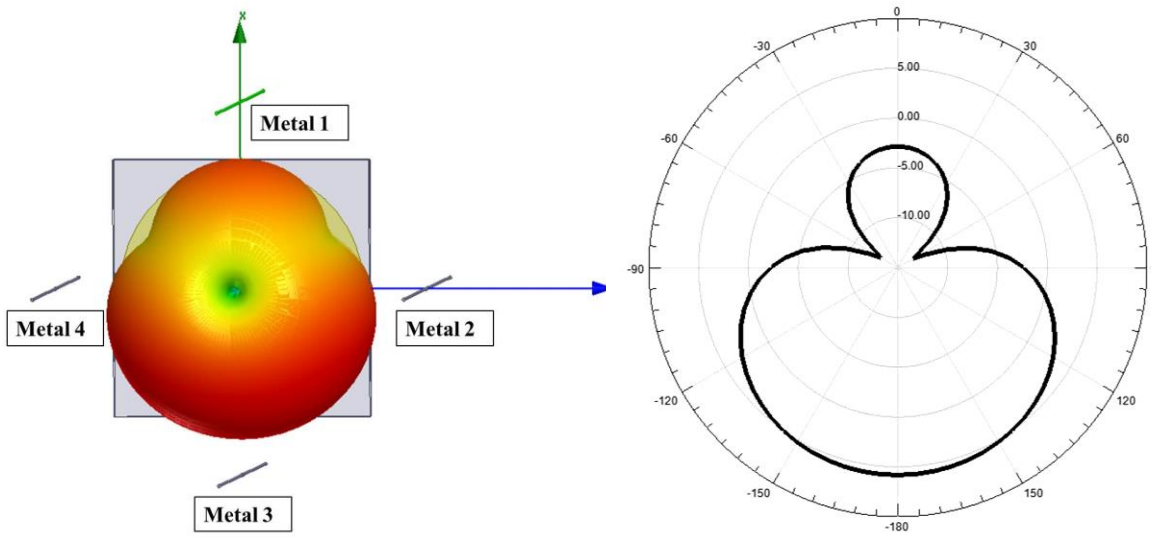

(a)

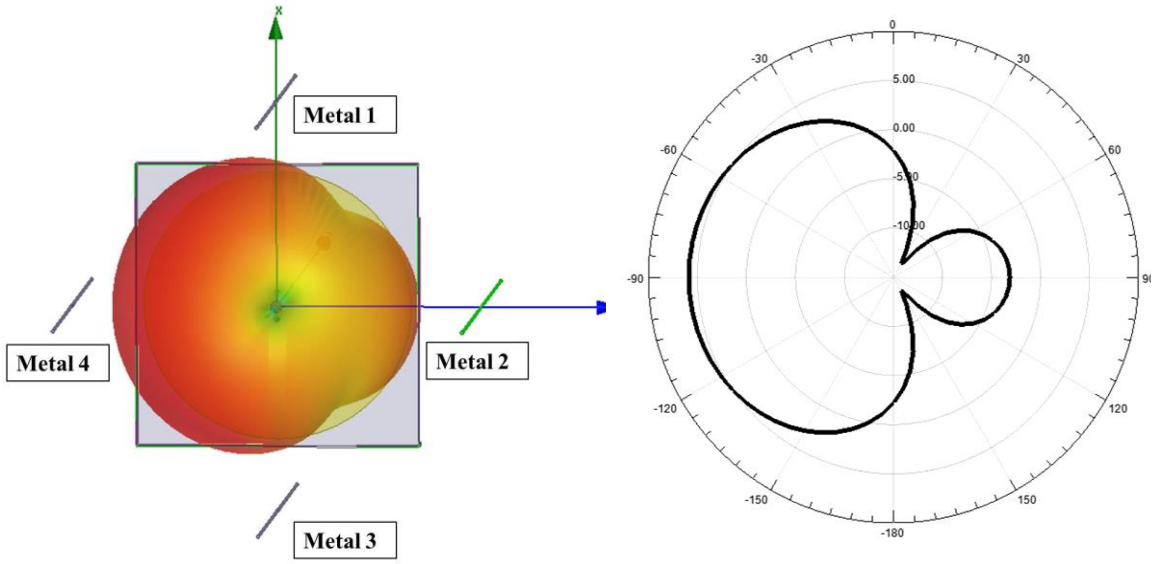

(b)

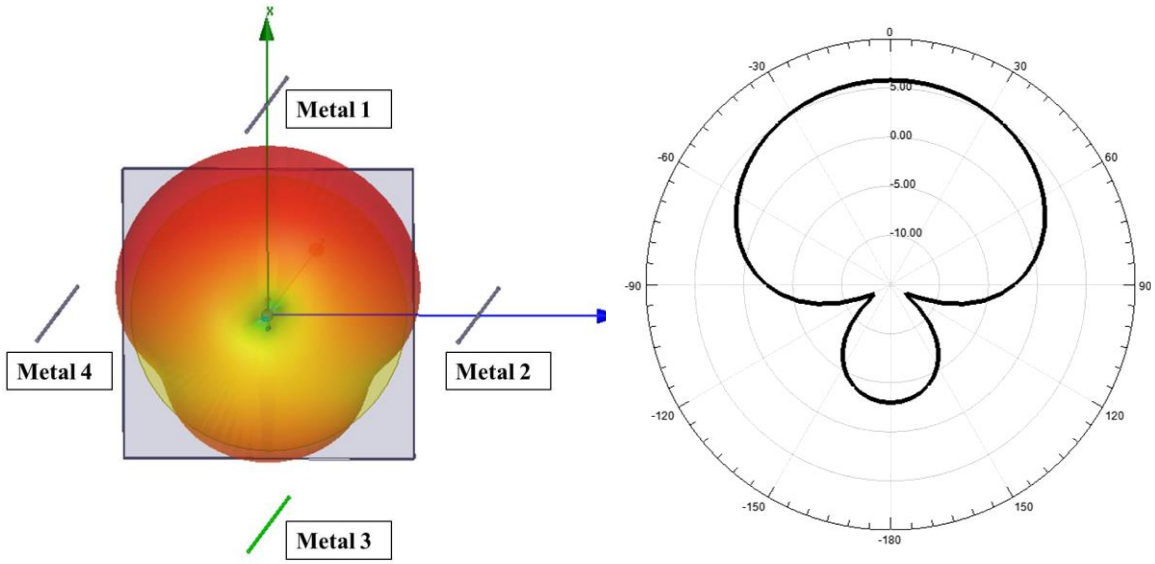

(c)

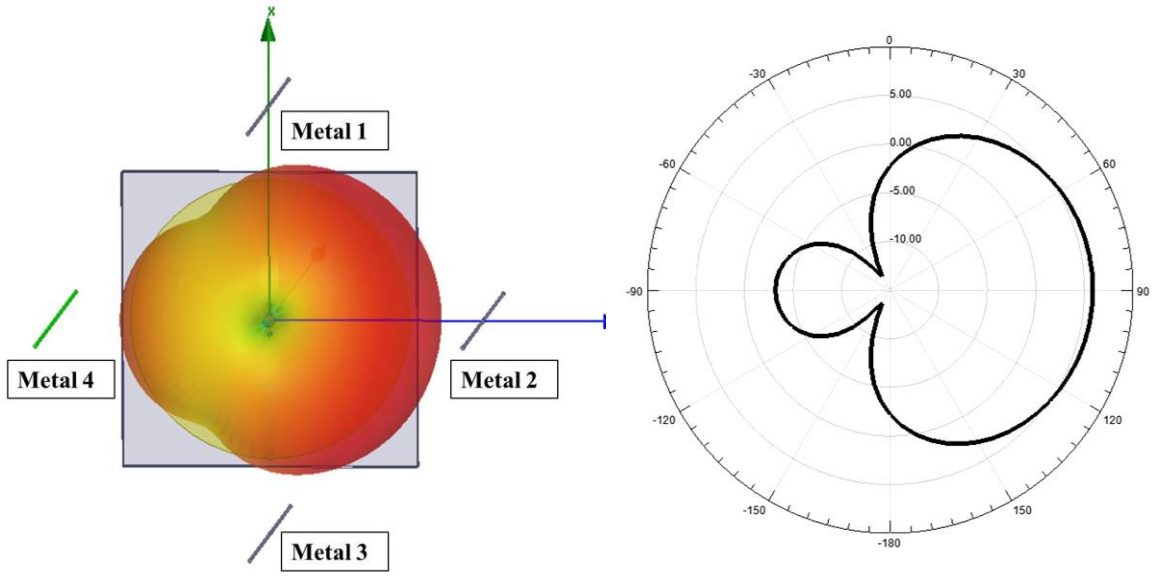

(d)

Figure 4.5 Radiation patterns on azimuth plane when different metal is activated (a)Metal 1 (b)Metal 2 (c)Metal 3 and (d)Metal 4

Subsequently, the metal rods are placed carefully next to each other. The finest beam resolution with adjacent elements activated is investigated and the changes in the radiation pattern are recorded. The metal rods are placed at 10° angle adjacent to each other. Figure 4.4 presents the simulated data on fine resolution radiation pattern. As can be seen from the figure, the radiation patterns of the antenna change accordingly when the metal rod is activated individually. However, based on the simulated data, there are some discrepancies in the radiation pattern when Metal C is activated. This might be due to the mutual coupling occurs when more metal rods are located close to each other.

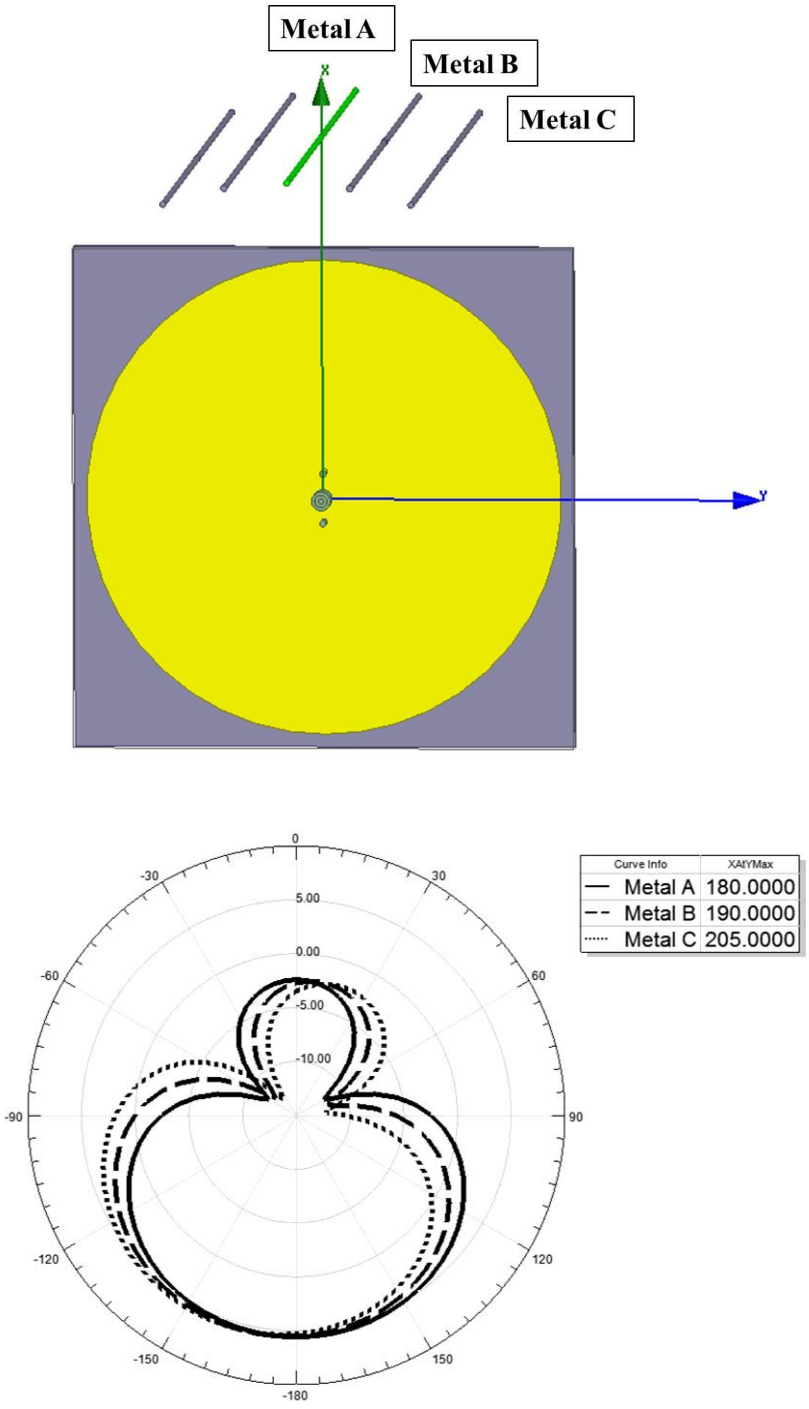

Figure 4.6 Radiation pattern on azimuth plane when different metal is activated.

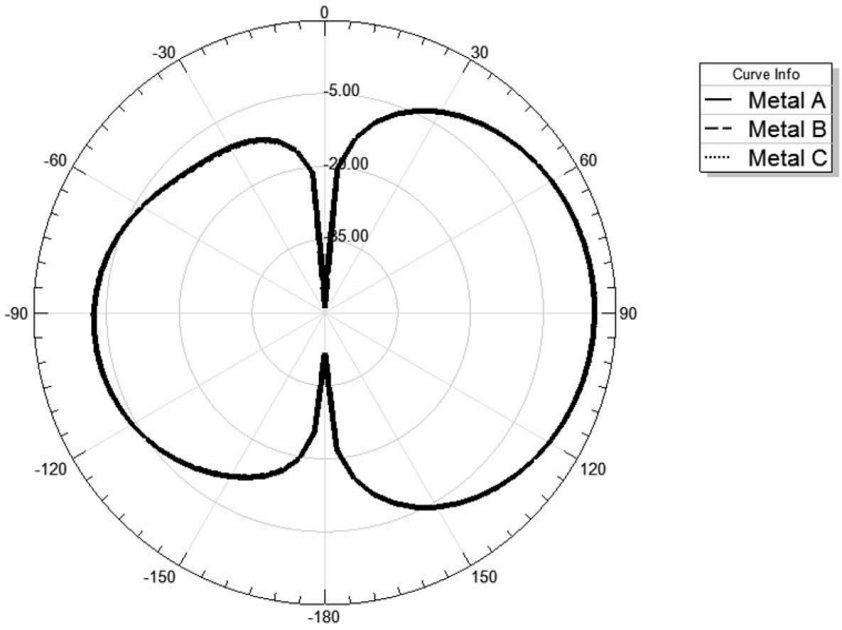

Figure 4.7 Vertical cut of the radiation pattern at their consecutive maximum direction.

4.3.2 Return loss

Although more focused is laid on the radiation pattern in this research, return loss and frequency response of the reconfigurable antenna is still crucial in the antenna design. A reconfigurable radiation pattern has a capability of changing the radiation pattern without affecting the frequency response of the antenna. The proposed antenna design is operating at 1 GHz frequency. As can be seen from Figure 4.8, the return loss and frequency response of the reconfigurable antenna is maintained at 1 GHz despite the addition of metal rods to the shorted circular patch antenna. However, there is some decrease in the antenna bandwidth when the metal rod is inserted.

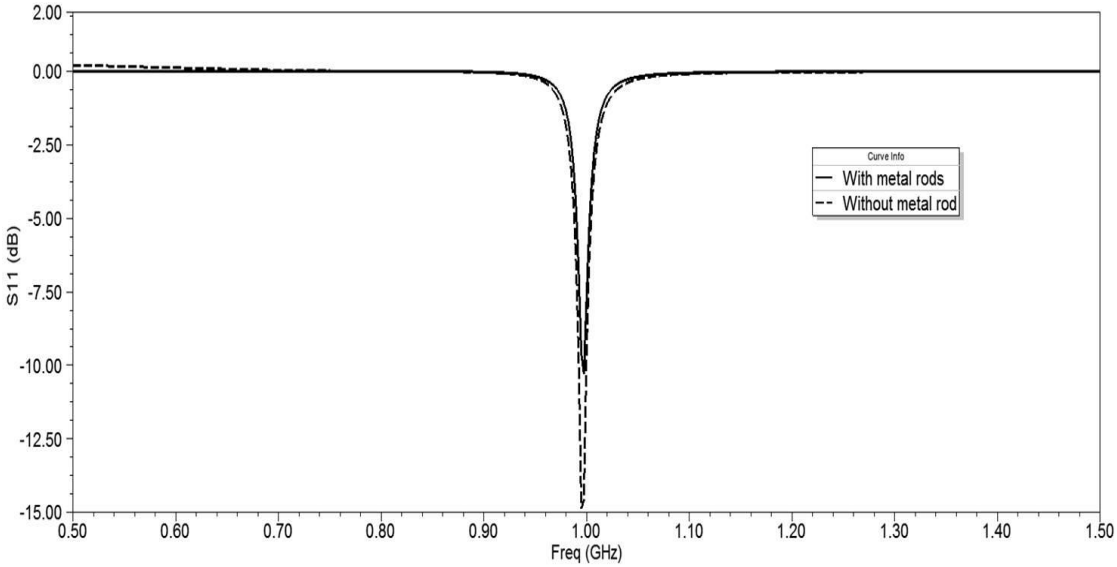

Figure 4.8 Simulated frequency response of the proposed antenna design with and without the insertion of metal rods.

4.4 Parametric analysis

Of all the investigated design parameters, two of them have a very noticeable effect in determining the performance of the antenna. The parameters that show the most effect are length and the distance between metal rod and centre of patch radiator. Length and position of metal rod have an impact on the maximum gain of radiation pattern. In order to check the changes of the radiation pattern, parametric studies for each parameter have been carried out and obtained from iterative simulation with initial data. Optimisation function in HFSS is utilised to give the optimal result.

The total phase of currents in the antenna design is not determined exclusively on length but also by the spacing to the relating elements. It is crucial to have the metal element to be placed appropriately so that it will act as a reflector. Later in 1973, Cheng and Chen[94] has proven that the maximum forward gain is obtained by optimising the spacing between the parasitic elements before published another paper on optimum element lengths for Yagi-Uda arrays[95]. Taking this approach, the proposed antenna design also paid extra consideration into the spacing of metal element to obtain maximum directivity.

4.4.1 Effect of changing the length of metal rod

The full length of metal rod when activated is around half free-space wavelength. In a configuration of Yagi-Uda antenna, the length of parasitic structure determines the behaviour of the element. A physical length of a reflector is slightly longer than resonant length and a director is typically shorter than resonant length[93]. The proposed antenna design applied the same concept; thus the length of metal rods is selected at half of free-space wavelength.

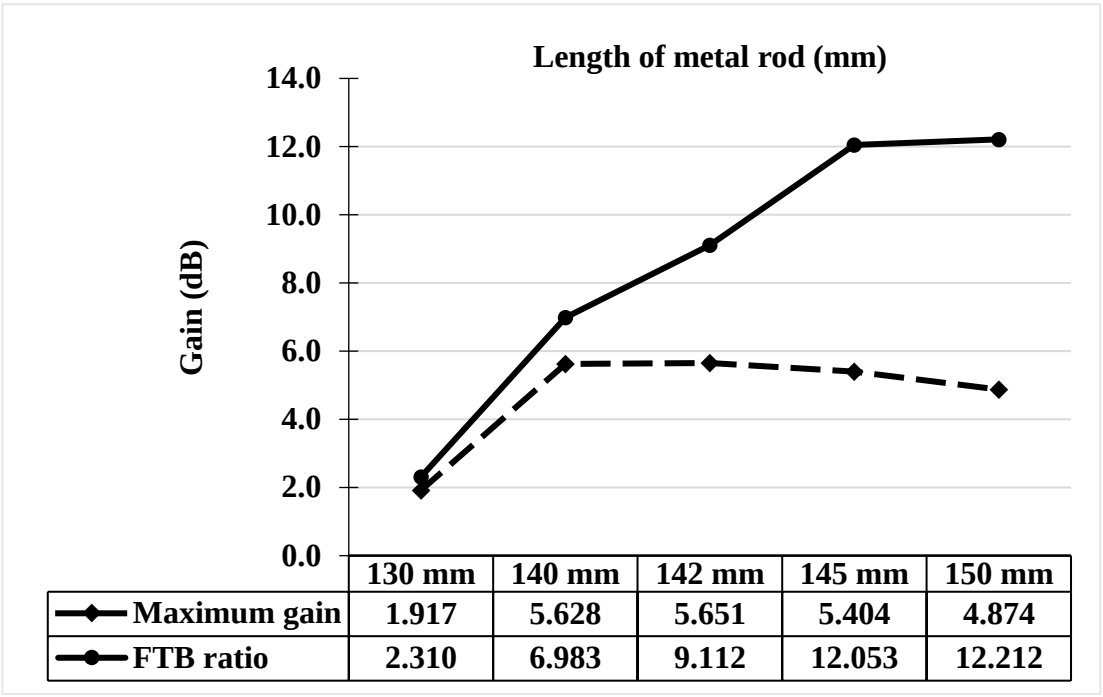

	130 mm	140 mm	142 mm	145 mm	150 mm
Maximum gain	1.917	5.628	5.651	5.404	4.874
FTB ratio	2.310	6.983	9.112	12.053	12.212

Figure 4.9 The relationship between length of metal rod and the maximum gain of antenna.

The maximum gain of the radiation pattern is observed for different length of metal rod to give a maximum gain. The maximum gain is measured opposing to the position of metal rods, assuming the metal rod behaves as a reflector. The graph of correlational analysis is presented in Figure 4.9 above. Closer inspection of the graph shows that there is a small decline in the maximum gain with the length of metal rod closer to $\lambda/2$. Also, the sudden drop in maximum gain at that particular direction is because the metal rod started to act more as a director and less as a reflector. Even though the maximum gain for the last measurement is reduced, the front-to-back ratio of the measurement is more significant than the earlier case. The front-to-back ratio for each case is also crucial when deciding the length of the metal rod. In Figure 4.10, there is a clear trend of decreasing in the back gain when the length of metal rod closer to $\lambda/2$.

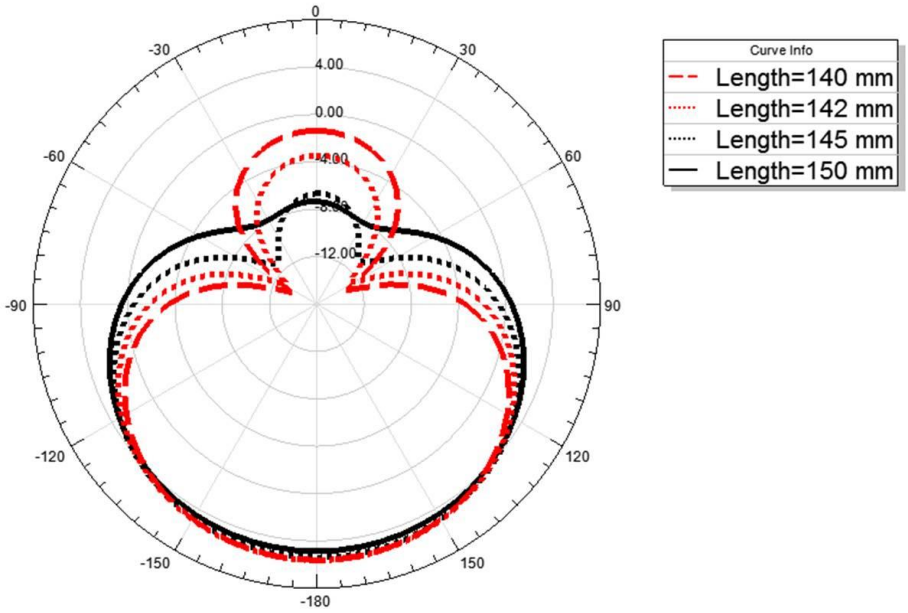

Figure 4.10 The comparison for different length of metal rods acting as a reflector.

Figure 4.11 depicted the radiation pattern for the proposed antenna when different length of metal rod is applied. When the length of metal is around λ/2, the metal rod acted as a reflector. When reducing the length even more, the metal rod started to serve as a director. To distinguish between these two manners, the maximum gain for both director and reflector is given in the radiation pattern below. The maximum gain for both cases is in the opposite direction. In this thesis, the length of metal rod is selected so as it acted as a reflector. This is due to a better front-to-back ratio presented by single metal rod in the radiation pattern report below.

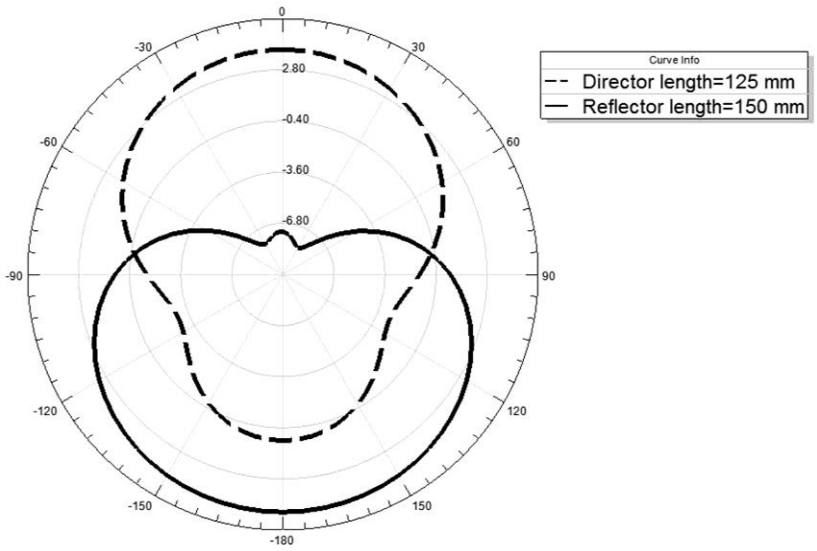

Figure 4.11 The gain comparison between director and reflector.

4.4.2 Effect of changing the distance

The distance between the metal elements and the centre of resonating conductor has minimal impact on the shape of radiation pattern. However, the impact is observed on the maximum gain and front-to-back ratio of the radiation pattern. The result from the preliminary analysis of radiation pattern is summarised in the graph below. The distance between the metal rod and the centre of resonating patch is varied and maximum gain for each case is obtained. From the graph, it can be seen that the maximum gain for the reconfigurable antenna is achieved when the metal rod is located 58 mm or one-fifth of the free-space wavelength from the centre of patch antenna. The maximum gain of the radiation pattern is improved when the distance increases. However, the highest front-to-back ratio is achieved when the metal rods are placed 42 mm from the centre patch.

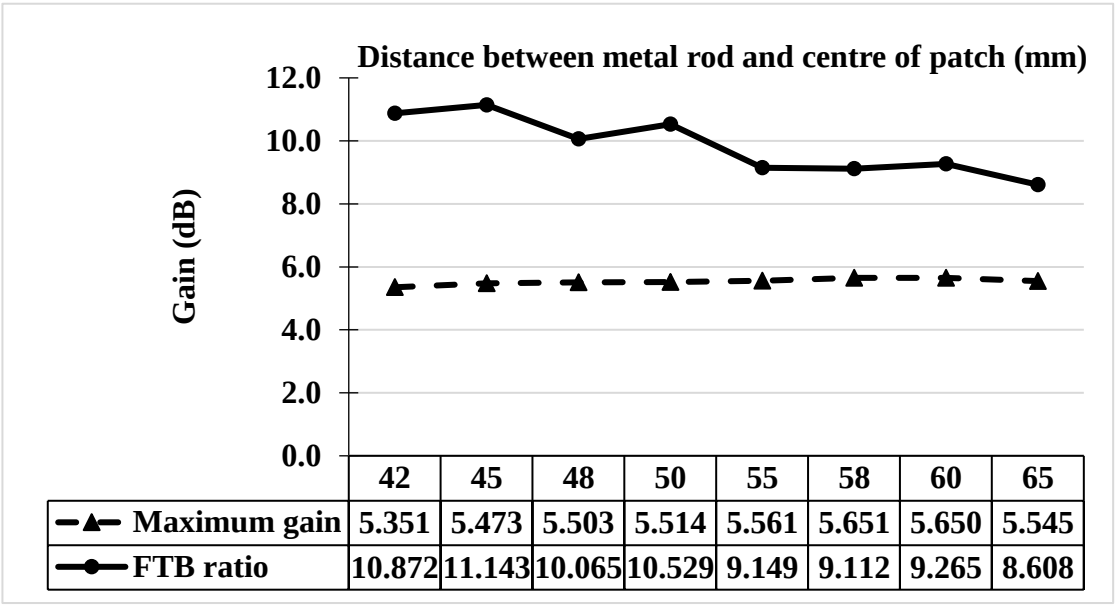

	42	45	48	50	55	58	60	65
Maximum gain	5.351	5.473	5.503	5.514	5.561	5.651	5.650	5.545
FTB ratio	10.872	11.143	10.065	10.529	9.149	9.112	9.265	8.608

Figure 4.12 The impact of the distance of metal rod and resonating conductor to the maximum gain of proposed antenna design.

4.4.3 Effect of increasing the number of metal rods

The number of directions covered by the proposed antenna depends on the number of metal rods attached to the patch antenna. As the shorted patch antenna has an omnidirectional radiation pattern, the reconfigured radiation patterns are covering the entire plane but limited to the complexity of the design. For instance, to have a large number of directions covered on single plane means the number of metal rods attached to the antenna is also increased. The position between the neighbouring metal rods will

be closer enough to introduce mutual coupling that will affect the fine beam resolution of the radiation pattern.

Table 4.1 below shows the number of metal rods attached to the antenna for different direction tuning. The expected main beam direction correlated to metal rod activated is also listed. The distance between the centre of the patch and the metal rod is maintained. However, there is a direction error occurs in Case D, E and F, as more metal cylinders are attached around the patch antenna.

Case	Number of metal rods	Expected beam direction	Actual beam direction	Reconfigurable direction
Case A	0	360°	360°	All direction
Case B	2	180°	180°	2
Case C	4	90°	90°	4
Case D	8	45°	45°	8
Case E	16	22.5°	25°	16
Case F	32	11.25°	10°	32

Table 4.1 The number of metal rods and its corresponding beam direction.

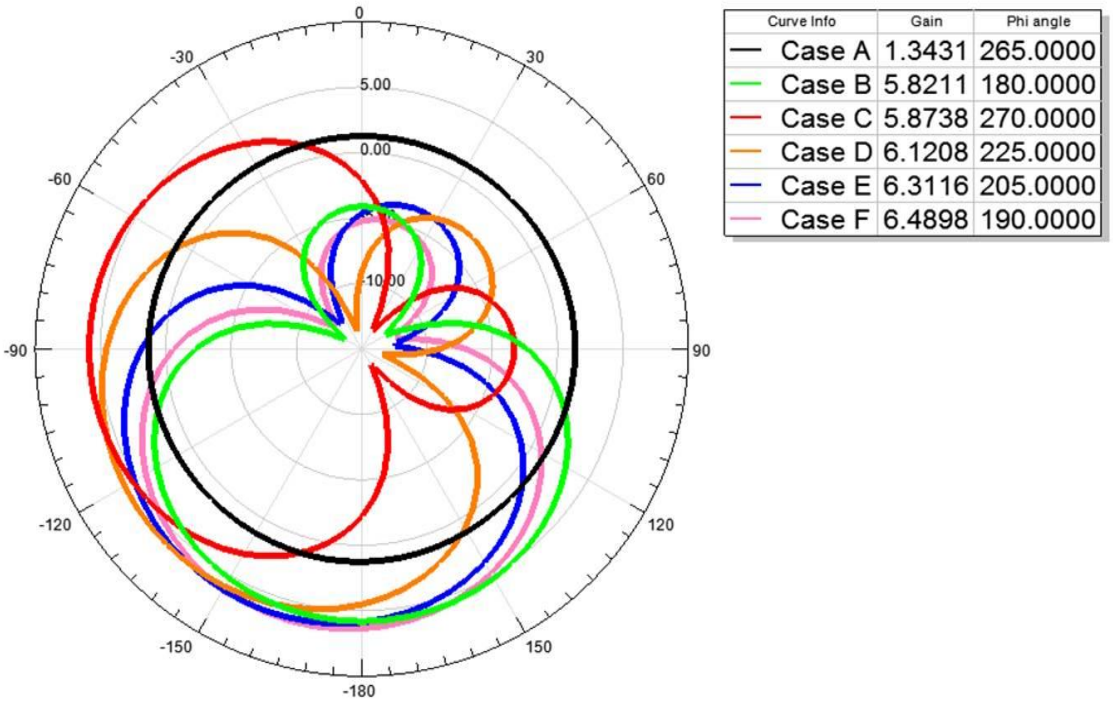

Figure 4.13 Radiation patterns for different number of metal rods attached to the shorted patch antenna.

4.5 Simulation and measurement

4.5.1 Return loss and S11

Simulations for the reconfigurable antenna were performed in HFSS to study the antenna performance. The measurement setup is conducted in a room big enough to reduce the multipath effect. The environment is kept clear and maintained stable position of the antenna. To measure the reflected power, the reconfigurable antenna is connected to the Port 1 of the Network Analyser. The simulation result demonstrates the reconfigurable radiation pattern resonates at 1 GHz, while a small shift is observed in the measured result towards 0.996 GHz. The magnitude of the reflection coefficient at this resonance is -11.202 dB as seen in Figure 4.14. The comparison between simulated and measured data shows that the magnitude of reflection coefficient during the practical experiment has reduced quite considerably. Furthermore, the starting point of the measured data does not correlate with simulated data. The errors might be caused by surrounding noises.

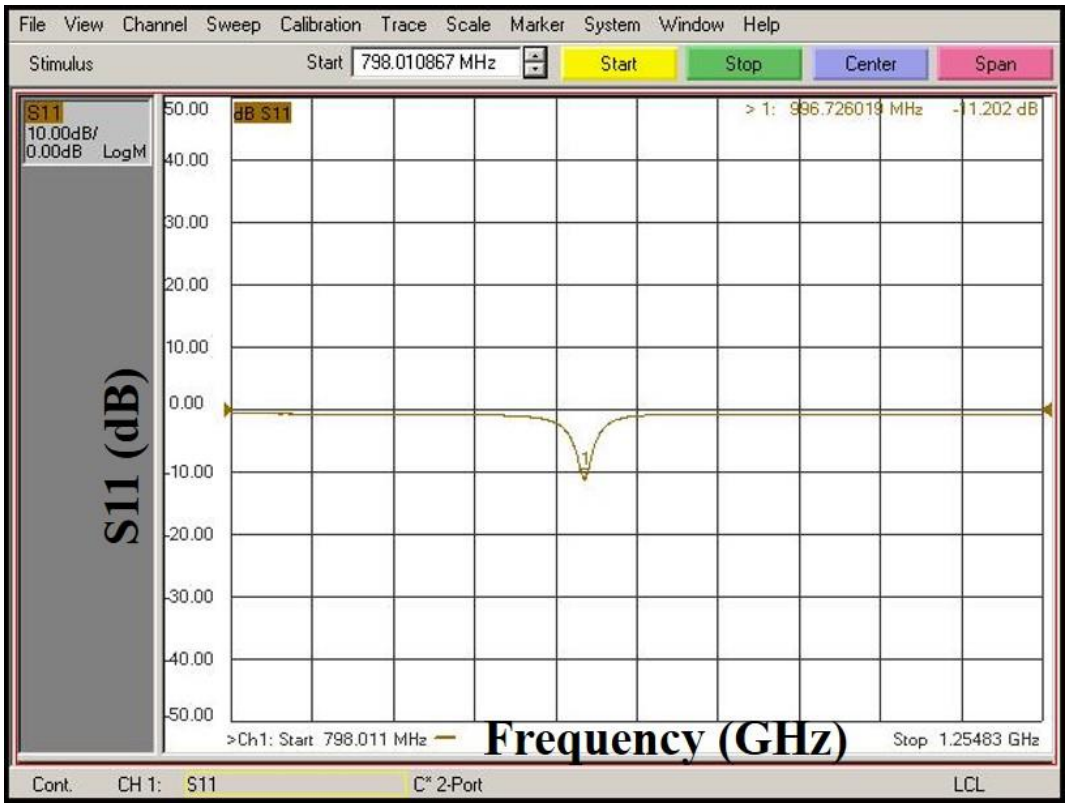

Figure 4.14 Measured return loss (S11) for the reconfigurable antenna as given by Network Analyser.

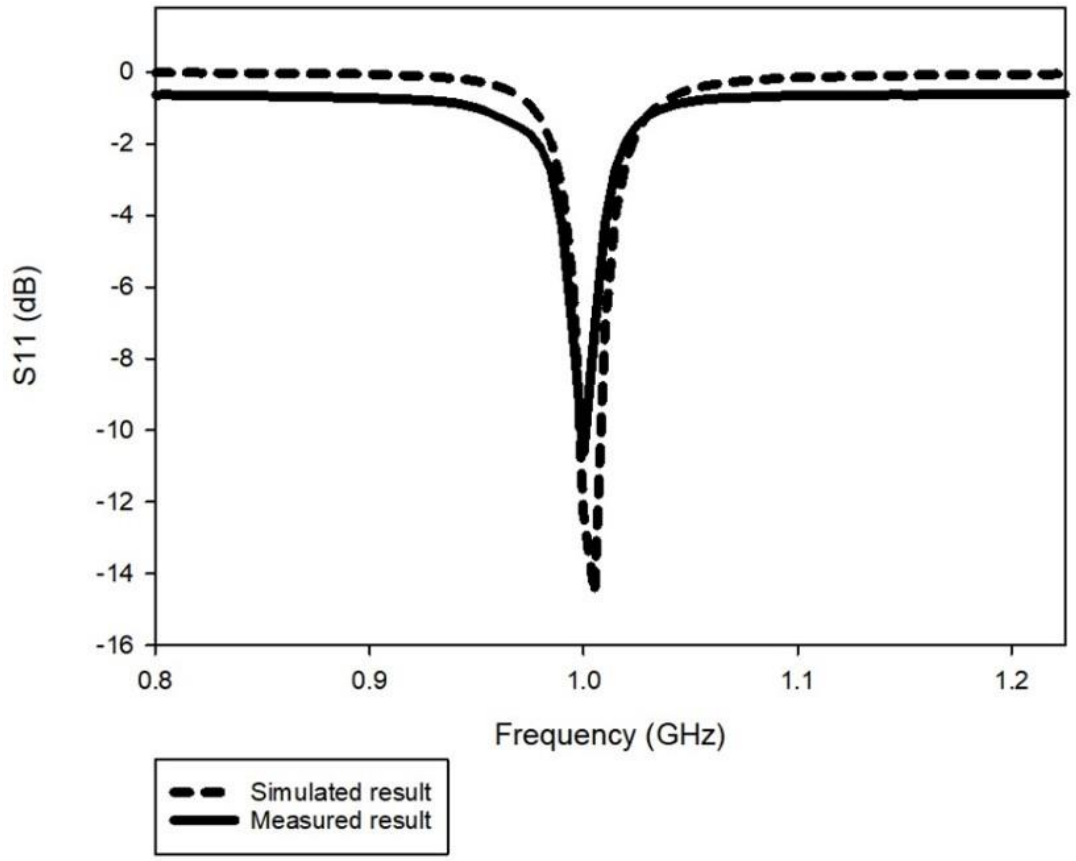

Figure 4.15 Simulated and measured return lost for the pattern reconfigurable antenna.

4.5.2 Radiation pattern measurement

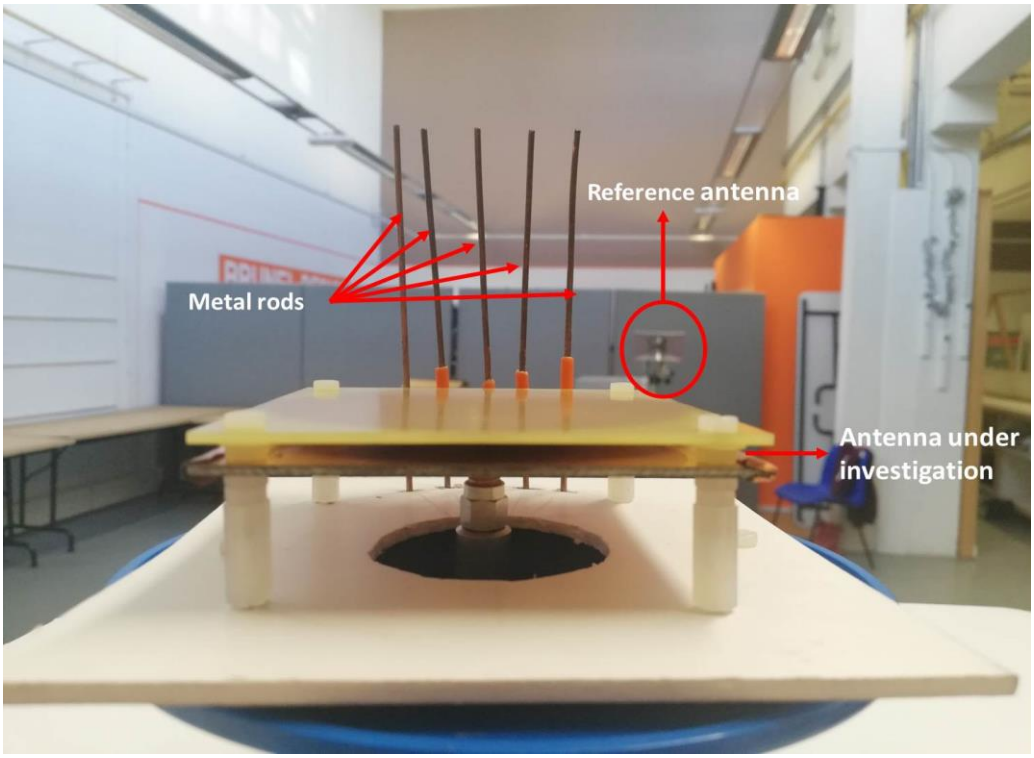

Figure 4.16 Measurement setup for the pattern reconfigurable antenna.

Figure 4.16 shows the setup of the pattern reconfigurable antenna during the measurement. Horn antenna is used as a reference antenna and positioned 5 metres from the antenna under investigation. For measuring the radiation pattern, reference antenna is connected to Port 1 as transmitter and antenna under investigation is connected to Port 2 as a receiver.

The result of radiation patterns for the different position of metal rods is shown below. For comparison purpose, the simulated and measured radiation patterns in the XY-plane at 1 GHz for different positions of metal rods are presented in Figure 4.17, 4.18, and 4.19. The comparison between the simulated and measured results shows a good agreement concerning the shape of radiation pattern. The maximum of radiation pattern is opposite to the position of metal rods, validating the proposed design. When the metal rod is activated at 0°, the maximum gain is at 180° as seen in Figure 4.17. In that order, when metal rod is activated at 10° and 20°, the maximum gain of radiation pattern can be seen at 190° and 200° respectively. However, the real antenna gain level for the measurement data is overlooked as more focused is put onto the shape of radiation pattern.

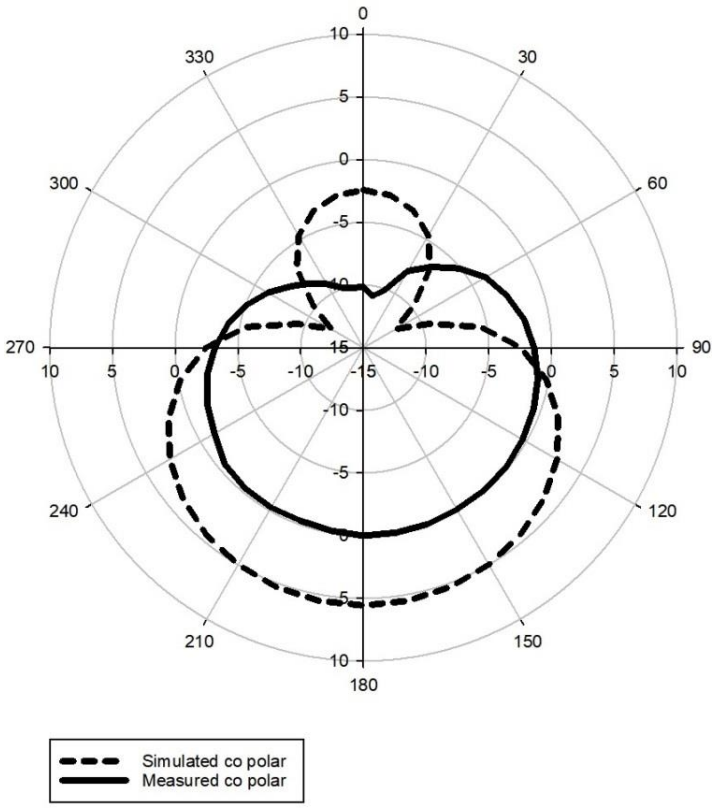

Figure 4.17 Radiation pattern of the reconfigurable antenna for metal rod activated at 0° on azimuth plane.

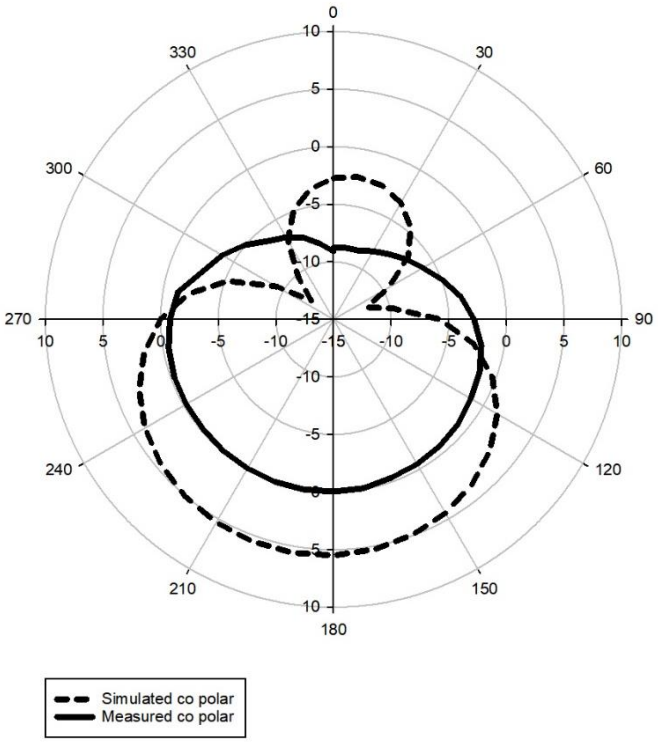

Figure 4.18 Radiation pattern of the reconfigurable antenna for metal rod activated at 10° on azimuth plane

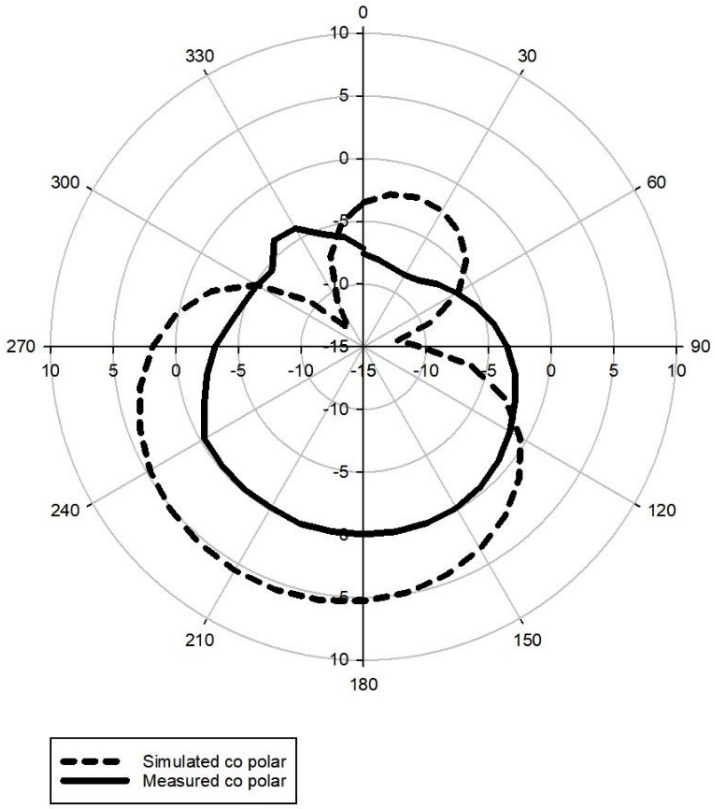

Figure 4.19 Radiation pattern of the reconfigurable antenna for metal rod activated at 20° on elevation plane.

To compare the changes in the direction of maximum gain clearly, the radiation pattern for different positions of metal rod is presented in a rectangular plot below. There are only small variations in the gain level of the reconfigurable antenna. In the case of metal rod positioned at 20°, there are some discrepancies in the measurement conducted. This might be due to the slight changing the environment of the experiment. Nevertheless, the measurement data analysis is consistent with the simulated data.

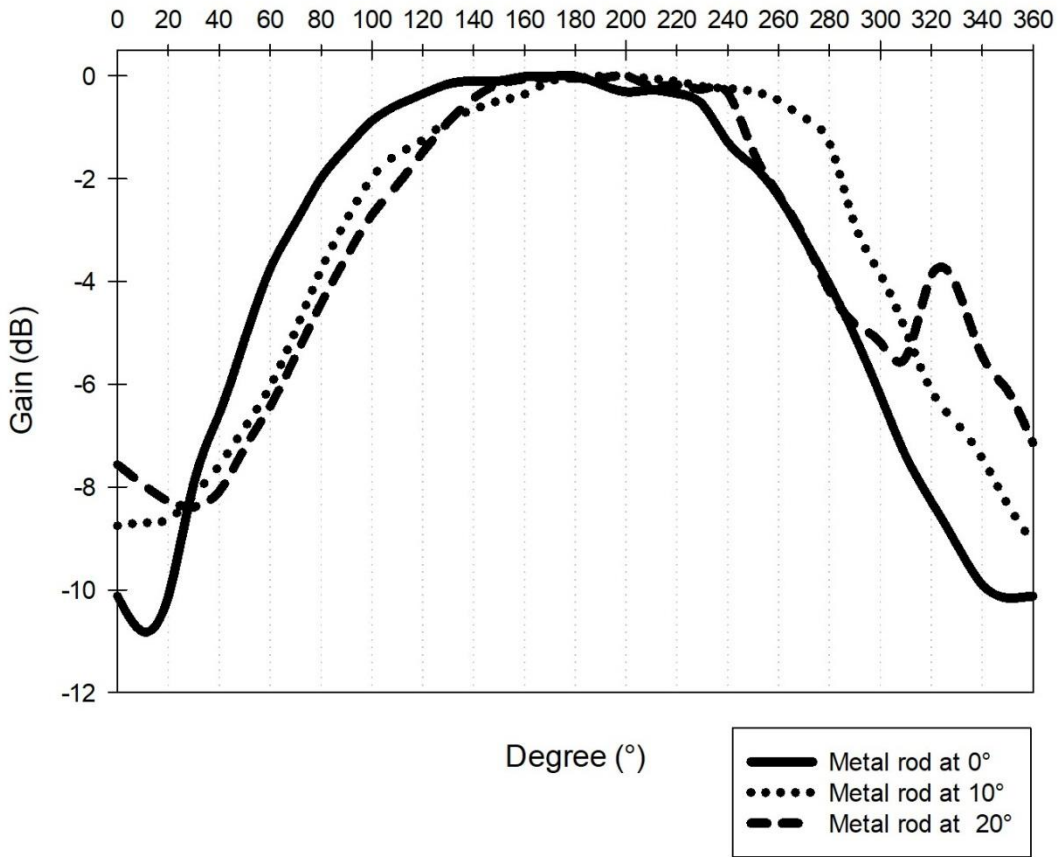

Figure 4.20 The changes in measured radiation pattern with different position of metal rods activated.

4.6 Summary

In this chapter, a pattern reconfigurable antenna is designed and fabricated. The radiation performance of the antenna is studied and compared with the simulated result. The radiation pattern changes as a metal rod is inserted into the shorted patch antenna design. The direction of maximum radiation pattern changes with different position of metal rods activated. The metal rod acted as a reflector when it is activated. The measurement data shows a good agreement on the change of radiation pattern shape. Some inconsistency in the measurement might be due to the multipath losses as the experiment is taken not in optimal environment. The PIN diodes are simulated as ideal lumped components without considering the actual P-I-N junction and depletion region.

Chapter 5 Miniaturisation of the radiation pattern reconfigurable antenna.

5.1 Introduction

The pattern reconfigurable antenna with fine direction resolution as proposed in the previous chapter has a quite large dimension in whole. The metal element functions as reflector has a length of half free-space wavelength stick out from the antenna. Miniaturisation is intended to reduce the overall size of the reconfigurable antenna without significant performance degradation to fit the design into a practical application. In this chapter, a miniaturisation on the antenna size as a whole is attempted. The metal rod size of half free-space wavelength (λ/2) reduced to almost one sixth of free-space wavelength (λ/6). The theory behind the miniaturisation of the parasitic structure is explained in detail in Section 5.2 of this chapter. The length of the metal rod is reduced by adding inductor with specific value to the parasitic structure. The performance analysis of the antenna is conducted in Section 5.3. The radiation pattern and frequency response of the proposed antenna design is studied and presented here. The parameters that show the most effect on the antenna design are the inductor value as well as the length and distance of the parasitic structure from the centre of radiating conductor. The parametric analysis of the antenna design is described in Section 5.4. Subsequently, the measurement data of the reconfigurable antenna is compared with simulation result. Any discrepancies from the expected result are reported in Section 5.5 of this chapter. Conclusively, all the result for this chapter is summarised in Section 5.6.

5.2 Miniaturisation techniques

Extensive research has shown that there a various techniques for antenna miniaturisation has been explored in the antenna designs up to this date. Large demand for a small and compact size of antenna with an acceptable degree of antenna performance has forced more antenna researchers to extend their designs. For a planar antenna, shorting and folding of the radiating patch has been a commonly used technique to reduce the size of the antenna[96][97]. This technique has been popular due to its cost efficient, but the shortcomings of the techniques come from the gain loss and low directivity[98].

The engagement of dielectric substrate with high effective permeability and permittivity values also has been proven to reduce the size of microstrip antenna[99]. However, the high cost of fabrication for such dielectric limited the use of this technique. Another technique is by reshaping the patch[100] or introducing slots into the patch[101][102]. This will result in antenna diminishment while maintaining high bandwidth. It has also proven to improve the gain and efficiency of the antenna[98].

Another interesting technique is by using metamaterial structure into the design which resulted in high degree of miniaturisation[103]. However, the technique has shortcomings of limited bandwidth and low efficiency. Due to the unnatural resources of metamaterial, the antenna geometry is complicated with no certain standard in antenna procedure.

One more miniaturisation technique is by incorporating reactive load into the transmission line structure. The reactive loads, either inductive or capacitive, introduces time delay (phase shift) and slows the wave propagation[104]. Antenna design with inductive loadings in [105][106] and capacitive loadings in [107][108][109] have shown to be successful in reducing the antenna size. Then again, this method has high ohmic losses due to the additional series resistance, which further reduce the gain.

5.3 Principle of operation

One of the major concerns in pattern reconfigurable antenna design in Part 4 is the length of metal rod. It is made longer than resonant length, so that the induced currents are in such a phase that it reflects the power away from the metal rod. In this chapter, miniaturisation of the metal rod is conducted by placing two inductors in series with parasitic structure. The main idea is to physically adding inductance to the parasitic structures as a replacement to the dimension.

The purpose of this chapter is to conduct a miniaturisation on the antenna design while having the same antenna characteristic and performance. The metal rod addition to the shorted circular patch antenna has been a trigger to the changes in the radiation pattern of patch antenna. A full-length metal rod has a size of $\lambda/2$ to operate, which is impractical for mobile application and small communication devices. Thus, the measurement is reduced by physically adding inductance to an element. There are multiple methods for miniaturisation. However, in this case, adding a lump inductor to the element is the most relevant. The inductors with specific value can compensate the inductive impedance introduce by a longer metal rod.

The full-length of metal rod is 150 mm, which is reduced to 45.5 mm which is three times smaller. The reduction is caused by the introduction of two inductors in series with the parasitic element. The value of the inductor is determined through optimisation function in HFSS. During the optimisation analysis, for every mesh point set, the value of appropriate inductor is selected to enable the parasitic to have a same behaviour as the full-length metal rod. Appropriate length of the parasitic element is also considered during the optimisation analysis.

During initial analysis, the shape of parasitic element is different. However, due to the practicality and also the availability of inductor with certain values in the current market, the shape of metal element is altered. The shape of the parasitic element is as shown in Figure 5.1 below.

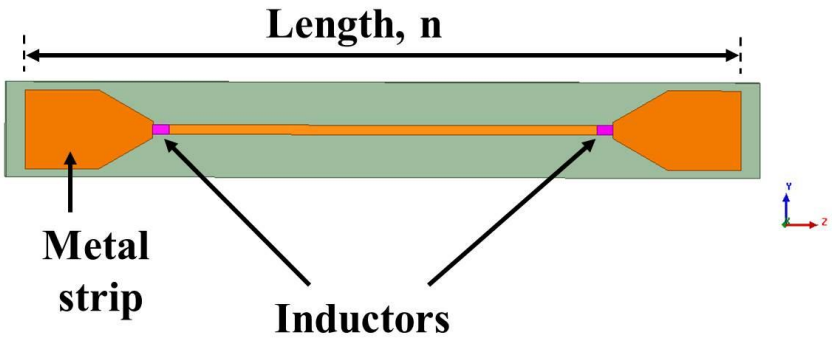

Figure 5.1 The build-up for the parasitic element with inductors in series for miniaturisation.

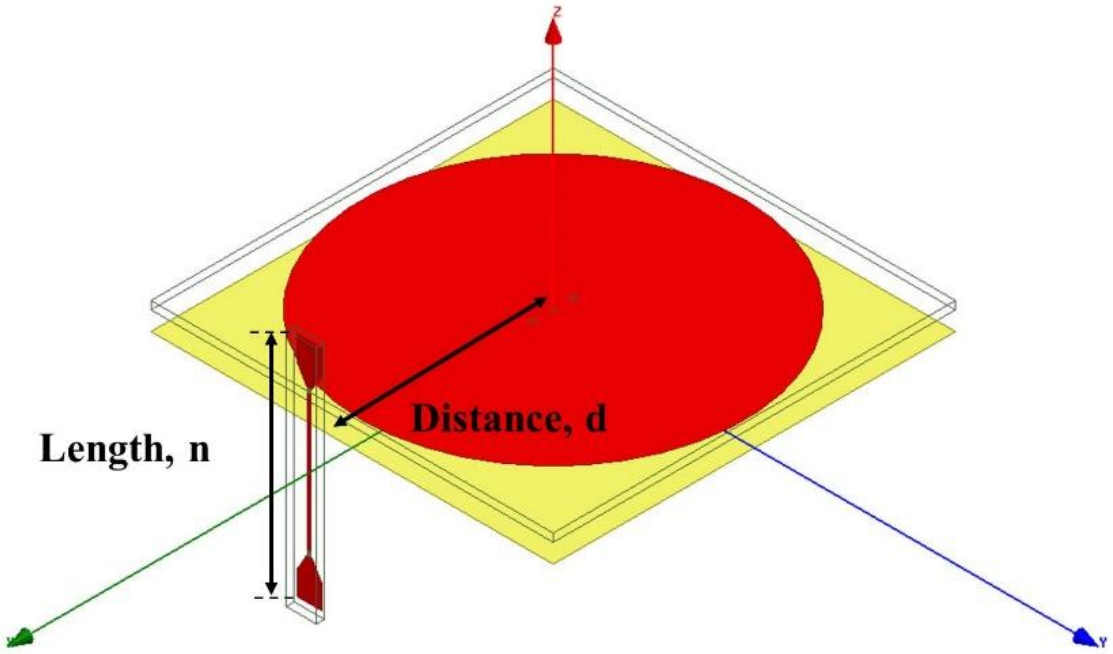

Figure 5.2 The construction of proposed antenna design for miniaturisation.

5.4 Performance analysis

5.4.1 Radiation pattern

The miniaturisation of full-length metal rod is conducted by the addition of two inductors in series to a parasitic element. The inductors with specific value of 53 nH are located at an equal distant from the middle of the parasitic element. The addition of real value inductors into the parasitic element has replaced the inductance introduced by the longer dimension of metal rod. Thus, the parasitic element with total length of 3/20 λ produces the same result as a full-length metal rod.

Figure 5.3 provides the overview of the changes in radiation pattern with the addition of a single parasitic element replacing a full-length metal rod to the proposed antenna design. The parasitic element with inductors in series appeared as a reflector. The maximum gain is in the opposite direction to the parasitic element. As can be seen from the figure, the omnidirectional radiation pattern of shorted circular patch antenna has transform into a directional radiation pattern where the maximum gain is in opposite direction of the position of parasitic element. This has proven that the parasitic element has conducted the same performance as the metal rod in previous chapter.

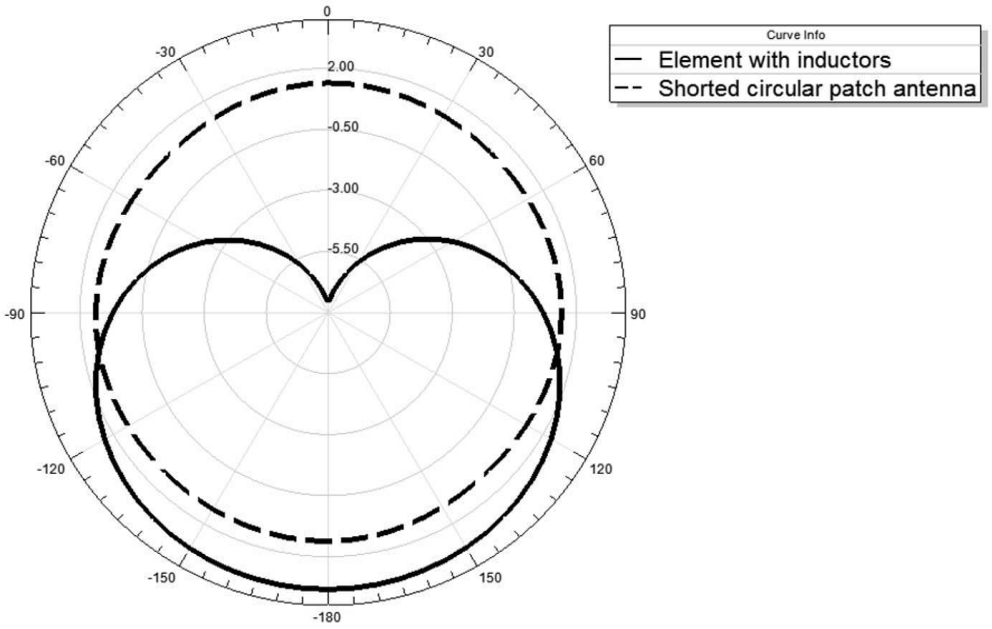

Figure 5.3 Radiation pattern with the insertion of single parasitic element.

In the above figure, there is a clear trend of the changes in the radiation pattern. The addition of inductor with specific value in series to the element has demonstrated the same performance as a full-length metal rod. The reduction in length of the element is about three times of the initial size. The comparison of the maximum gain for both elements is shown in the Figure 5.4 below. The front-to-back ratios for both cases are also observed. It is clear that the maximum gain for metal rod is greater than the element with inductors. However, it is noteworthy to notice that the front-to-back ratio for element with inductor is more significant compared to metal rod.

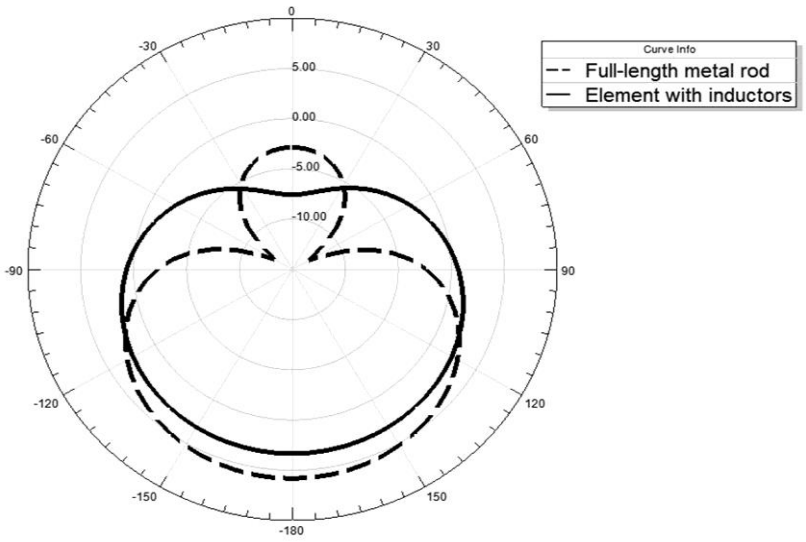

Figure 5.4 Comparison of radiation patterns when using metal rod and parasitic element.

To investigate the changes of radiation pattern, an element is placed at different position and activated individually. The individual parasitic element is placed at 0°, 10° or 20° from the centre of the antenna. It is important to investigate the changes in radiation pattern with regards to the slightest change in location of single element. Each of the elements is activated individually and the change in radiation pattern is observed. From the Figure 5.5, it is clear that the parasitic element with inductors inserted has the same capability as metal reflector in previous study. Furthermore, as seen from the figure, the antenna is quite sensitive as the radiation pattern changes accordingly with different position of activated element.

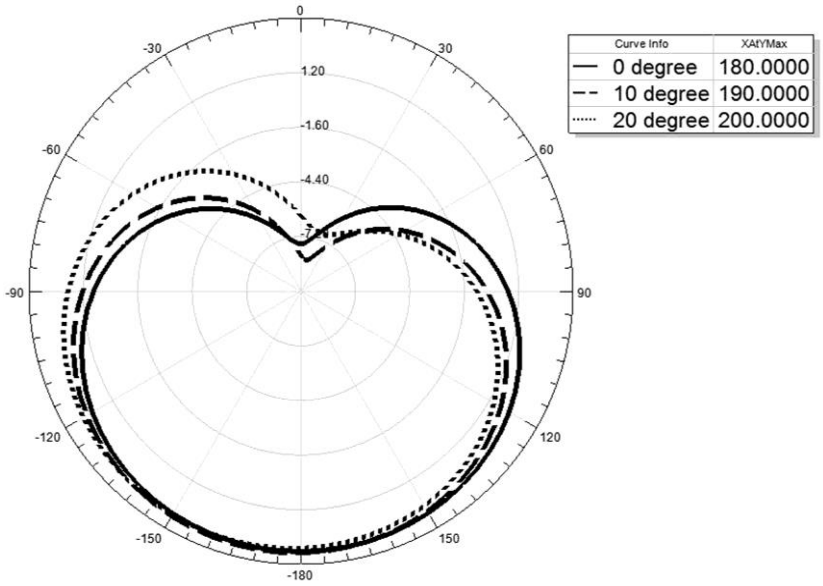

Figure 5.5 Radiation patterns when single activated parasitic element is located at different location.

Subsequently, the changes in the radiation pattern with the activation of parasitic element at different location are studied. Multiple parasitic elements are situated around the shorted circular patch antenna with 10° distance to each other. Each of the parasitic elements is activated individually. The changes in radiation pattern can be observed in Figure 5.6 below. As can be seen in the figure below, the maximum gain for each case has diminished drastically. In general, the direction of the maximum gain still present the parasitic element has been behaving as a reflector. However, the reduced in the maximum gain is possibly caused by the mutual coupling occurred when the parasitic elements are located adjacent to each other.

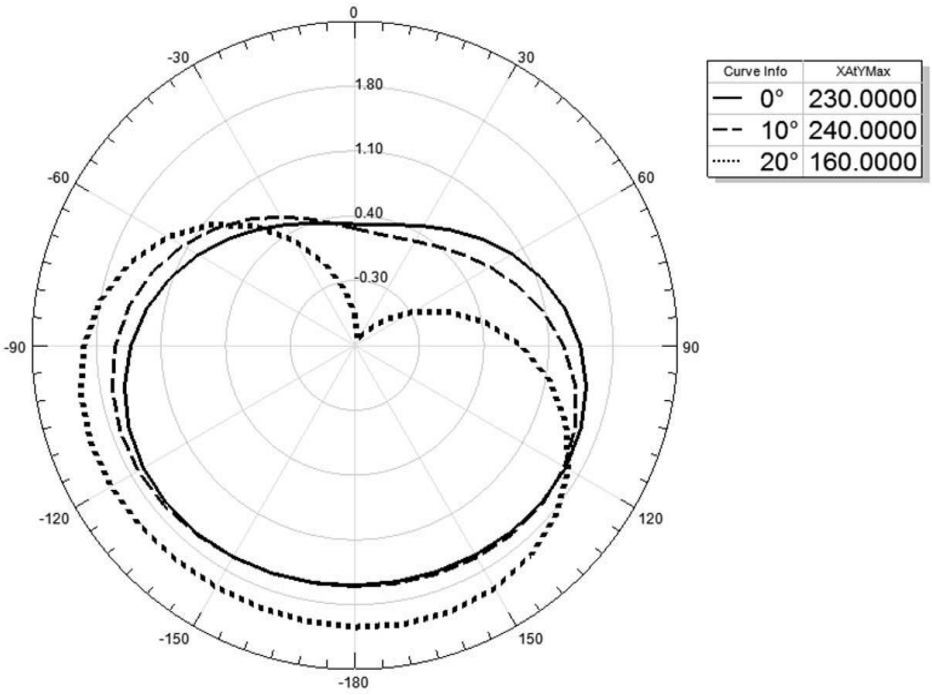

Figure 5.6 Radiation patterns when multiple elements are placed around patch antenna with single activation.

5.4.2 Return loss

Return loss or frequency response of the proposed antenna design is maintained at 1 GHz. The figure below depicted the S11 for the case where the metal rod is replaced by the parasitic element. When simulated in HFSS, the frequency response for the proposed antenna design is maintained at 1 GHz and only the radiation pattern of the antenna performance is change. In this way, the pattern reconfigurable antenna can be achieved. Figure 5.7 shows the return loss of the shorted patch antenna when the metal rod is replaced by the element with inductors. As seen in the figure, the S11 is maintained at 1 GHz, plus the amount of radiated power is increase when using parasitic element with inductors.

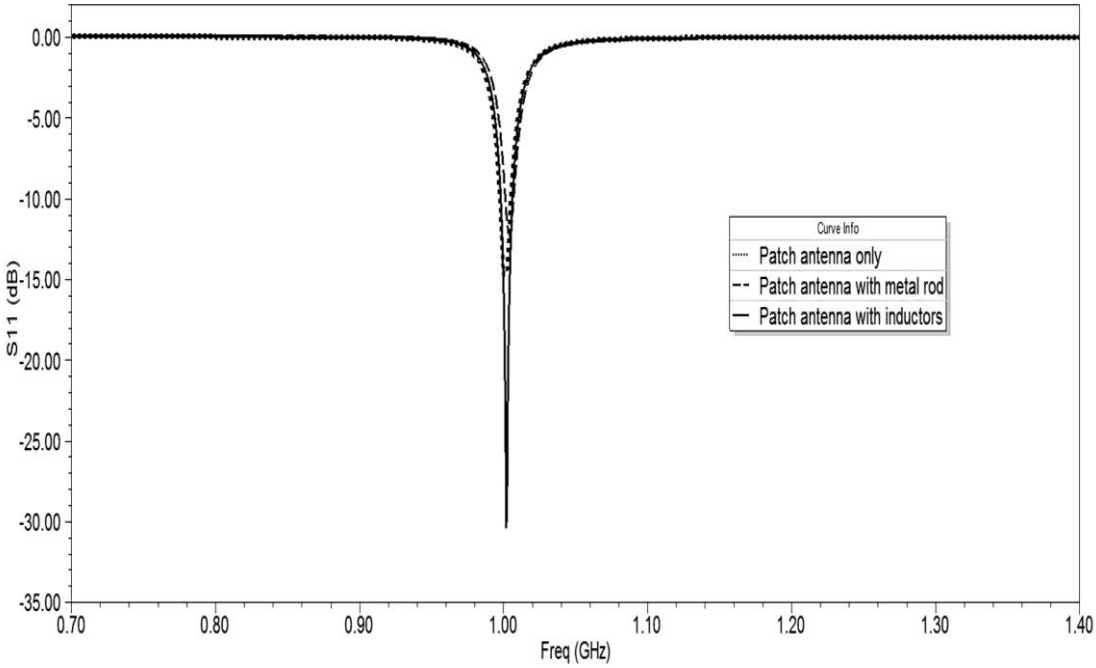

Figure 5.7 Simulated return loss for the proposed antenna.

5.5 Parametric analysis

The real value inductors are placed into the element as a substitute to the inductance acquired from the longer length of metal rod. The configuration of the parasitic element using single inductor is studied in this part of the chapter. While the inductance value is crucial, the formation of parasitic element is equally important to ensure the same radiation performance as metal rod. Another aspect to be considered is the value of the inductors. The values of the inductors need to be practical and real-world value. The impact of the parameters on the radiation pattern is described concisely in this part of the chapter. The parametric analysis and optimisation function in HFSS is operated to give the best result.

5.5.1 Single inductor configuration

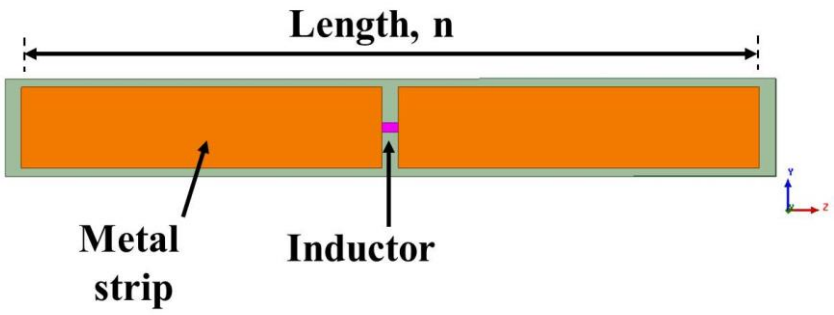

Figure 5.8 Parasitic element configuration using single inductor.

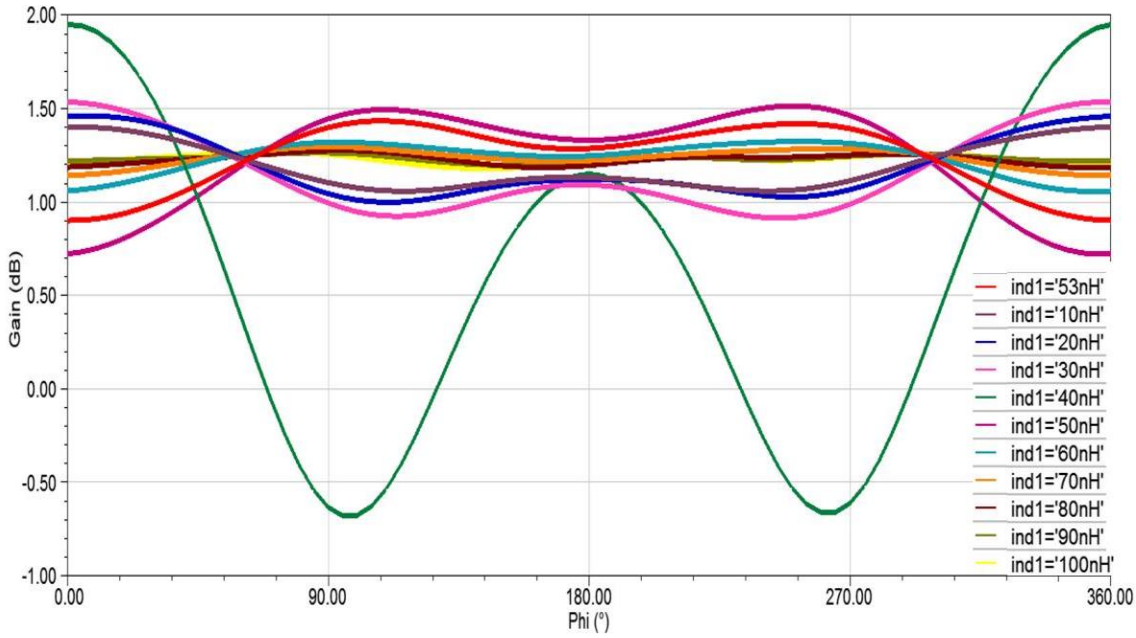

Figure 5.9 Radiation pattern for different values of inductor in a single inductor configuration.

During the antenna design process, other configuration of the parasitic elements has also been considered. The figure above shows the configuration of metal strip with single inductor. The radiation performance of the antenna is plotted in rectangular graph for better understanding and given in the Figure 5.9. The size of inductor is maintained at 1 mm, the same size of practical inductor available in the market. Although the inductance values are varied, the parasitic element still failed to operate as a reflector. As can be seen in the graph, at some value of inductor, the parasitic element serves as a poor director. For that reason, the number and position of inductors, as well as the shape

of the metal strip are similarly crucial for the parasitic element to serve as a reflector and maintain the same radiation performance given by metal rod. Thus, the proposed antenna is designed using two inductors in the parasitic element to serve as a good reflector.

5.5.2 Different values of inductors

The reflector capabilities of metal rod is due to the element being inductive, which means the current induced lags the current induced by the radiating patches, thus causes phase distribution to occur. Two real value inductors are inserted into the design to replace the inductance coming from longer length of metal rod. Thus, the parasitic element can have a shorter dimension and at the same time behaving as equal as the full length metal rod. However, another aspect to be considered is the real world value of the inductor. The real value inductor has a fixed inductance which is available in the market. There are some values that are not available in the market as well.

The parametric analysis conducted on different value of inductors placed in series with the metallic element to see the changes in the radiation pattern. As can be seen from the graph below, the radiation patterns show that at certain value of inductance the element does not behave as a reflector. When using 50nH inductor, the parasitic element has enough inductance to act like a reflector and thus, causes the radiation pattern to have a maximum gain in the opposite direction of the element. Other value of inductors does not provide sufficient inductance which indicates that the element fails to behave as a reflector.

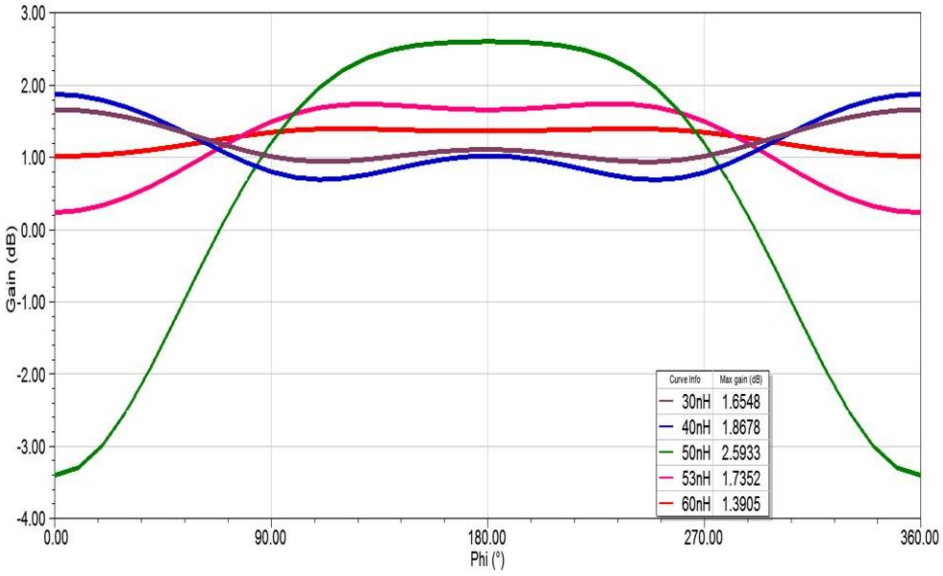

Figure 5.10 Radiation pattern in rectangular plot for different inductor values.

5.6 Simulation and Measurement

5.6.1 Return loss and S11

The measurement for pattern reconfigurable antenna using miniaturise element to replace the metal rod is conducted in a capacious room. The experiment area is kept clear from any devices that can cause multipath effect. The measurement of S11 for the reconfigurable antenna is repeated using miniaturised reflector. The pattern reconfigurable antenna is connected to Port 1 of the Network Analyser. Simulation data obtained from HFSS is compared to the measurement data from the experiment. As seen from the Figure 5.12 below, the antenna resonates at 1 GHz during the simulation whilst the frequency shifted a bit during the experiment.

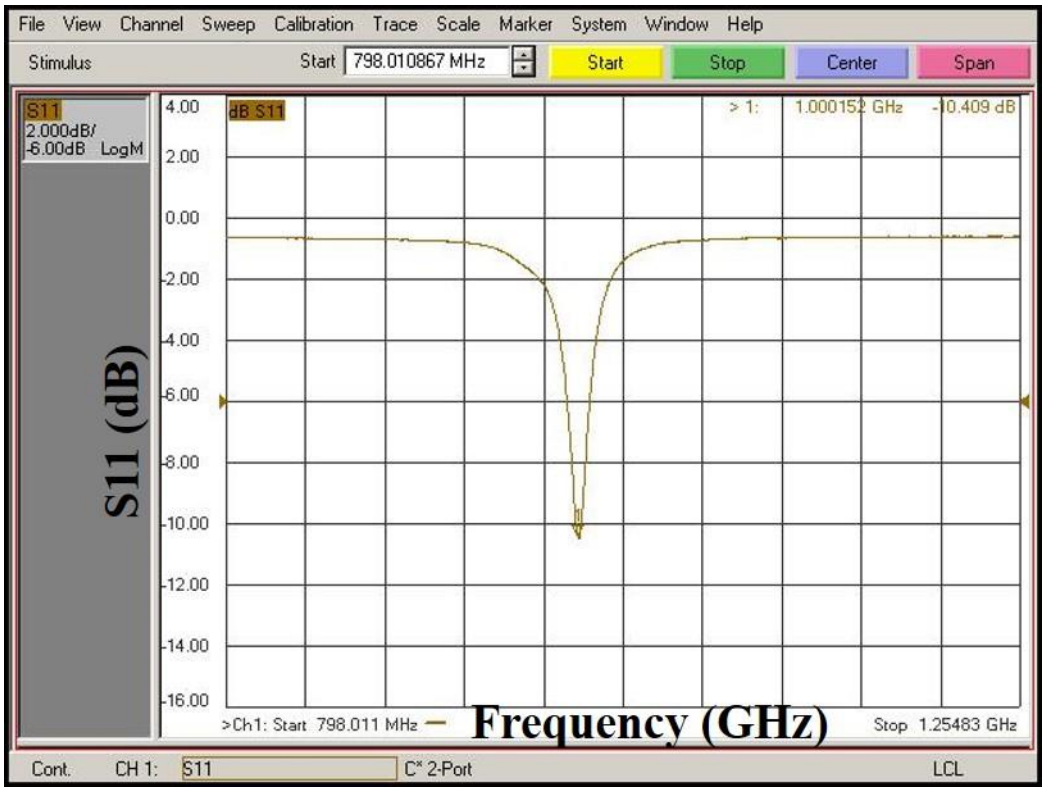

Figure 5.11 Measured return loss (S11) for the reconfigurable antenna with miniaturised reflector as given by Network Analyser.

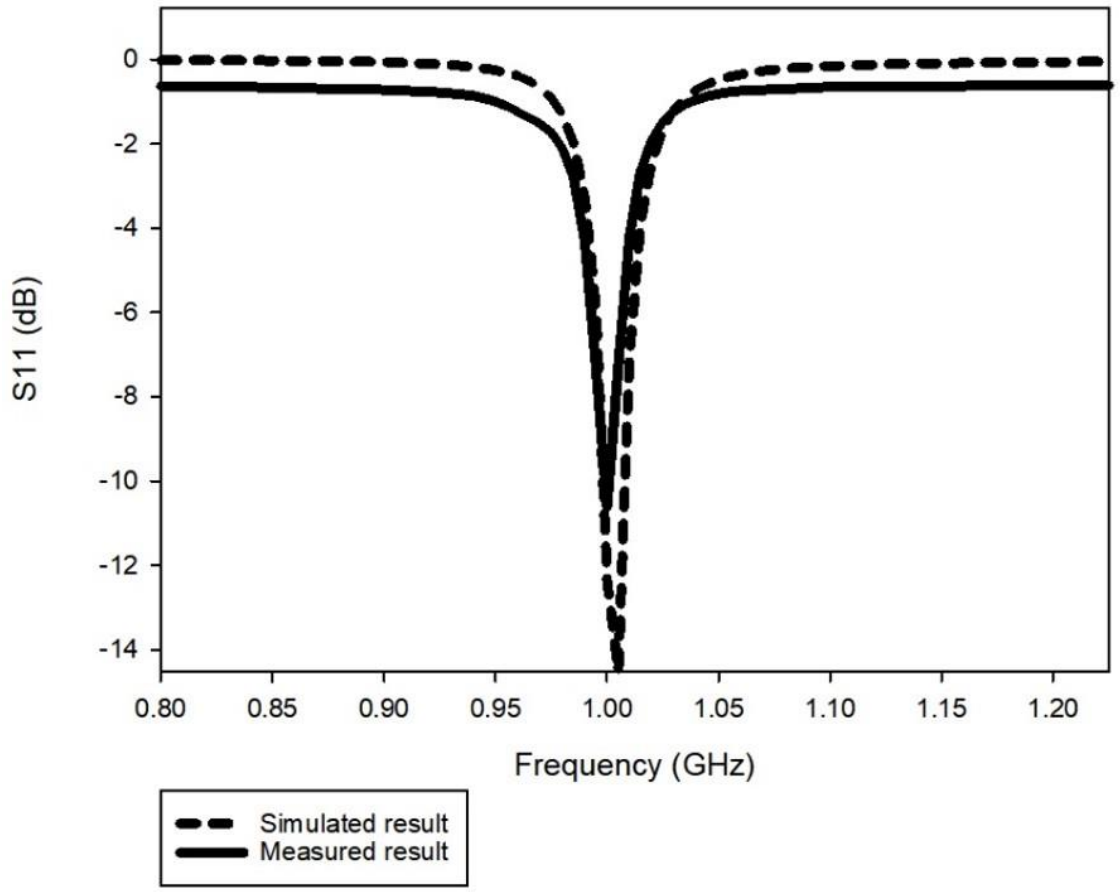

Figure 5.12 Simulated and measured return lost for the reconfigurable antenna with miniaturised reflector.

5.6.2 Radiation pattern measurement

During the measurement of radiation pattern, the horn antenna is connected to Port 1 of the Network Analyser while the proposed antenna is connected to Port 2. Both antennas are elevated far above the ground to reduce reflection from floor. Figure 5.13 shows the arrangement for the measurement of radiation pattern. As seen in Figure 5.9, two inductors are soldered to Element 1 which signifies the element is activated. Element 1 is positioned at 20° from the centre of radiating patch. The parasitic element is positioned in 0°, 10° and 20° from the centre of radiating patch. During the preparation of the experiment, inductors value of 53 nH is chosen as it gives the best result for practical measurement.

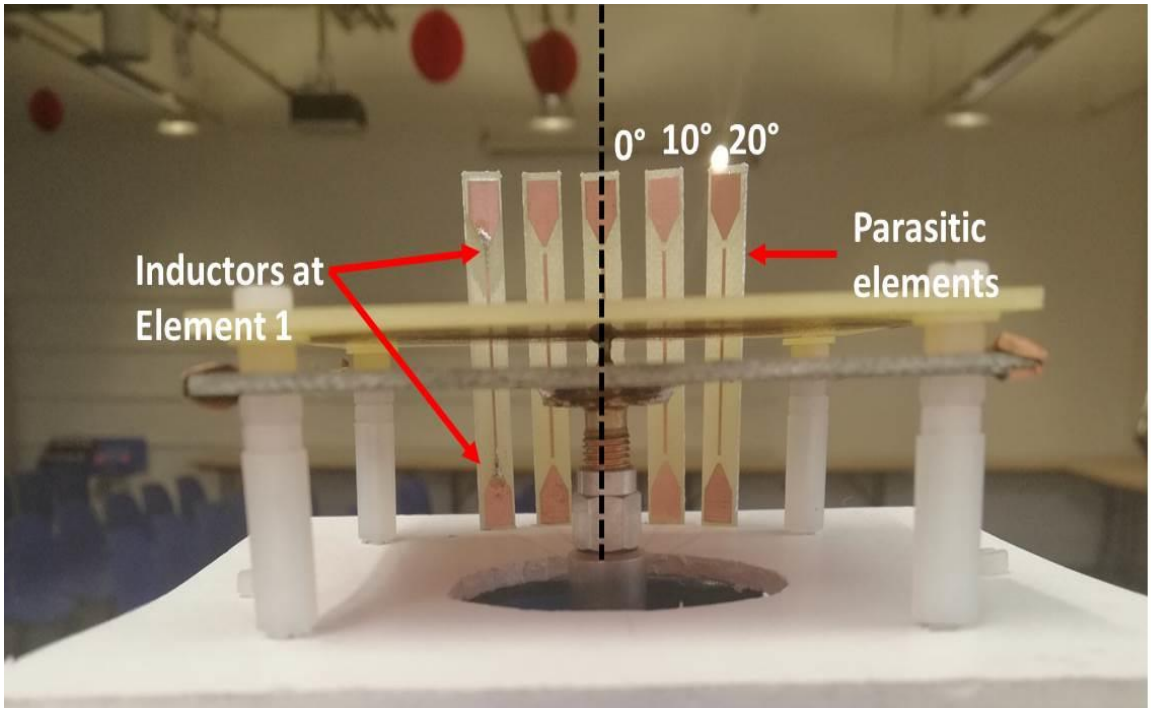

Figure 5.13 Measurement setup for the pattern reconfigurable antenna using parasitic element with inductors.

The purpose of this chapter is to miniaturise the size of metal rod while maintaining the same behaviour of the reflector. The result of comparison between the simulation conducted in HFSS and experimental results are presented below. When the element at 0° is activated, the radiation pattern is shown in Figure 5.14. The radiation patterns when single element activated at 10° and 20° are presented in Figure 5.15 and 5.16 respectively. The results comprises of radiation pattern on azimuth plane at 1 GHz for different position of element activated around the patch antenna. From the results presented, the shape of radiation pattern did change accordingly when different position of element is activated. However, the maximum beam direction is not exactly according to the position of the element. There are some discrepancies in the direction of maximum gain when individual element is activated. The maximum gain is at 210° when element at 0° is activated and the maximum gain occurs at 220° for both cases where the element at 10° and 20° is activated. The inconsistencies might be due to the mutual coupling occurred between the elements positioned close to each other.

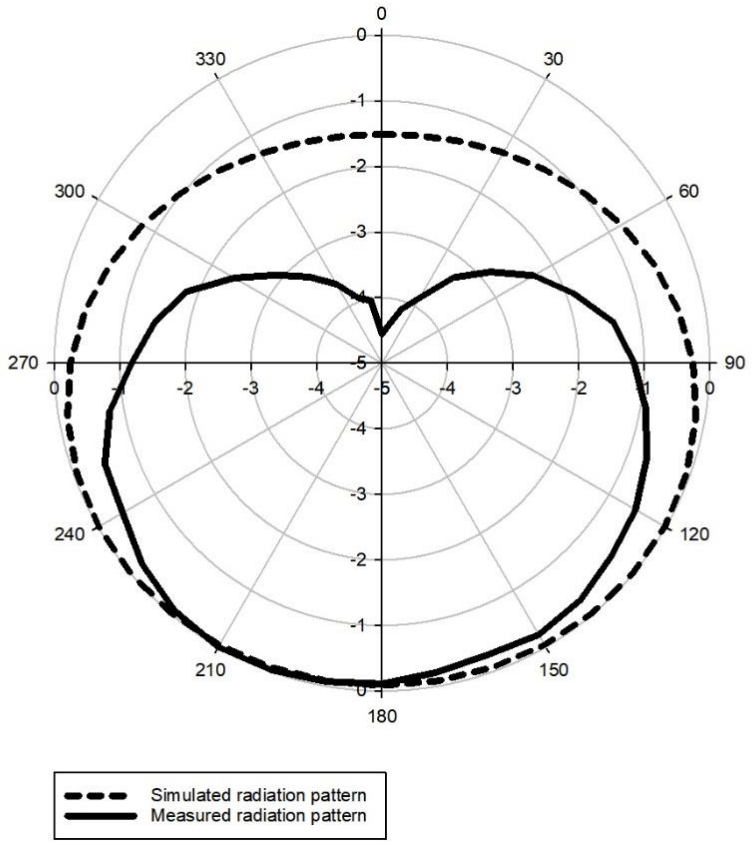

Figure 5.14 Radiation pattern of the reconfigurable antenna for element activated at 0°.

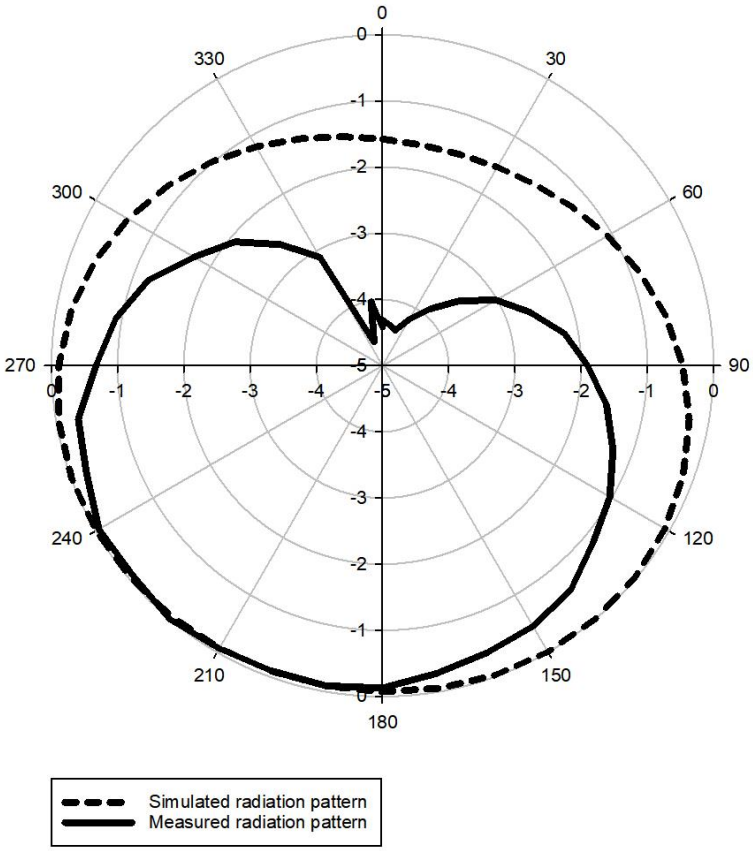

Figure 5.15 Radiation pattern of the reconfigurable antenna for element activated at 10°.

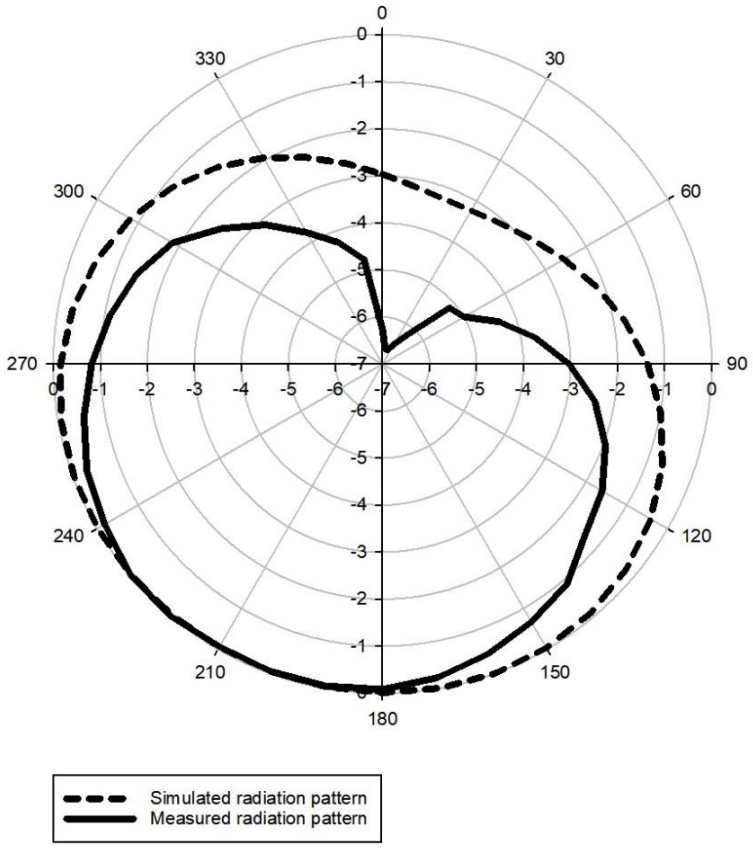

Figure 5.16 Radiation pattern of the reconfigurable antenna for element activated at 20°.

The comparison for each case where different elements is activated at different position is well presented in a rectangular plot below. From the graph, it is clearly shown that the direction of maximum gain for each case is not in consequences to the location of reflector. The inconsistencies of the maximum gain direction may perhaps influence by the close position of the elements. The elements are located close enough to each other to initiate a mutual coupling which affected the direction of maximum gain. Also, the multipath effect as well as power reflection from the ground might impact the measurement results. Even though the noises are kept at minimum and the surrounding area is kept clear of any electromagnetic devices, without the Anechoic chamber, the environment is still not optimum for the experiment.

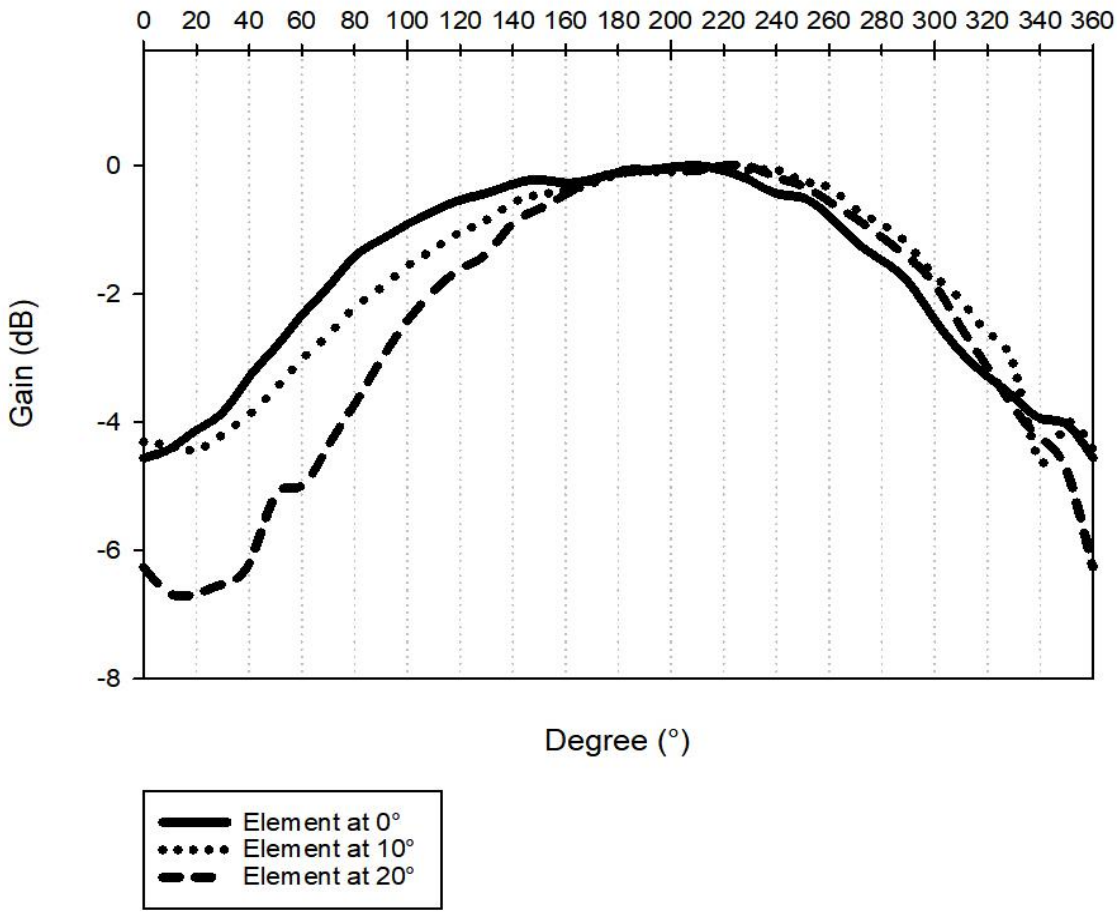

Figure 5.17 Rectangular plot for radiation patterns activated at different positions.

5.7 Summary

In this chapter, a miniaturisation on the pattern reconfigurable antenna is accomplished by exercising reactive loading (inductive) into the antenna design. The radiation performance of the miniaturised antenna is compared with the full-size reconfigurable antenna. There is a clear pattern of changes in direction of radiation pattern. However, the gain has reduced significantly. The simulation and measurement results are compared and show good agreement until the parasitic element are placed 10° apart from each other. When the parasitic element is position too close between each other, mutual coupling arises which affected the result. Another factor might be due to the multipath losses from the surrounding.

Chapter 6 Conclusion

6.1 Discussion

Advanced wireless system necessitate an antenna with the ability to transmit and receive signal in all horizontal direction equally, and at the same time can be a directional antenna when preferred. Therefore, the construction of radiation pattern antenna is crucial to feed the demand. Reconfigurable antenna has a capability to change its parameter; i.e. frequency, radiation pattern and polarisation, without significant change in antenna structure.

Throughout this thesis, a patch antenna with an omnidirectional radiation pattern is designed and tested. A patch antenna is widely used because of its low profile design. A standard patch antenna has a directional radiation pattern. In the proposed antenna design, air dielectric is utilised to give the omnidirectional radiation pattern. By having an omnidirectional radiation pattern, it will be beneficial to incorporate the shorted patch antenna for an application that transmit or receive signal from wide variety of directions. The proposed antenna design also allows a full coverage of transmission in horizontal direction. Furthermore, the incorporation of shorting pin resulted in a size reduction of the patch antenna. Integrating more than one shorted pin into the patch antenna ensure a more stable design.

The antenna in aforementioned chapter is modified, so that its radiation properties change by insertion of metal rod. The metal rod with full length of $\lambda/2$ acted as a reflector, thus gives significant change in the direction of radiation pattern. The optimal length and distance of the metal cylinder is acquired through parametric analysis in HFSS. The hardware prototype of the antenna is fabricated. The frequency response and radiation performance of the antenna is measured and compared with simulation result. The measurement data shows a good agreement on the change of radiation pattern shape. Some inconsistency in the measurement might be due to the multipath losses as the experiment is taken not in optimal environment. The PIN diodes are simulated as ideal lumped components without considering the actual PIN junction and depletion region.

The problem with radiation pattern reconfigurable antenna in the previous chapter is the large dimension of the whole antenna. The size of metal rod affected the size of whole antenna design. Thus, a miniaturisation of the metal rod is attempted in the subsequent chapter. The miniaturisation of the antenna is accomplished by exercising reactive loading (inductive) into the antenna design. The metal rod is reduced to one third of its initial half-wavelength size by integrating two equivalent inductors on each side of the parasitic element. The shape as well as the best inductor value is obtained through parametric analysis conducted in HFSS. The comparison between the miniaturised antenna and full-size reconfigurable antenna shows a good agreement in terms of the direction of radiation pattern. The simulation and measurement results are compared and show good agreement until the parasitic element are placed 10° apart from each other. When the parasitic element is positioned too close between each other, mutual coupling arises which affected the result. Another factor might be due to the multipath losses from the surrounding.

6.2 Future works

The experiments are all conducted in a huge-spaced room to ensure minimal multipath effect. All preventive measures are taken into considerations. However, the experiment should be conducted in Anechoic chamber for a more accurate result. All the noises and losses can be eliminated. The orientation of the reference antenna and antenna-under-test must be aligned as well, which is the trickiest part of the experiment.

During this study, the application of PIN diode as a switch is not studied. The PIN diode has specific value of resistance during ON state. Even though the value is small, the effect it has on the signal should be investigated. Furthermore, the incorporation of PIN diode would require dc bias for activation, thus might affecting the signal as well. In the upcoming study, the impact of PIN diode should be highlighted to extensively comprehend the antenna design.

List of References

[1] I. A. and P. Society, *IEEE Standard for Definitions of Terms for Antennas*, vol. 2013. 2013.

[2] C. A. Balanis, "Antenna Theory: A Review," *Proc. IEEE*, 1992.

[3] Y. Huang and K. Boyle, *Antennas: From Theory to Practice*. 2008.

[4] T. D. Antenna, "FCC-1," vol. 510.

[5] C. A. Balanis, "Chapter 14," in *Antenna Theory: Analysis Design, Third Edition, by Constantine A. Balanis*, 2005, pp. 811–882.

[6] J. Wu, Z. Zhao, M. S. Ellis, Q.-H. Liu, and Z. Nie, "Printed double-dipole antenna with high directivity using a new feeding structure," *IET Microwaves, Antennas Propag.*, vol. 8, no. 14, pp. 1186–1191, 2014.

[7] P. Bevelacqua, "Antenna basics." [Online]. Available: http://www.antenna-theory.com/basics/gain.php. [Accessed: 01-Dec-2018].

[8] C. A. Balanis, "Chapter 2," in *Antenna Theory: Analysis Design, Third Edition, by Constantine A. Balanis*, no. 3, 2005, p. 34.

[9] N. A. Aziz, A. H. Radhi, and R. Nilavalan, "A reconfigurable radiation pattern annular slot antenna," in *2016 Loughborough Antennas & Propagation Conference (LAPC)*, 2016, pp. 1–4.

[10] M. S. Shakhirul, M. Jusoh, Y. S. Lee, and C. R. Nurol Husna, "A Review of Reconfigurable Frequency Switching Technique on Micostrip Antenna," *J. Phys. Conf. Ser.*, vol. 1019, p. 012042, Jun. 2018.

[11] Q. Li, T. Li, Z. Li, and J. Fang, "Unidirectional frequency reconfigurable bow-tie antenna array with AMC reflector," in *2017 11th European Conference on Antennas and Propagation, EUCAP 2017*, 2017, pp. 2221–2223.

[12] L. Ge and K. M. Luk, "Frequency-reconfigurable low-profile circular monopolar patch antenna," *IEEE Trans. Antennas Propag.*, vol. 62, no. 7, pp. 3443–3449, 2014.

[13] L. Ge and K. M. Luk, "A band-reconfigurable antenna based on directed dipole," *IEEE Trans. Antennas Propag.*, vol. 62, no. 1, pp. 64–71, 2014.

[14] A. Boukarkar, X. Q. Lin, Y. Jiang, and X. F. Yang, "A Compact Frequency-Reconfigurable 36-States Patch Antenna for Wireless Applications," *IEEE Antennas Wirel. Propag. Lett.*, vol. 17, no. 7, pp. 1349–1353, Jul. 2018.

[15] B. Suryakanth, "Design and Development of Aperture Coupled Rectangular Microstrip Antenna for Wide Band Operation," pp. 356–360, 2013.

[16] M. Shirazi, J. Huang, T. Li, and X. Gong, "A Switchable-Frequency Slot-Ring Antenna Element for Designing a Reconfigurable Array," *IEEE Antennas Wirel. Propag. Lett.*, vol. 17, no. 2, pp. 229–233, 2018.

[17] H. a. Majid, M. K. a. Rahim, M. R. Hamid, M. F. Ismail, and M. R. Sani, "Frequency reconfigurable microstrip patch antenna," *2012 IEEE Asia-Pacific Conf. Appl. Electromagn.*, vol. 1, no. APACE, pp. 342–345, 2012.

[18] B. A. Cetiner, G. Roqueta Crusats, L. Jofre, and N. Biyikli, "RF MEMS integrated frequency reconfigurable annular slot antenna," *IEEE Trans. Antennas Propag.*, vol. 58, no. 3, pp. 626–632, 2010.

[19] C. Borda-Fortuny, K.-F. Tong, and K. Chetty, “Low-cost mechanism to reconfigure the operating frequency band of a Vivaldi antenna for cognitive radio and spectrum monitoring applications,” *IET Microwaves, Antennas Propag.*, vol. 12, no. 5, pp. 779–782, Apr. 2018.

[20] Z. Liang, J. Liu, Y. Li, and Y. Long, “A Dual-Frequency Broadband Design of Coupled-Fed Stacked Microstrip Monopolar Patch Antenna for WLAN Applications,” *IEEE Antennas Wirel. Propag. Lett.*, vol. 15, pp. 1289–1292, 2016.

[21] K. Kavitha, S. Arivazhagan, and R. T. Jerin, “Reconfigurable microstrip stacked array antenna,” in *Proceedings of 2016 Online International Conference on Green Engineering and Technologies, IC-GET 2016*, 2017.

[22] N. Ramli, M. T. Ali, A. L. Yusof, M. T. Islam, and S. Muhamud-Kayut, “Reconfigurable Microstrip Stacked Array Antenna with Frequency and Pattern Characteristics,” *Prog. Electromagn. Res. C;2014, Vol. 49, p47*, vol. 49, pp. 47–58, 2014.

[23] L. Ge, M. Li, J. Wang, and H. Gu, “Unidirectional Dual-Band Stacked Patch Antenna with Independent Frequency Reconfiguration,” *IEEE Antennas Wirel. Propag. Lett.*, vol. 16, pp. 113–116, 2017.

[24] M. Abou Al-alaa, H. A. Elsadek, E. A. Abdallah, and E. A. Hashish, “Pattern and frequency reconfigurable monopole disc antenna using PIN diodes and MEMS switches,” *Microw. Opt. Technol. Lett.*, vol. 56, no. 1, pp. 187–195, Jan. 2014.

[25] I. Ben Trad, J. M. Floc’H, H. Rmili, M. Drissi, and F. Choubani, “A planar reconfigurable radiation pattern dipole antenna with reflectors and directors for wireless communication applications,” *Int. J. Antennas Propag.*, vol. 2014, 2014.

[26] J. Dong, Y. Li, and B. Zhang, “A survey on radiation pattern reconfigurable antennas,” in *7th International Conference on Wireless Communications, Networking and Mobile Computing, WiCOM 2011*, 2011, pp. 1–4.

[27] R. L. Haupt and M. Lanagan, “Reconfigurable antennas,” *IEEE Antennas Propag. Mag.*, vol. 55, no. 1, pp. 49–61, 2013.

[28] S. K. Sharma, F. Fideles, and A. Kalikond, “Planar Yagi-UDA antenna with reconfigurable radiation patterns,” *Microwave and Optical Technology Letters*, vol. 55, no. 12, pp. 2946–2952, 2013.

[29] W. S. Kang, J. A. Park, and Y. J. Yoon, “Simple reconfigurable antenna with radiation pattern,” *Electron. Lett.*, vol. 44, no. 3, p. 182, 2008.

[30] Zhan Shi, Ruping Zheng, Jun Ding, and Chenjiang Guo, “A Novel Pattern-Reconfigurable Antenna Using Switched Printed Elements,” *IEEE Antennas Wirel. Propag. Lett.*, vol. 11, pp. 1100–1103, 2012.

[31] T. Aboufoul, C. Parini, X. Chen, and A. Alomainy, “Pattern-Reconfigurable Planar Circular Ultra-Wideband Monopole Antenna,” *IEEE Trans. Antennas Propag.*, vol. 61, no. 10, pp. 4973–4980, Oct. 2013.

[32] W. Kang, S. Lee, and K. Kim, “Design of symmetric beam pattern reconfigurable antenna,” *Electron. Lett. (Volume46 , Issue 23)*, vol. 46, no. 23, pp. 1536–1537, 2010.

[33] J. Zhang, X. S. Yang, J. L. Li, and B. Z. Wang, “Triangular patch yagi antenna with reconfigurable pattern characteristics,” *Appl. Comput. Electromagn. Soc. J.*, vol. 27, no. 11, pp. 918–924, 2012.

[34] Y.-F. Cheng, X. Ding, B.-Z. Wang, and W. Shao, “An Azimuth-Pattern-Reconfigurable Antenna With Enhanced Gain and Front-to-Back Ratio,” *IEEE Antennas Wirel. Propag. Lett.*, vol. 16, pp. 2303–2306, 2017.

[35] G. Bertin, B. Piovano, R. Vallauri, F. Bilotti, and L. Vegni, “Metamaterial-inspired antennas for telecommunication applications,” in *Proceedings of 6th European Conference on Antennas and Propagation, EuCAP 2012*, 2012, pp. 2739–2740.

[36] F. Fezai, C. Menudier, M. Thevenot, E. Arnaud, and T. Monediere, “Reconfigurable Parasitic Element Antenna Using Reflection Phase Shifters,” *IEEE Antennas Wirel. Propag. Lett.*, vol. 14, pp. 775–778, 2015.

[37] A. Edalati and T. A. Denidni, “Reconfigurable antenna with high-directive beam using active cylindrical PRS,” in *IEEE Antennas and Propagation Society, AP-S International Symposium (Digest)*, 2009.

[38] W. Cao, B. Zhang, A. Liu, T. Yu, D. Guo, and K. Pan, “A Reconfigurable Microstrip Antenna With Radiation Pattern Selectivity and Polarization Diversity,” *Antennas Wirel. Propag. Lett. IEEE (Volume11)*, vol. 11, pp. 453–456, 2012.

[39] R. Mehmood and J. W. Wallace, “Interference suppression using parasitic reconfigurable aperture (RECAP) antennas,” in *Final Program and Book of Abstracts - iWAT 2011: 2011 IEEE International Workshop on Antenna Technology: Small Antennas, Novel Structures and Innovative Metamaterials*, 2011, pp. 82–85.

[40] D. Rodrigo, B. A. Cetiner, and L. Jofre, “Frequency, Radiation Pattern and Polarization Reconfigurable Antenna Using a Parasitic Pixel Layer,” *IEEE Trans. Antennas Propag.*, vol. 62, no. 6, pp. 3422–3427, Jun. 2014.

[41] Y. Fan, Y. Cui, and R. Li, “Polarization reconfigurable omnidirectional antenna using crossed dipoles,” *IEEE Antennas Propag. Soc. AP-S Int. Symp.*, vol. 2015–Octob, pp. 2371–2372, 2015.

[42] C. C. Chen, C. Y. D. Sim, and H. L. Lin, “Annular ring slot antenna design with reconfigurable polarization,” *Int. J. RF Microw. Comput. Eng.*, vol. 26, no. 2, pp. 110–120, 2016.

[43] J. Y. Sze, C. I. G. Hsu, M. H. Ho, Y. H. Ou, and M. T. Wu, “Design of circularly polarized annular-ring slot antennas fed by a double-bent microstripline,” *IEEE Trans. Antennas Propag.*, vol. 55, no. 11 II, pp. 3134–3139, 2007.

[44] A. Panahi, X. L. Bao, K. Yang, O. O’Conchubhair, and M. J. Ammann, “A simple polarization reconfigurable printed monopole antenna,” *IEEE Trans. Antennas Propag.*, vol. 63, no. 11, pp. 5129–5134, 2015.

[45] Z. X. Yang, H. C. Yang, J. S. Hong, and Y. Li, “Bandwidth enhancement of a polarization-reconfigurable patch antenna with stair-slots on the ground,” *IEEE Antennas Wirel. Propag. Lett.*, vol. 13, pp. 579–582, 2014.

[46] S. Karamzadeh, V. Rafii, M. Kartal, and H. Saygin, “Reconfigurable CP cavity back with ability to change polarisation diversity,” *Electron. Lett.*, vol. 51, no. 25, pp. 2080–2082, 2015.

[47] Z. Wang, P. S. Hall, J. R. Kelly, and P. Gardner, “Wideband Frequency-Domain and Space-Domain Pattern Reconfigurable Circular Antenna Array,” *IEEE Trans. Antennas Propag.*, vol. 65, no. 10, pp. 5179–5189, Oct. 2017.

[48] H. A. Majid, M. K. A. Rahim, M. R. Hamid, and M. F. Ismail, “Frequency and Pattern Reconfigurable Slot Antenna,” *Antennas Propagation, IEEE Trans. (Volume62 , Issue 10)*, vol. 62, no. 10, pp. 5339–5343, 2014.

[49] M. Ye and P. Gao, “Back-to-back F semicircular antenna with frequency and pattern reconfigurability,” *Electron. Lett.*, vol. 51, no. 25, pp. 2073–2074, 2015.

[50] S. Nikolaou *et al.*, “Pattern and Frequency Reconfigurable Annular Slot Antenna Using PIN Diodes,” *Antennas Propagation, IEEE Trans. (Volume54 , Issue 2)*, vol. 54, no. 2,

pp. 439–448, 2006.

[51] S. Nikolaou, B. Kim, and P. Vryonides, “Reconfiguring Antenna Characteristics Using PIN Diodes,” in *Antennas and Propagation, 2009. EuCAP 2009. 3rd European Conference*, 2009, pp. 3748–3752.

[52] W. Kang, S. Lee, K. Kim, S. Korea, and S. Korea, “A pattern-reconfigurable antenna using pin diodes,” *Microwave and Optical Technology Letters*, vol. 53, no. 8, pp. 1883–1887, May-2011.

[53] T. Li, H. Zhai, X. Wang, L. Li, and C. Liang, “Frequency-reconfigurable bow-tie antenna for bluetooth, WiMAX, and WLAN applications,” *IEEE Antennas Wirel. Propag. Lett.*, vol. 14, pp. 171–174, 2015.

[54] L. Pazin and Y. Leviatan, “Reconfigurable slot antenna for switchable multiband operation in a wide frequency range,” *IEEE Antennas Wirel. Propag. Lett.*, vol. 12, pp. 329–332, 2013.

[55] Guang-Min Zhang, Jin-Song Hong, Bing-Zhong Wang, Gangbing Song, and Peng Li, “Design and Time-Domain Analysis for a Novel Pattern Reconfigurable Antenna,” *IEEE Antennas Wirel. Propag. Lett.*, vol. 10, pp. 365–368, 2011.

[56] X. CAI, A. WANG, N. MA, and W. LENG, “Novel radiation pattern reconfigurable antenna with six beam choices,” *J. China Univ. Posts Telecommun.*, vol. 19, no. 2, pp. 123–128, Apr. 2012.

[57] D.-K. N. A. Editors, “How and Why to Use PIN Diodes for RF Switching,” 2016. [Online]. Available: https://www.digikey.co.uk/en/articles/techzone/2016/dec/how-and-why-to-use-pin-diodes-for-rf-switching. [Accessed: 11-Apr-2018].

[58] C. G. Christodoulou, Y. Tawk, S. A. Lane, and S. R. Erwin, “Reconfigurable antennas for wireless and space applications,” in *Proceedings of the IEEE*, 2012.

[59] G. H. Huff and J. T. Bernhard, “Integration of packaged RF MEMS switches with radiation pattern reconfigurable square spiral microstrip antennas,” *IEEE Trans. Antennas Propag.*, vol. 54, no. 2, pp. 464–469, 2006.

[60] O. Bayraktar, O. A. Civi, and T. Akin, “Beam switching reflectarray monolithically integrated with RF MEMS switches,” *IEEE Trans. Antennas Propag.*, vol. 60, no. 2 PART 2, pp. 854–862, 2012.

[61] J. M. Kovitz, H. Rajagopalan, and Y. Rahmat-Samii, “Design and implementation of broadband MEMS RHCP/LHCP reconfigurable arrays using rotated e-shaped patch elements,” *IEEE Trans. Antennas Propag.*, vol. 63, no. 6, pp. 2497–2507, 2015.

[62] A. Zohur, H. Mopidevi, D. Rodrigo, M. Unlu, L. Jofre, and B. A. Cetiner, “RF MEMS reconfigurable two-band antenna,” *IEEE Antennas Wirel. Propag. Lett.*, vol. 12, pp. 72–75, 2013.

[63] C. G. Christodoulou, “RF-MEMS and its applications to microwave systems, antennas and wireless communications,” *Proc. 2003 SBMO/IEEE MTT-S Int. Microw. Optoelectron. Conf. - IMOC 2003. (Cat. No.03TH8678)*, vol. 1, pp. 525–531, 2003.

[64] I. Kim and Y. Rahmat-Samii, “RF MEMS switchable slot patch antenna integrated with bias network,” *IEEE Trans. Antennas Propag.*, vol. 59, no. 12, pp. 4811–4815, 2011.

[65] A. Grau Besoli and F. De Flaviis, “A multifunctional reconfigurable pixeled antenna using MEMS technology on printed circuit board,” *IEEE Trans. Antennas Propag.*, vol. 59, no. 12, pp. 4413–4424, 2011.

[66] W. Tian, P. Li, and L. X. Yuan, “Research and analysis of MEMS switches in different frequency bands,” *Micromachines*, vol. 9, no. 4, 2018.

[67] H. A. C. Tilmans *et al.*, “MEMS packaging and reliability: An undividable couple,” *Microelectron. Reliab.*, vol. 52, no. 9–10, pp. 2228–2234, 2012.

[68] S. Yong and J. T. Bernhard, “A Pattern Reconfigurable Null Scanning Antenna,” *Antennas Propagation, IEEE Trans. (Volume60 , Issue 10)*, vol. 60, no. 10, pp. 4538–4544, 2012.

[69] H. Zakaria, M. Hindy, and A. El-Henawi, “Optically controlled UWB antenna using photonic crystal waveguides,” *Int. J. Microw. Wirel. Technol.*, pp. 1–6, 2017.

[70] D. Patron, A. S. Daryoush, and K. R. Dandekar, “Optical control of reconfigurable antennas and application to a novel pattern-reconfigurable planar design,” *J. Light. Technol.*, vol. 32, no. 20, pp. 3394–3402, 2014.

[71] G. Ruvio, M. J. Ammann, and Z. N. Chen, “Wideband Reconfigurable Rolled Planar Monopole Antenna,” *IEEE Trans. Antennas Propag.*, vol. 55, no. 6, pp. 1760–1767, Jun. 2007.

[72] Y. Dong, P. Liu, D. Yu, G. Li, and F. Tao, “Dual-Band Reconfigurable Terahertz Patch Antenna with Graphene-Stack-Based Backing Cavity,” *IEEE Antennas Wirel. Propag. Lett.*, vol. 15, pp. 1541–1544, 2016.

[73] H. Yan *et al.*, “Tunable infrared plasmonic devices using graphene/insulator stacks,” *Nat. Nanotechnol.*, 2012.

[74] S. H. Lee *et al.*, “Switching terahertz waves with gate-controlled active graphene metamaterials,” *Nat. Mater.*, 2012.

[75] F. N. Ayoub, C. D. Woehrle, Y. Tawk, D. T. Doyle, C. G. Christodoulou, and J. Costantine, “Frequency-tunable patch array using highly anisotropic liquid crystal,” in *IEEE Antennas and Propagation Society, AP-S International Symposium (Digest)*, 2014.

[76] M. A. Iskander, M. T. Chryssomallis, and D. E. Anagnostou, “Reconfigurable coplanar metamaterial unit cell for antenna array applications,” in *Radio Science Meeting (Joint with AP-S Symposium), 2013 USNC-URSI*, 2013, p. 85.

[77] T. Debogovic and J. Perruisseau-carrier, “MEMS-Reconfigurable Metamaterials and Antenna Applications,” *Int. J. Antennas Propag. Vol. 2014*, pp. 1–6, 2014.

[78] A. Dadgarpour, B. Zarghooni, and B. S. Virdee, “Beam Tilting Antenna Using Integrated Metamaterial Loading,” *Antennas Propagation, IEEE Trans. (Volume62 , Issue 5)*, vol. 62, no. 5, pp. 2874–2879, 2014.

[79] B. Kwaha, O. Inyang, and P. Amalu, “The Circular Microstrip Patch Antenna-Design And Implementation.,” *Int. J. Res. Rev. Appl. Sci.*, vol. 8, no. July, pp. 86–95, 2011.

[80] C. A. Balanis, *Antenna Theory: Analysis and Design, 3rd Edition - Constantine A. Balanis*. 2005.

[81] B. D. Orban and G. J. K. Moernaut, “The Basics of Patch Antennas,” *RF Glob.*, p. 2, 2011.

[82] C. U. Ndujiuba and A. O. Oloyede, “Selecting Best Feeding Technique of a Rectangular Patch Antenna for an Application,” *Int. J. Electromagn. Appl.*, vol. 5, no. 3, pp. 99–107, 2015.

[83] R. Waterhouse, “Small microstrip patch antenna,” *Electron. Lett.*, vol. 31, no. 8, p. 604, 1995.

[84] N. W. Liu, L. Zhu, and W. W. Choi, “A Low-Profile Wide-Bandwidth Planar Inverted-F Antenna under Dual Resonances: Principle and Design Approach,” *IEEE Trans. Antennas Propag.*, vol. 65, no. 10, pp. 5019–5025, 2017.

[85] A. Mishra, P. Singh, N. P. Yadav, J. A. Ansari, and B. R. Vishvakarma, "Compact Shorted Microstrip Patch Antenna for Dual Band Operation," *Prog. Electromagn. Res. C*, vol. 9, pp. 171–182, 2009.

[86] R. B. Waterhouse, S. D. Targonski, and D. M. Kokotoff, "Design and performance of small printed antennas," *IEEE Trans. Antennas Propag.*, vol. 46, no. 11, pp. 1629–1633, 1998.

[87] A. A. Deshmukh and K. P. Ray, "Analysis of shorted-plate compact and broadband microstrip antenna," *IEEE Antennas Propag. Mag.*, vol. 55, no. 6, pp. 100–113, 2013.

[88] X. Zhang and L. Zhu, "Patch Antennas with Loading of a Pair of Shorting Pins Toward Flexible Impedance Matching and Low Cross Polarization," *IEEE Trans. Antennas Propag.*, vol. 64, no. 4, pp. 1226–1233, 2016.

[89] J. S. Row, "A simple impedance-matching technique for patch antennas fed by coplanar microstrip line," *IEEE Trans. Antennas Propag.*, vol. 53, no. 10, pp. 3389–3391, 2005.

[90] P. R. Urwin-Wright, "A tuneable electrically-small antenna operating in the 'DC' mode," in *5th European Personal Mobile Communications Conference 2003*, 2003, vol. 2003, pp. 524–528.

[91] H. Yagi, "Beam Transmission of Ultra Short Waves," *Proc. IRE*, vol. 16, no. 6, pp. 715–740, Jun. 1928.

[92] D. M. Pozar, "Beam transmission of ultra short waves: an introduction to the classic paper by H. Yagi," *Proc. IEEE*, vol. 85, no. 11, pp. 1857–1863, 1997.

[93] C. A. Balanis, "Chapter 10," in *Antenna Theory: Analysis Design, Third Edition, by Constantine A. Balanis*, 2005.

[94] D. Cheng and C. Chen, "Optimum element spacings for Yagi-Uda arrays," *IEEE Trans. Antennas Propag.*, vol. 21, no. 5, pp. 615–623, Sep. 1973.

[95] C. Chen and D. Cheng, "Optimum element lengths for Yagi-Uda arrays," *IEEE Trans. Antennas Propag.*, vol. 23, no. 1, pp. 8–15, Jan. 1975.

[96] A. Holub and M. Polívka, "A novel microstrip patch antenna miniaturization technique: Meanderly folded shorted-patch antenna," in *Proceedings of the 14th Conference on Microwave Techniques, COMITE 2008*, 2008.

[97] S. Wang, H. W. Lai, K. K. So, K. B. Ng, Q. Xue, and G. Liao, "Wideband shorted patch antenna with a modified half U-slot," *IEEE Antennas Wirel. Propag. Lett.*, 2012.

[98] M. S. Sharawi, M. U. Khan, and R. Mittra, "Microstrip patch antenna miniaturisation techniques: a review," *IET Microwaves, Antennas Propag.*, vol. 9, no. 9, pp. 913–922, 2015.

[99] S. Kumar and D. K. Vishwakarma, "Miniaturisation of microstrip patch antenna using an artificial planar magneto-dielectric meta-substrate," *IET Microwaves, Antennas Propag.*, vol. 10, no. 11, pp. 1235–1241, Aug. 2016.

[100] J. P. Gianvittorio and Y. Rahmat-Samii, "Fractal antennas: A novel antenna miniaturization technique, and applications," *IEEE Antennas Propag. Mag.*, 2002.

[101] S. Sufyar and C. Delaveaud, "A miniaturization technique of a compact omnidirectional antenna," *Radioengineering*, vol. 18, no. 4, pp. 373–380, 2009.

[102] S. K. M. Haque and K. M. Parvez, "Slot antenna miniaturization using slit, strip, and loop loading techniques," *IEEE Trans. Antennas Propag.*, 2017.

[103] J. Choi and S. Lim, "Frequency and Radiation Pattern Reconfigurable Small Metamaterial Antenna using its Extraordinary Zeroth-Order Resonance," *J.*

Electromagn. Waves Appl., vol. 24, pp. 2119–2127, 2010.

[104] M. Fallahpour and R. Zoughi, "Antenna Miniaturization Techniques: A Review of Topology- and Material-Based Methods," *IEEE Antennas Propag. Mag.*, vol. 60, no. 1, pp. 38–50, Feb. 2018.

[105] R. Azadegan and K. Sarabandi, "A novel approach for miniaturization of slot antennas," *IEEE Trans. Antennas Propag.*, vol. 51, no. 3, pp. 421–429, 2003.

[106] C. W. Harrison, "Monopole with Inductive Loading," *IEEE Trans. Antennas Propag.*, vol. AP-11, no. 4, pp. 394–400, 1963.

[107] R. S. S. Kumari and M. K. Kumar, "A Realistic Approach for Antenna Miniaturization," *Int. J. Appl. Comput.*, vol. 4, no. 2, pp. 93–99, 2011.

[108] L. Loizou, J. Buckley, M. Belcastro, J. Barton, B. O. Flynn, and C. O. Mathuna, "Miniaturized Inverted-F Antenna with Capacitive Loading," in *Antennas and Propagation (EuCAP), 2013 7th European Conference on*, 2013, pp. 3111–3114.

[109] M. C. Scardelletti, G. E. Ponchak, J. L. Jordan, and S. J. Merritt, "Reduced size folded slot antennas with capacitive loading," *2008 IEEE Int. Symp. Antennas Propag. Usn. Natl. Radio Sci. Meet. APSURSI*, vol. 44135, no. 1, pp. 3–6, 2008.